FABRICATION AND CHARACTERIZATION OF GRISEOFULVIN LOADED NANOPOROUS SCAFFOLDS FOR ANTIFUNGAL DRUG DELIVERY

THESIS SUBMITTED FOR THE DEGREE OF
MASTER OF PHARMACY

JADAVPUR UNIVERSITY
2023

By

PRATEEP SENGUPTA

Roll No. – 002111402009

Examination Roll No. – M4PHP23028

Registration No. – 160243 of 2021-22

DEPARTMENT OF PHARMACEUTICAL TECHNOLOGY

FACULTY OF ENGINNERING AND TECHNOLOGY

JADAVPUR UNIVERSITY

KOLKATA – 700032

INDIA

JADAVPUR UNIVERSITY
KOLKATA – 700032

Title of the thesis

FABRICATION AND CHARACTERIZATION OF GRISEOFULVIN LOADED NANOPOROUS SCAFFOLDS FOR ANTIFUNGAL DRUG DELIVERY

Name, Designation and Institution of the supervisor:

Dr. Kajal Ghosal, Assistant Professor

Department of Pharmaceutical Technology

Jadavpur University

Kolkata – 700032, India.

DEPARTMENT OF PHARMACEUTICAL TECHNOLOGY
FACULTY OF ENGINEERING AND TECHNOLOGY
JADAVPUR UNIVERSITY

CERTIFICATE OF APPROVAL

This is to certify that the thesis entitled "**Fabrication and Characterization of Griseofulvin Loaded Nanoporous Scaffolds for Antifungal Drug Delivery**" submitted by **Prateep Sengupta**, of Jadavpur University, for the course of **Master of Pharmacy** is absolutely based upon his work under the supervision of **Dr. Kajal Ghosal**, Assistant Professor, Department of Pharmaceutical Technology, Jadavpur University, Kolkata and that neither his thesis nor any part of the thesis has been submitted for any degree/diploma or any other academic award anywhere before.

Kajal Ghosal

(Signature of M.Pharm thesis Guide)

12.09.23

Asst. Prof. Kajal Ghosal

Dr. Kajal Ghosal
Assistant Professor
Department of Pharm. Tech
Jadavpur University
Kolkata - 700032

Department of Pharmaceutical Technology

Jadavpur University, Kolkata – 700032.

Head
Dept. of Pharmaceutical Technology
Jadavpur University
Kolkata-700032, W.B. India

12/9/23

(Signature of Head of the Department)

Saswati Mazumdar

12.9.23

(Signature of Dean)

Prof. (Dr.) Sanmoy Karmakar

Faculty of Engineering and Technology

Department of Pharmaceutical Technology

Jadavpur University, Kolkata – 700032.
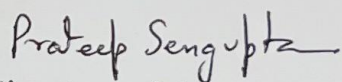
Jadavpur University, Kolkata – 700032.

DEAN
Faculty of Engineering & Technology
JADAVPUR UNIVERSITY
KOLKATA-700 032

3

DECLARATION BY THE CANDIDATE

I do hereby declare that the work incorporated in the thesis entitled "**Fabrication and Characterization of Griseofulvin Loaded Nanosponge for Antifungal Drug Delivery**" has been carried out by me in the Department of Pharmaceutical Technology, Jadavpur University under the supervision of Dr. Kajal Ghosal, Assistant Professor, Department of Pharmaceutical Technology, Jadavpur University, Kolkata – 700032. Neither the thesis nor any part therefore has been submitted for any other degree.

Date: 12/9/23

Place: Kolkata, India

Prateep Sengupta

Signature of the candidate

(PRATEEP SENGUPTA)

4

Dedicated to my Guide and My Family

ACKNOWLEDGEMENT

I express my deepest gratitude to my supervisor, Dr. Kajal Ghosal for providing me a scope to work in her laboratory. I owe to her for all the suggestions and guidance support extended.

This thesis has become a reality only due to her. Her wide knowledge and way of thinking know no bounds. Her encouragement and human quality are two never exhaustible things which I have felt. During these years, I have witnessed Dr. Kajal Ghosal as a sympathetic and a principled person. Her enthusiasm and view of research and her mission for achieving quality work without any compromise, has made a deep impression on me.

I would like to convey my sincerest gratitude to Prof. Jasmina Khanam for sharing her valuable knowledge and letting me use her laboratory for project work. I am highly indebted to Prof. Pranab Kumar Mondal, IIT Guwahati, for letting me use their instruments and all facilities of IITG for characterization purpose.

I am very thankful to Prof. Sanmay Karmakar, Head, Department of Pharmaceutical Technology, Jadavpur University, and all the faculty members of this department for their individual suggestions and kind co-operation.

I express my deepest gratitude to my labmate Ms. Amrita Das, my senior Ms. Prateechee Padma (IITG), Mrs. Shreya Chatterjee, my juniors Mr. Souvik Singha and Mr. Samrat Chowdhury for creating a congenial environment, kind support and active participation in project related discussions and encouragement throughout my research work.

I prefer to say thanks to all of my friends of Jadavpur University who helped me directly or indirectly to progress my research work.

I am thankful to the authority of Jadavpur University for providing me facilities to complete my work successfully. I am also sincerely thankful to all the non-teaching staff of the department of Pharmaceutical Technology.

I gratefully acknowledge my parents, my dog, and my relatives for their active encouragement, moral support, unlimited blessing, and their presence in my life which enabled me to reach till this point.

Date: 12/9/23   PRATEEP SENGUPTA

PREFACE

The present thesis work entitled "**Fabrication and Characterization of Griseofulvin Loaded Nanoporous Scaffolds for Antifungal Drug Delivery**" deals with development of sustained release nanoporous scaffolds which were developed by incorporating emulsion solvent diffusion technique. Further by using passive loading, griseofulvin has been encapsulated in the scaffold matrix and further efficacy of griseofulvin loaded nanoporous scaffolds as an antifungal drug delivery system have been assessed.

- Chapter 1 deals with the introduction part of the thesis, it describes about the characteristics and types of nanosponges (nanoporous scaffolds), their preparations and thereafter prospect of nanosponge being used as an antifungal delivery system. Some discussions about the drug, polymer and cross-linker types utilized in nanoporous scaffolds fabrication were highlighted.

- Chapter 2 represents a careful selection on recent developments in the field of topical delivery of antifungal drugs using nanosponges related to the present topic of work.

- The aims and objectives of this work are laid sequentially and logically in Chapter 3.

- Chapter 4 enlists the drug and polymer profile used in the project.

- Chapter 5 consists of the preparation procedures used in fabricating nanoporous scaffolds and the characterization methods employed

- Chapter 6 highlights the results and discussions.

- The conclusions drawn from the entire work are detailed in Chapter 7.

- Chapter 8 gives comprehensive list of references which were cited in the text.

- Chapter 9 enlists various recent publications based on the thesis work.

Contents

List of Tables

Table no.	Title
1.	List of polymers used for synthesis of nanosponge.
2.	List of crosslinkers used for synthesis of nanosponge.
3.	List of BCS class II drugs used in nanosponge formulation.
4.	List of marketed cyclodextrin based nanosponges.
5.	Application of nanosponges with respect to their possible advantages.
6.	Plant extracts encapsulated as nanosponge for anti-fungal use.
7.	Formulation chart of Griseofulvin loaded nanosponges.
8.	Absorbance of various concentrations of GRI at λmax 295nm.
9.	Solubility of GRI in various solvents.
10.	Physical properties of GRI.
11.	Percentage yield and entrapment efficiency result of the formulations.
12.	Mean Particle Size, PDI and Zeta potential values.
13.	%CDR Calculation of F1 formulation
14.	%CDR Calculation of F2 formulation
15.	%CDR Calculation of F3 formulation
16.	Summary of r^2 value of various models
17.	Calculation of zero-order kinetics
18.	Calculation of first-order kinetics
19.	Calculation of Hixon-Crowell model.
20.	Calculation of Higuchi model.
21.	Calculation of Korsmeyar-Peppas model.
22.	Zones of Inhibition Interpretative Standard for some important Test Microorganisms.
23.	Zone of inhibition diameter of pure drug and formulations F1, F2 and F3.

List of Figures

20.	In-vitro antifungal activity assessed for BTF, BTF loaded BNS3 gel and Marketed preparation.
21.	Antifungal activity of F9 hydrogel formulation after integration with lemongrass loaded NS, after 2 and 4 days.
22.	In-vitro release profiles of six formulations CA1, CA2, CA3, CA4, CA5 and CA6 at λmax 210 nm.
23.	Skin deposition of THCL nanosponge, THCL hydrogel and Marketed Cream.
24.	Zone of Inhibition of Babchi Oil and BONS4: optimized Babchi Oil loaded NS.
25.	In vitro release profile of marketed CTZ gel and CTZ loaded hydroxylpropyl β-CD NS- based in situ vaginal gel.
26.	Proposed nanosponge structure of β-CD.
28.	In-vitro release profiles of GRI and GRI loaded NS.
29.	Standard calibration curve of GRI in phosphate buffer solution of pH 7.2
30.	Nanosponges prepared by quasi emulsion solvent diffusion method. Where A: F1 formulation, B: F2 formulation, C: F3 formulation, D: griseofulvin.
31.	Particle size distribution of three nanosponge formulations: F1, F2 and F3.
32.	Images of Griseolfulvin nanosponge from trinocular microscope, where a: F1, b: F2, and c: F3.
33.	FTIR spectra of Griseofulvin, blank nanosponge and drug loaded nanosponge (F1, F2 and F3).
34.	XRD spectra of GRI.
35.	XRD spectra of blank nanosponge and formulations F1, F2 and F3.
36.	DSC thermogram of drug loaded nanosponges (F1, F2 and F3).
37.	SEM images of all formulations, where a: blank nanosponges, b: F1, c: F2 and d: F3.
38.	TEM images of F1 nanosponge, scale 100 and 50 nm.
39.	% Cumulative drug release vs. Time of F1, F2 and F3.
40.	Zero-order release kinetics.
41.	First-order release kinetics.
42.	Hixon-Crowell Kinetics.

43.	Higuchi release kinetics.
44.	Korsmeyar-Peppas kinetics.
45.	Antifungal activity assay, where a: after 24 hours, b: after 48 hours, c: after 72 hours.

List of Abbreviations

PS: Particle size

PDI: Polydispersity index

ZP: Zeta potential

EE: Entrapment efficiency

DL: Drug loading

THCL: Terbinafine hydrochloride

PY: Production yield

TEM: Transmission Electron Microscopy

DCM: Dichloromethane

EC: Ethyl Cellulose

PVA: Polyvinyl alcohol

LGO: Lemongrass oil

DDSs: Drug delivery systems

DLS: Dynamic Light Scattering study

CIP: Ciprofloxacin

NAC: N-acetyl cysteine

BO: Babchi oil

CTZ: Clotrimazole

PF-127: Pluronic F-127

PF-68: Pluronic F-68

EN: Econazole nitrate

GRI: Griseofulvin

NS: Nanosponge:

Chapter 1
Introduction

1.1 Introduction to Novel Drug Delivery System

Day by day the understanding of pharmacokinetics and pharmacodynamic behaviour of drugs offer more rational approaches to the development of more optimal drug delivery systems. Any type of active agent may be more effective and safer using an improved drug delivery system and it may present more lucrative marketing opportunities for pharmaceuticals and be effective for mankind as it improves the treatment strategy. Properly designed drug delivery systems deliver a specified amount of drug to the target site at an appropriate time and rate. Conventional dosage forms such as tablets and capsules are incapable of controlling the rate of drug delivery to the target site. As a result, the massive distribution of drugs in non-target tissues and body fluids necessitate therapeutic doses that could far exceed the amount required in target cells. Also, higher doses can lead to severe adverse effects during treatment. In that case novel drug delivery system (NDDS) becomes helpful to maintain the drug concentration in therapeutic range for a long time and to reduce the dosing interval [1].

1.2 Advantages of NDDS [1]:

1. Pre-determined release rate for an extended period of time may be achieved.
2. Increase the duration of short half-life of drugs
3. Elimination of side effects by targeting the site of action
4. Wastage of drugs and frequent dosing may be reduced.
5. Better patient compliance can be achieved.
6. Optimal therapeutic drug concentration in the blood and tissue fluids can be maintained for a prolonged period of time.

1.3 Introduction to Nanoporous scaffolds:

To lessen systemic and localised negative effects, the best pharmacological therapies concentrate the medicine at the affected area for a predetermined amount of time. To achieve an effective therapeutic effect, it is necessary to regulate the drug's intake rate once it has been transported and delivered to the site of action. It is thus puzzling that the medicine would be dispersed to other tissues, which might be both wasteful and harmful. What we mean by "targeted drug delivery" is the restricted access to non-target areas combined with the selective localisation of the medication at therapeutic concentrations at the intended site of action [2].

Site specific delivery can be classified according to the level of specificity achieved:

1. Delivery to individual organs or tissues. (**Organ targeting**)
2. Targeting a specific cell type within a tissue. (**Cellular targeting**)
3. Delivery to different intracellular compartments in target cells by engineering the internalization of drug and drug carrier construct via specific transport pathways. (**Intracellular targeting**)

However, medical professionals have long struggled to design effective customised drug delivery systems that can transport medications to the appropriate site in the body and regulate their release to prevent overdose. The development of innovative, complex molecules called nanosponges has been proposed as a possible answer to these problems [3].

Nanosponge aka nanoporous scaffolds are a novel class of materials made of small particles with perforations just a few nanometers wide, that can encapsulate a broad range of compounds. They can boost the solubility of molecules by including both lipophilic and hydrophilic components into their chambers [4]. Nanosponges are tiny, mesh-like structures with the potential to improve the treatment of a wide range of ailments and also enhance solubility of a wide range of BCS class II drugs. Preliminary research has shown that this technology is approximately five times more effective at delivering drugs for breast cancer than conventional methods [5].

The "backbone" (a three-dimensional scaffold structure) of the virus-sized nanosponge is comprised of biodegradable polyester (figure 1). Smaller molecules called cross-linkers bind to specific areas of the polyester strands in a solution containing long polyester strands. They create a sphere with multiple compartments by cross-linking sections of the polyester to accommodate medication. Since the biodegradation of the polyester can be predicted, the medicine will be released at fixed intervals when the drug (nanosponges) disintegrates in the body [6]. One of the main benefits of this technology over other nanoparticle delivery systems currently being tested is its predictability of release. Many other nanoparticle delivery techniques rapidly and uncontrollably release the major fraction of their medicine once they reach their destination. This is known as the "burst effect," in which it is hard to determine an effective dose. Fortunately, nanosponges make it possible to mitigate this problem to a significant extent [7].
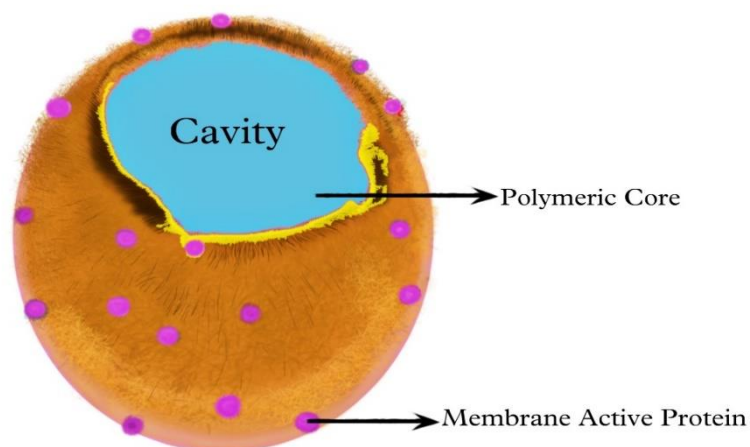
Figure 1: Visual representation of nanosponge embedded with membrane active proteins. Nanosponges are encapsulating nanoparticle that may safely enclose medication molecules inside its core. The nanoparticles may be broken down into several categories based on how they combine with drugs [8].

- **Encapsulating nanoparticles:** Nanosponges and nanocapsules are examples of these. Alginate nanosponges, for example, have numerous pores that convey the drug molecules. Poly (isobutyl-cyanoacrylate) (IBCA) nanocapsules are also used to encapsulate nanoparticles. They have the ability to abduct pharmaceutical molecules in their aqueous core.
- **Complexing nanoparticles:** The molecules are attracted to these nanoparticles by electrostatic charges.
- **Conjugating nanoparticles**: A strong covalent connection connects these nanoparticles to pharmaceutical molecules so that they may work together.

Nanosponges are an unusual kind of nanoparticle that may be synthesised from natural products. They can withstand temperatures up to 300°C, are soluble in water and organic solvents, and have a higher porosity and lower toxicity than conventional nanoparticles. Thanks to its nanomeric sized gaps and changeable polarity, nanosponges are able to selectively release a broad variety of chemicals [9]. These solids can be formed into injectable, oral, topical (transdermal patches and gel), and inhalational dosage forms. They can be combined with excipients in the case of oral dosage formulations. For parenteral preparations, they may be mixed with water for injection, saline, or other aqueous solutions. When administered topically, they pair well with hydrogel and patches to increase retention onto the skin, lessen the likelihood of side effects, and reduce discomfort compared to other topical delivery systems.

This suggests that nanosponges may hold great promise as a topical medication delivery vehicle [10, 11].

By adjusting the cross-linker to polymer ratio during manufacturing, the nanosponges can be tailored to a specific size and timed drug release. This results in formation of various kinds of nanosponges (figure 2). Nanosponge has more engineering potential than many other nanoscale drug delivery systems due to the simplicity of its chemistry, which consists of polyesters and cross-linking peptides [12]. These nanosponges may be magnetised if they are produced in the company of substances having magnetic properties, thus unlocking more potential [13]. A good disguise enables nanosponge to soak up toxins from drug resistant infections or poisons [14]. Their tiny shapes also enable efficient pulmonary delivery [15]. Nanosponges can be dissolved in water without dissolving chemically. They combine with water and employ it as a transport fluid. They are able to change liquids into solids and mask off undesirable flavours. The nanosponge is able to bind preferentially to the target spot because of the chemical linkers [16].
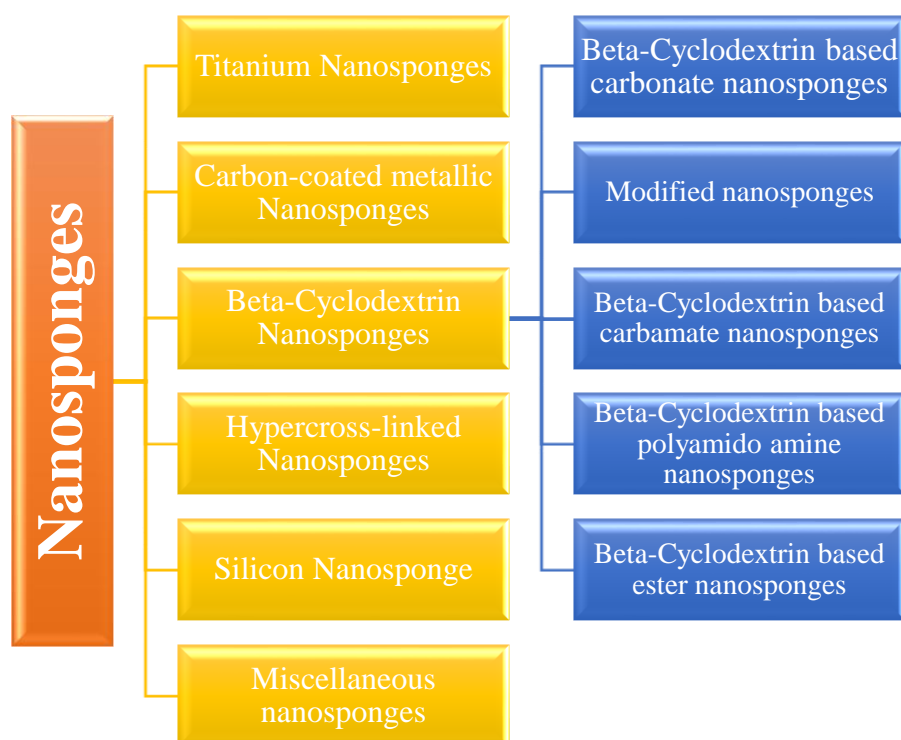

Figure 2: Types of nanosponge (adapted from Ref no. 4)

1.4 Examples of various works on drug loaded nanosponges

Drugs	Disease	Polymer and Crosslinker used	Aim of the study	Models used	Major findings	Reference
Itraconazole	Fungal infection	β-Cyclodextrin (β-CD), copolyvidonum	Solubility study	Higuchi	Solubilty increased by many folds.	17
Quercitin	Lung cancer, COVID-19	β-CD, 2-HPβCD, Diphenyl carbonate	Solubility study, anti-proliferation, anti-SARS-COV-2 activity	A549(lung cancer cell line), vero-E6 cell	Improved solubility, improved biological activity against lung cancer, and SAR-CoV-2	18
Camptothecin	Cancer	β-CD, Diphenyl carbonate	Haemolytic activity	HT-29 (human colon cancer cell line)	Stability of the drug increased, prolonged drug release profile	19
Dexamethasone	Anti-estrogen	β-CD, Diphenyl carbonate	In-vitro release	Dialysis membrane	Prolonged drug release	20
Paclitaxel	Cancer	β-CD, Diphenyl carbonate	Bioavailability (BA) study, cytotoxicity study	Sprague Dawley rats for BA study, MCF-7 Cell line (for cytotoxicity study)	Increased bioavailability, better cell proliferations inhibition	21,22
Telmisartan	Hypertension	β-CD, Diphenyl carbonate	Solubility	___	Solubility of the drug increased	23

Rilpivirin	Anti-HIV	β-CD, Diphenyl carbonate	Bioavailability	Sprague Dawley rats	Bioavailability increased	24
Griseofulvin	Fungal infection	β-CD, Diphenyl carbonate	Dissolution study, oral bioavailability (BA)	Dialysis membrane	Solubility of the drug increased, increased oral BA with masking bitter taste, improved dissolution	25
Resveratrol	Dermatitis, gonorrhoea, antioxidant	β-CD, carbonyldiimidazole	Permeation study, cytotoxicity study	Pigskin (ex-vivo) for permeation study, HCPC-I cell line	Better permeation, inhibition of cells proliferation	26
Tamoxifen	Anti-estrogen	β-CD, carbonyldiimidazole	Solubility, cytotoxicity study	MCF -7 cell line	Solubility of drug increased, better inhibition of cells proliferation	27
Oxygen delivery	Hypoxic condition	α, β, γ - CD, carbonyldiimidazole	Cytotoxicity study, in vitro release	Vero cells for cytotoxicity study, teflon vials for IV release	Non-toxic to vero cells, burst release initially followed by slow, prolonged release	28
Erlotinib	Lung cancer	β-CD, Pyromellitic dianhyride	Cytotoxicity study	A549 Cell (human lung	Showed higher inhibitory effect at lower dose for	29

				carcinoma cell)	extended period of time as compared to conventional drug	

2.1 The Human Skin, Structure and Functions [30]

The skin is the largest organ in the body, comprising about 15% of body weight. The total skin surface of an adult ranges from 12-20 square feet. In terms of chemical composition, the skin is about 70% water, 25% protein and 2% lipids.

The skin consists of three main layers: Epidermis, Dermis and Subcutaneous tissue.
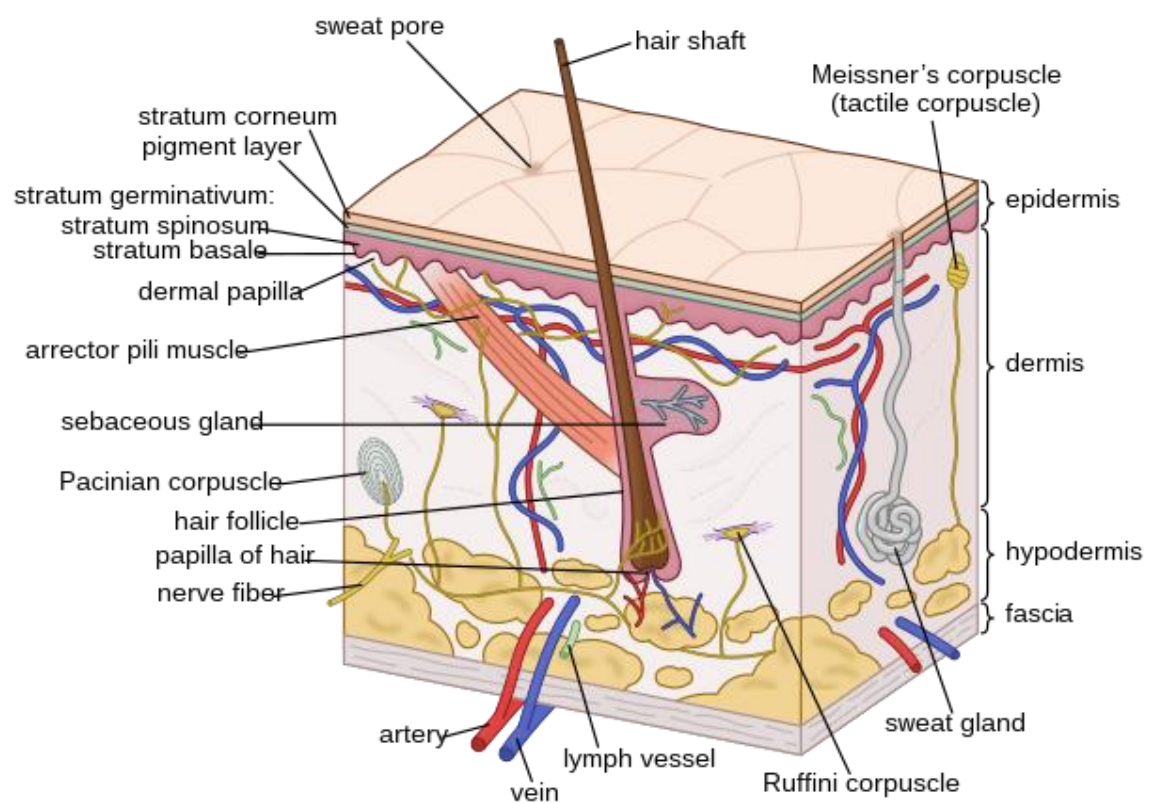

Figure 3: Structure of skin

Epidermis

The epidermis is the most superficial layer of the skin and is composed of *stratified keratinized squamous epithelium,* which varies in thickness in different parts of the body. It is thickest on

the palms of the hand and soles of the feet. There are no blood vessels or nerve endings in the epidermis, but its deeper layer is bathed in interstitial fluid from the dermis, which provides oxygen and nutrients, and drains away as lymph.

There are several layers (strata) of cells in the epidermis which extend from the deepest germinative layer to the most superficial *stratum corneum* (a thick horny layer). The cells on the surface are flat, thin, non-nucleated, dead cells or *squames*, in which the cytoplasm has been replaced by the fibrous protein *keratin*. These cells are constantly being rubbed off and replaced by cells that originated in the germinative layer and have undergone gradual changes as they progressed towards the surface. Complete replacement of the epidermis takes about a month.

Melanin, a dark pigment derived from amino acid tyrosine and secreted by *melanocytes* in the deep germinative layer, is absorbed by surrounding epithelial cells. The amount is genetically determined and varies between different parts of the body. It protects the skin from the harmful effects of sunlight. Exposure to sunlight promotes synthesis of melanin. Langerhans cells are a specialized population of dendritic cells that are found in the epidermis of the skin. They prevent unwanted foreign substances from penetrating the skin.

Dermis

The dermis is tough and elastic. It is formed from connective tissue and the matrix contains collagen fibres interlaced with elastic fibres. Rupture of elastic fibres occurs when the skin is overstretched, resulting in permanent striae or stretch marks, that may be found in pregnancy and obesity. Collagen fibres bind water and give the skin its tensile strength, but as this ability declines with age, wrinkles develop. Fibroblasts, macrophages and mast cells are the main cells found in the dermis. Underlying its deepest layer there is areolar tissue and varying amounts of adipose tissue. The structures in the dermis are: blood vessels, lymph vessels, sensory nerve endings, sweat glands and their ducts, hairs, arrector pili muscles and sebaceous glands.

Blood and lymph vessels

Arterioles form a fine network with capillary branches supplying sweat glands, sebaceous glands, hair follicles and the dermis. Lymph vessels form a network throughout the dermis.

Sensory nerve endings

Sensory receptors (specialized nerve endings) sensitive to *touch, temperature, pressure* and *pain* are widely distributed in the dermis. Incoming stimuli activate different types of sensory receptors. The Pacinian corpuscle is sensitive to deep pressure. The skin is an important sensory organ through which individuals receive information about their environment. Nerve impulses, generated in the sensory receptors in the dermis are conveyed to the spinal cord by sensory nerve, then to the sensory area of the cerebrum where the sensations are perceived.

Sweat glands

These are widely distributed throughout the skin and are most numerous in the palms of the hand, soles of the feet, axillae and groins. They are formed from epithelial cells. The bodies of the glands lie coiled in the subcutaneous tissue. There are two types of sweat gland. The commonest type opens onto the skin surface through tiny pores, and the sweat produced here is clear, watery fluid important for regulating body temperature. The second type opens into hair follicles, and is found, for example, in the axilla. Bacterial decomposition of these secretions causes an unpleasant odour. A specialized example of this type of gland is the ceruminous gland of the outer ear, which secretes earwax.

The most important function of sweat is in the regulation of body temperature. Excessive sweating may lead to dehydration and serious depletion of sodium chloride unless intake of water and salt is appropriately increased. After 7 to 10 days exposure to high environmental temperature the amount of sweat lost is substantially reduced but water loss remains high.

Hairs

These are formed by a down growth of epidermal cells into the dermis or subcutaneous tissue, caller hair follicle. At the base of the follicle is a cluster of cells called the *papilla* or *bulb.* The hair is formed by multiplication of cells of the bulb and as they are pushed upwards, away from their source of nutrition, the cells die and become keratinized. The part of the hair above the skin is the shaft and the remainder, the root.

Arrector pili

These are little bundles of smooth muscle fibres attached to the hair follicles. Concentration makes the hair stand erect and raises the skin around the hair, causing 'goose flesh'. The muscles are stimulated by sympathetic nerve fibres in response to fear and cold. Erect hairs

trap air, which acts as an insulating layer. This is an efficient warming mechanism, especially when accompanied by shivering, i.e., involuntary contraction of skeletal muscles.

Sebaceous glands

These consist of secretory epithelial cells derived from the same tissue as the hair follicles. They secrete an oily substance, *sebum*, into the hair follicles and are present in the skin of all parts of the body except the palms of the hands and the soles of the feet. They are most numerous in the skin of the scalp, face, axillae and groins. In regions of transition from one type of superficial epithelium to another, such as lips, eyelids, nipple, labia minora and glans penis, there are sebaceous glands that are independent of hair follicles, secreting sebum directly onto the surface.

Sebum keeps the hair soft and gives it a shiny appearance. On the skin it provides some waterproofing and acts as a bactericidal and fungicidal agent, preventing infection. It also prevents drying and cracking of skin, especially on exposure to heat and sunshine. The activity of these glands increases at pub   erty and is less at the extremes of age, rendering the skin of infants and older adults prone to the effects of excessive moisture (maceration).

Subcutaneous layer

Subcutaneous tissue is the innermost layer of the skin located under the dermis consisting of connective tissue and fat molecules. Subcutaneous fat acts as a shock absorber and heat insulator protecting underlying tissues from cold mechanical trauma. The loss of subcutaneous tissue, often accounting with age, leads to facial sagging and wrinkles.

Functions of the skin

Human skin has multifunctional activities:

- Acts as protective barrier against the ingress of foreign materials (pathogenic microbes and chemical agents) and it provides safety against physical injury.
- Helps to balance fluid and restrict loss of endogenous material such as water.
- Helps to prevent excessive water absorption by imparting water resistance to the skin.
- Helps to transport active solute molecules by passive diffusion.
- It is involved in temperature regulation of body.
- It is the body's main sensory organ for temperature, pressure, touch and pain.

- Provides protection from UV light.

- Plays a key role in metabolism, including vitamin D synthesis and biotransformation of some chemicals. Lack of vitamin can lead to soft bones and many associated problems.

## 2.2 Physiological and Pathological conditions of skin [31]

- **Reservoir effect of horny layer** – Skin's deeper layer or horny layer has a reservoir effect which can bind irreversibly with a part of drug.

- **Lipid film** – The lipid film on the skin surface prevents the removal of moisture from the skin and maintains skin's barrier function.

- **Skin hydration** – Skin can be hydrated by covering or occluding with a plastic sheet, hence accumulation of sweat can enhance the penetration

- **Skin temperature and pH** – Increased temperature can cause easier penetration as energy required for diffusion is easily achieved. The pH is normally acidic, ranging from 4-6. If the formulation has very low or very high pH value then it may cause destruction of the skin.

- **Regional variation** – Variation in climates of different region and the thickness can affect the permeability.

- **Pathological injuries to skin** – Injury that disrupt the continuity of the skin layers can cause easy permeation, caused by increased vasodilation

- **Cutaneous self-metabolism** – Epidermis or cutaneous layer having catabolic enzymes may render the drug inactive by metabolism as well as bioavailability of the topical drug.

- **Skin barrier properties in young and adult** – The pH of the skin of the neonates or newborns is higher than adult skin. Skin surface is slightly hydrophobic in case of young infants. Whereas, the adult's skin is smooth and rigid. Moisture content decreases within the age.

- **Race** – Racial differences between white and black skin have different anatomical and physiological functions. Black skin is having increased intracellular cohesiveness, lipid content and electrical resistance.

2.3 Fungal effects on skin [32]

Fungal infections have been common throughout the world, infecting mainly the skin. Fungal infections of the skin, also known as dermatophytosis or ringworm, can have various effects on the skin. Fungal infections are caused by different species of fungi, such as *Trichophyton,*

Microsporum, and *Epidermophyton*, which thrive in warm and moist environments. Candida species are responsible for the majority of human infections caused by fungal pathogens. Members of these species include the most frequent cause of opportunistic infections, *Candida albicans*, the drug-resistant *Candida glabrata*, the new global public health threat *Candida auris*, and other emerging species such as *Candida tropicalis*. These infections can occur on any part of the body, including the scalp, feet, groin, nails, and body folds. The most commonly experienced symptoms are:

1. **Itching and Redness:** Fungal infections often lead to intense itching and redness in the affected area. The skin may become inflamed and may appear swollen or irritated.

2. **Scaling and Peeling:** Infected skin may exhibit scaling and peeling, resulting in the formation of small flakes or larger patches of dry, flaky skin. The affected skin may also become thickened or develop a raised, scaly border.

3. **Rash:** A fungal infection can cause a rash, which may be characterized by a circular or oval-shaped pattern with a well-defined edge. The rash may have a reddish or brownish color and can be accompanied by small, raised bumps or blisters.

4. **Cracking and Fissuring:** In some cases, the skin affected by a fungal infection may crack or develop small fissures. This can be especially common in areas where the skin is naturally thin or subject to friction, such as between the toes or in the groin area.

5. **Hair and Nail Changes:** Fungal infections can also affect the hair and nails. Scalp infections may result in hair loss, while fungal nail infections (onychomycosis) can cause thickening, discoloration, and brittleness of the nails.

6. **Secondary Infections:** Prolonged fungal infections can weaken the skin's natural barrier, making it more susceptible to secondary bacterial infections. These secondary infections can lead to increased redness, swelling, and pus formation
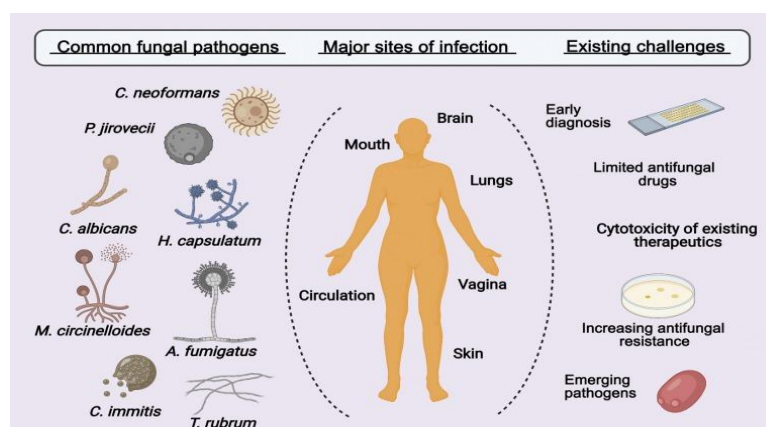
Treatment for **Figure 4:** The entire scenario of fungal infections and its challenges.

fungal skin infections typically involves antifungal medications, such as topical creams, powders, or oral medications (figure 4). Conventional antifungal usually requires long-term therapy, due to which adverse effects may increase after systemic administration. To avoid this, the topical preparation of anti-fungal drugs is developed. Anyhow, most of the topical antifungals, have less residence time and thereby show poor therapeutic actions. Hence due to their low efficacy, they require a high amount of active pharmaceutical agents to show therapeutic effect. Nanosponge loaded with antifungal drugs reduces the side effects associated with the conventional delivery system [33].

2.4 Conventional antifungal drug delivery vs. novel antifungal drug delivery

Fungal infections lead to a significant risk of mortality and morbidity worldwide. Out of 250,000 species of Fungi known, most of the infections are caused by opportunistic pathogens such as *Aspergillus*, *Candida* and *Cryptococcus* spp [34]. Conventional antifungal delivery systems have been used for many years to combat the same via orally, by injection, or as a topical cream or ointment. These methods have been effective in treating certain fungal diseases, but they have some drawbacks. The drugs are not always localized to the areas of infection, and can cause unwanted side effects in other parts of the body, common antifungal drugs such as clotrimazole, ciclopirox olamine, ketoconazole, miconazole, and ketoconazole may cause liver damage, kidney damage, and gastrointestinal issues in certain individuals [35]. Amphotericin B which is choice of drug for the systemic mycoses, however it can induce moderate to severe nephrotoxicity which limits the use of this drug [36]. The conventional drugs may not be effective against certain types of fungi, as they may not be able to penetrate the cell walls of the organism, additionally, some fungi can develop resistance to antifungal drugs over time, rendering the drugs ineffective [37]. The cost is also a huge issue which prevents frequent dosing and reduces patient compliance; the echinocandin drug caspofungin costs around $1,000 per dose, and the triazole drug itraconazole costs around $250 per month [38].

In recent years, researchers have been exploring new methods of antifungal drug delivery. These include nanoparticles and nanofibers, drug-containing liposomes, polymeric-based systems and solid-lipid nanoparticles (SLNs) [39]. Nanoparticles and nanofibers have the potential to deliver antifungal drugs directly to the site of infection, and they can be designed to penetrate cell walls more effectively than conventional drugs [40]. Drug-containing liposomes are small vesicles that can encapsulate antifungal drugs, protecting them from degradation in the body and allowing them to be released over a sustained period of time [41]. Polymeric-based systems are also under development, which involve using polymers to bind antifungal drugs

together and then releasing them into the bloodstream. These systems could potentially provide sustained release of antifungal drugs with fewer side effects than conventional delivery systems. In mycoses treatment, lipid formulations such as Amphotericin B or nystatin are used to reduce the toxicity [42]. The controlled release property makes SLNs a popular treatment of topical skin infections because of its prolonged release effect and high skin permeation. These systems mainly help in reducing the toxicity and increase the efficacy of antifungal drugs and thus increase the therapeutic effect in antifungal drug treatment [43].

Recently an increase in interest of nanosponges being used as novel antifungal delivery systems has emerged. Their large and porous cavitites even enable the encapsulation of high molecular weight drugs like Griseofulvin [44]. These innovative spherical nanocarriers are able to reduce the side effects associated with antifungal treatments, as they are able to target the infected areas without affecting the rest of the body [45]. They can reduce drug toxicity as nanosponges can be designed to remain in the body for a certain amount of time before the drug is released. This also makes them ideal for use in topical applications, as they can be applied directly to the affected area [46]. Additionally, nanosponges can be used to treat fungal infections that are resistant to conventional treatments, such as *Candida albican*s and *Aspergillus* spp.

2.5 Nanosponge: prospective drug delivery system for antifungal drugs

Recently, researchers have been exploring ways to use nanosponge technology to deliver antifungal drugs such as amphotericin B, a polyene macrolide antibiotic that has been used to treat fungal infections for decades. The basic idea behind nanosponges is to attach specific ligands, or molecules, to the nanosponge surface that are able to bind to the fungal cells [47]. The specific ligands used to bind to fungal cell walls include α-1,3-glucan, β-1,3 and β-1,6-glucan, chitin, chitosan, mannoproteins, and other GPI-anchored molecules [48]. Furthermore, research has shown that antifungal agents such as caspofungin can disrupt the cell wall architecture and make the β (1-3)-glucan layer more accessible, thus allowing for greater binding by dectin-1 [49]. Additionally, the carboxyl terminus of AGA2 has been found to be a high affinity ligand for the α-agglutinin molecule Sag1p, which is expressed on mating-type α cells [50]. This allows the nanosponge to be specifically targeted to only the fungal cells, thus increasing the drug's effectiveness.

In addition to being able to target specific cells, nanosponges also increase the drug's half-life when administered. This is due to the nanosponge's ability to sequester and release drugs in a controlled manner, preventing rapid clearance from the body and allowing for a longer duration

of action. Furthermore, nanosponges can also be used to significantly enhance drug solubility, allowing for improved penetration into the fungal cell wall, and to target drug delivery to specific sites of action [51].

3.1 Characteristics of nanosponge [52,53]

The capacity of nanosponges to enhance the bioavailability of medications is one of the most significant benefits offered by these particles. This may be accomplished by a number of different processes, including as the capacity of the nanosponges to slowly release the medication over an extended period of time, to target certain cells or tissues, and to shield the drug from being degraded.

- Targeted and site-specific drug delivery can be easily achieved
- Nanosponges exhibit high drug-loading capacities due to their porous structure. The drugs can be encapsuled within the cavities or absorbed onto the surface of the nanosponges. This property allows for efficient loading of both hydrophobic and hydrophilic drugs.
- Improved stability, increased elegance, and enhanced formulation flexibility.
- Nanosponge systems are non-irritating, non-mutagenic, non-allergic and non-toxic as they are made of biocompatible materials.
- A nanosponge provides continuous action up to 12 hours at the site of action I.e., extended release.
- It minimizes irritation on topical applications and it gives better tolerance which leads to improved patient compliance.
- Allows incorporation of immiscible liquids which improves material processing. Liquid can be converted to powders.
- The formulations are stable over a wide range of pH (1-11) and temperature (up to 150°C).
- These are self-sterilizing as their average pore size is 0.25 µm where bacteria cannot penetrate.
- These are free flowing, highly compatible with a wide variety of ingredients and cost effective.
- They have better thermal, physical, and chemical stability.
- Nanosponge particles are soluble in water, so encapsulation can be done within the nanosponge, by the addition of chemicals called an adjuvant reagent. Also the porous structure allows easy encapsulation of drug substances and entraps them for sustained release at the site of action.

The polyesters and cross-linking peptides in nanosponges have relatively simple chemistry, which adds to their engineering potential when compared to other nanoscale drug delivery methods. Nanosponges may be dissolved in water without experiencing any chemical breakdown. Instead, they use water as a carrier fluid after mixing with it. In addition to masking off-putting tastes, they may also be used to solidify liquids. The nanosponge is able to selectively bind to the target site thanks to the chemical linkers.

Nanosponges have a solid structure. They've been shown to be safe for use in both the oral and invasive administration of medications. As a result of their diminutive size, nanosponges may be administered through the respiratory system and the circulatory system. The complexes may be formulated into capsules and tablets by dispersing them in a matrix containing excipients, diluents, lubricants, and anti-caking agents. The compound is readily portable in sterile water, saline, or other aqueous solutions for intravenous or intramuscular injection. They are easily incorporated into hydrogels for topical administration.

3.2 Merits of Topical delivery using Nanosponge:

Since nanosponges have a diameter of less than 1µm, they are superior to microsponges, which have a diameter of 10-25µm and a void size of about 5-300µm. They are capable of transporting hydrophilic and lipophilic materials. Additionally, they have the ability to make things more water soluble. Without causing patients any discomfort, high efficacy and regulated distribution are accomplished. When combined with cross-linkers, nanosponges are more likely to adhere to their intended targets. The chemistry of crosslinkers and polymers does not provide many obstacles for preparing nanosponges, so it can certainly be extended to commercial levels. Washing and stripping with mildly inert gases, eco-friendly solvents, modest heating, or a change in ionic/pH value are just some of the simple procedures that can be used to regenerate them [54].

3.3 Demerits of Topical delivery using Nanosponge [55]:

1. Nanosponges can include only minute molecules, limiting its use from the wide domain of antifungal drugs.
2. The degree of crystallisation has an effect on the drug-loading capacity. The drug loading capability of crystalline and paracrystalline nanosponges was found to be distinct in the case of cafadroxil Nanosponge.

4.1 Factors to be concerned for nanosponge dose calculation [56]: -

Physicochemical	Pharmacokinetic	Biological
Solubility	Half life	Site of application
Crystallinity	Total body clearance	Skin toxicity
Molecular weight	Peak plasma concentration	Skin metabolism
Polarity	Volume of distribution	Allergic reaction
Melting point	Bioavailability	Skin barrier properties

4.2 Factors influencing nanosponge formation

Type of polymer [9]

The type of polymer utilised can affect both the development and performance of Nanosponges. For complexation to occur, it is necessary that the nanosponge's cavity be large enough to hold the target drug molecule.

Type of drugs [57]

To be complexed with nanosponges, drug molecules must possess features such as:

- Molecular weight of drug should be in the range of 100-400 Da.
- Drug molecule consists of less than 5 condensed rings
- Solubility in water should be less that 10mg/ml (favourably a BCS Class II drug)
- Melting point of the drug substance should be less than 250°C.

Temperature [58]

Changes in temperature can impact the degree of drug-nanosponge complexation. Generally, an increase in temperature diminishes the magnitude of the apparent stability constant of the drug/nanosponge complex. This can be explained by the decrease in drug/nanosponge contact forces, such as van-der Waal forces and hydrophobic forces, when the temperature increases.

Method of preparation [59]

Complexation between the drug and the nanosponge may be modified by how the drug is loaded onto the nanosponge. Despite the fact that the success of a method depends on the nature of the drug and polymer, freeze drying has been proven to be the most effective way for drug complexation in many instances.

Degree of substitution

The kind, number, and location of the substituent on the parent molecule can significantly impact the nanosponge's complexation capability.

4.3 Factors affecting drug release from nanosponge [60]

There are several factors that can affect drug release from nanosponges. These include:

1. The size and shape of the nanosponges: The size and shape of the nanosponges can influence their ability to release the drug they are carrying. For example, smaller nanosponges may be more efficient at releasing the drug, as they have a higher surface area-to-volume ratio and therefore more surface area for drug release.

2. The type of drug being delivered: The properties of the drug being delivered can also affect its release from the nanosponges. For example, drugs with low solubility may be more difficult to release from the nanosponges than drugs with higher solubility.

3. The nature of the nanosponge material: The material used to make the nanosponges can also affect drug release. For example, some materials may be more porous and therefore more efficient at releasing the drug.

4. The pH and temperature of the application site: The pH and temperature of the skin can also affect drug release from the nanosponges. For example, a lower pH or higher temperature may increase drug release, while a higher pH or lower temperature may decrease drug release.

5. The duration of drug release: The length of time over which the drug is released from the nanosponges can also be a factor. Some nanosponges may release the drug more slowly over a longer period of time, while others may release the drug more quickly over a shorter period of time.
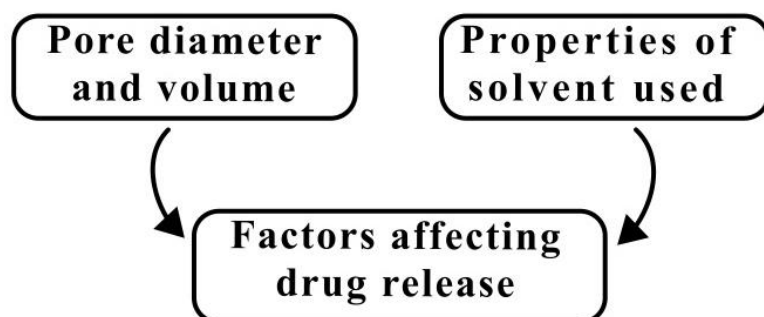

Figure 5: Overall factors affecting drug release from nanosponge.

5.1 Composition and structure of Nanosponges [16]:

Nanosponges are intricate structures formed from long linear molecules that have been folded via cross-linking into a roughly spherical shape, resembling a protein. The three primary parts of nanosponges are polymer, crosslinker and drug.

1. Polymer

Both the formation and the functionality of Nano sponges are susceptible to the polymer used. The functional groups and active groups that will be substituted affect the polymer's capacity for cross-linking. The polymer chosen for controlled medication delivery must be compatible with the drug it will encapsulate. The polymer must possess the ability to bind to the targeted ligands.

2. Crosslinker

Cross-linking agents are chosen based on the structure of the polymer and the drug that is to be encapsulated.

Polymers used for synthesis of Nanosponges are listed in Table 1; Table 2 contains a list of crosslinkers and their uses in Nanosponge synthesis.
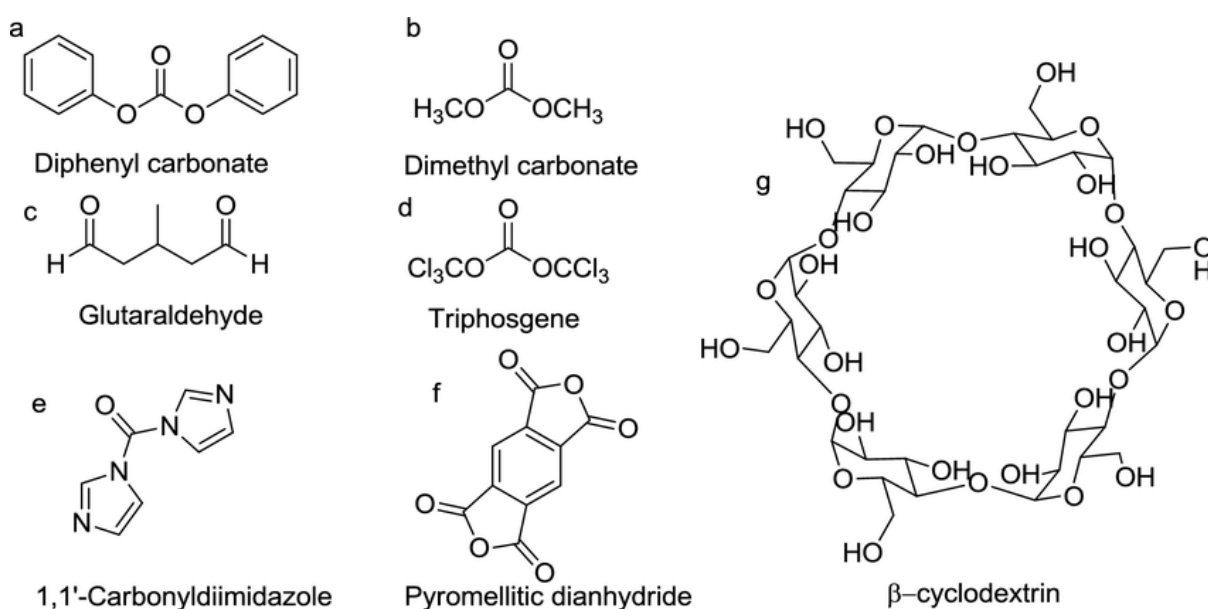

Figure 6: Various cross-linkers (a–f) and β-cyclodextrin (g) used in fabrication of cyclodextrin nanosponges.

Table 1: List of polymers used for synthesis of nanosponge

Polymers	Use	Particle Size
Cyclodextrins and their derivatives	Solubility enhancement, cytotoxicity, hemolytic activity	Below 500 nm
Titanium dioxide	Coating of polystyrene microspheres	100-130 nm
B-Cyclodextrin and copolyvidonum	Saturation solubility study	Below 500 nm
Ethyl cellulose and Polyvinyl alcohol	Irritation study	230-470 nm
Poly (Valerolactone-allylvalerolactone Oxepanedione) and poly (Valerolactone-allylvalerolactone)	Drug release study	Not reported

Table 2: List of crosslinkers used for synthesis of nanosponge

Crosslinker	Uses
Diphenyl carbonate	Solubility enhancement, hemolytic activity, cytotoxicity
Diaryl carbonates	Solubility enhancement, Bioavailability enhancement and drug release studies
Diisocyanates	Saturation solubility studies
Pyromellitic anhydride	Gelling agent
Carbonyl diimidazoles	Cytotoxicity
2,2-Bisacrylamidoacetic acid or polyamide amine	Bovine serum albumin (BSA)
Dichloromethane	Solubility enhancement

3. Drug substance

Nanosponges are most suited for drug molecules with a molecular weight between 100 and 400 Da, a solubility of less than 10mg/ml in water, and a melting point of less than 250°C. Drugs from many different classes, such as antibiotics, anticoagulants, anticonvulsants, antidiabetic, antiepileptic, antifungal, antihistamine, antihypertensive, cardiac, antioxidant, anthelmintic, diuretics, antipsychotic, NSAID, steroid, etc., can be utilised. Table 3 includes a comprehensive list of the drug substances formulated as nanosponges.

Table 3: List of BCS class II drugs used in nanosponge formulation

Anti-anxiety drugs	Lorazepam
Antiarrhythmic agents	Amiodarone hydrochloride
Antibiotics	Azithromycin, Ciprofloxacin, Erythromycin, Ofloxacin, Sulfamethoxazole
Anti-cancer	Camptothecin, Docetaxel, Etoposide, Exemestane, Flutamide, Irinotecan, Paclitaxel, Raloxifene, Tamoxifen, Topotecan
Anticoagulants	Warfarin
Anticonvulsants	Carbamazepine, Felbamate, Oxcarbazepine, Primidone
Antidiabetic and Antihyperlipidemic drugs	Atorvastatin, Fenofibrate, Glibenclamide, Lovastatin, Troglitazone
Antiepileptic drugs	Phenytoin
Anti-fungal	Econazole nitrate, Griseofulvin, Itraconazole, Ketoconazole, Voriconazole
Anti-histamine	Terfenadine
Antihypertensives	Felodipine
Antioxidants	Resveratrol
Antipsychotics	Chlorpromazine hydrochloride, Tiapride
Antiretroviral	Indinavir, Nelfinavir, Ritonavir, Saquinavir
Antiulcer	Lansoprazole, Omeprazole
Anti-helminthics	Albendazole, Mebendazole, Praziquantel
Cardiac drugs	Carvedilol, Digoxin
Diuretics	Chlorthalidone, Spironolactone
Gastroprokinetic agents	Cisapride
Immunosuppressants	Cyclosporine, Sirolimus, Tacrolimus
NSAIDs	Dapsone, Diclofenac, Diflunisal, Etodolac, Etoricoxib, Flurbiprofen, Ibuprofen, Indomethacin, Ketoprofen, Mefenamic acid, Naproxen, Nimesulide, Oxaprozin
Steroids	Danazol, Dexamethasone
Miscellaneous	Atovaquone, Melarsoprol, Phenazopyridine, Ziprasidone

6.1 Cyclodextrin based Nanosponges

$$H-O-\beta-CD-OH + X-CO-X \rightarrow -(\beta-CD-OCOO-\beta-CD-OCOO)\,n-$$
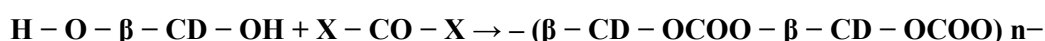
(Where X=chlorine, imidazolyl, or a –OR group in which R is C1-C4 alkyl and n is an integer.)

Cyclodextrin-based nanosponges are made up of non-reducing oligosaccharides that are cyclic and toroidal cone-shaped, and whose arrangement stands in for an outer torus area (hydrophilic) and an interior lipophilic region. It is only the lipophilic cavity of native cyclodextrins that can generate inclusion compounds; hydrophilic molecules or those with a higher molecular weight are never involved. Improvements in inclusion constants above 103 are quite uncommon. Cross-linked polystyrene cyclodextrins are insoluble in water and most organic solvents, are non-toxic, porous, and can withstand temperatures beyond 300 degrees Celsius, making them ideal for use in the fabrication of nanosponges, which can then be used to encapsulate and transport drug substances. Nanosponges based on CDs have been shown to form inclusion and non-inclusion complexes with various hydrophobic and hydrophilic molecules, and the resulting derivatives have been found to improve the native CDs' ability to perform their intended function. It was discovered that CDs had a strong ability to form complexes of drug conjugates with a wide variety of chemicals, and therefore it was chosen for use as a drug carrier. Nanosponges derived from β-cyclodextrins have the advantages of being more stable and complexing than those derived from natural sources like α and γ [61].

In the past, CD-based Nanosponges were utilised for water purification [62]. They have recently been discovered to be effective solubilizing or Nanocarrier agents in Drug delivery systems. Approximately 30% of CD products have made it to global markets, and its derivatives have been utilised to improve the capacity of nanoparticles, nanosponges, microsponges, and liposomes [63]. They can also create intricate pathways (called nanochannels) for drugs to transit. In addition to increased output and reduced production costs, they also facilitate enhanced output. β -cyclodextrin was shown to be the most sought-after component for making Nanosponges. Multiple instances of this reaction between CDs and cross-linkers of carbonyl or dicarboxylate compounds have occurred [64]. The formation of nanosponges from cyclodextrin and carbonyl compounds is depicted in the accompanying figure 7.
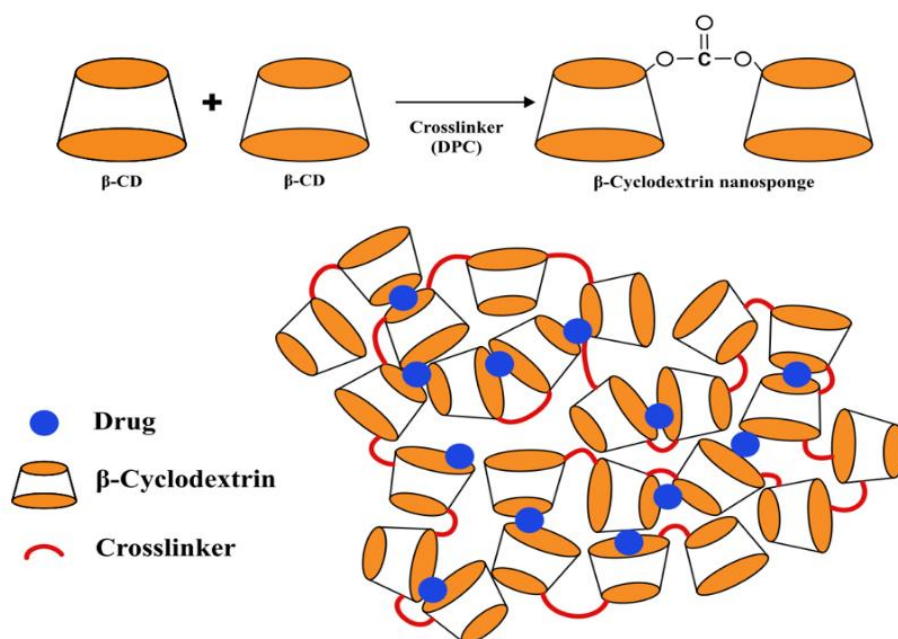
Figure 7: Diphenyl carbonate based cyclodextrin nanosponge

6.2 Marketed preparations of cyclodextrin based nanosponges

A variety of drugs ranging from NSAIDs to anti-cancer and anti-viral have been incorporated with cyclodextrin based nanosponges due to their unique crosslinking nature. All such drugs available in market have been summarized in table 4.

Table 4: List of marketed cyclodextrin based nanosponges

Drugs	Nanosponge vehicle	Therapeutic Uses	Reference
Prostaglandin E1	α-cyclodextrin	Occlusive peripheral arterial disease	65
Piroxicam	β-cyclodextrin	Analgesic	22
Quercitin, Curcumin	β-cyclodextrin,DPC	Anti-cancer	4,66
Erlotinib	β-cyclodextrin, CDI	Anti-cancer	29
Acyclovir	β-cyclodextrin, CDI	Anti-viral	67
Camptothecin	β-cyclodextrin, DPC	Anti-cancer	68
Bovine serum albumin	β-cyclodextrin, 2,2-bisacodyl amino acetic acid	Protein supplement	15
Resveratrol	β-cyclodextrin, CDI	Anti-hyperlipidemia, Treatment of gonorrhea	26
Meloxicam	β-cyclodextrin, PMDA, DCM	NSAID	69
Dexamethasone	β-cyclodextrin, DPC	Anti-inflammatory, Brain tumor	70
Tamoxifen	β-cyclodextrin, CDI	Anti-cancer	27

Paclitaxel, Docetaxel	β-cyclodextrin	Breast cancer	21
Raloxifene	β-cyclodextrin	Invasive Breast cancer	71
Itraconazole	β-cyclodextrin, copolyvidonum	Anti-fungal	72

6.3 Patent report on β-cyclodextrin nanosponges [9]

Sl no.	Patent/App no. Year of issue	Applicant	Title
1.	WO2003041095A1 (2003)	Alberto Bocanegra Diaz	Process of composites preparation between particulate mateirals and cyclodextrin derivatives.
2.	WO2003085002A1 (2003)	Sea Marconi Technologies Diw	Cross-linked polymers based on cyclodextrin for removing polluting agents
3.	DE10008508A1 (2001)	Bayer Ag	New polycarbonate with cyclodextrin units, used ex: as a chromatographic stationary phase, catalyst especially for removing organic compunds from water
4.	EP0502194A1 (1992)	Toppan Printings co. Ltd.	Cyclodextrin polymer and cyclodextrin film formed

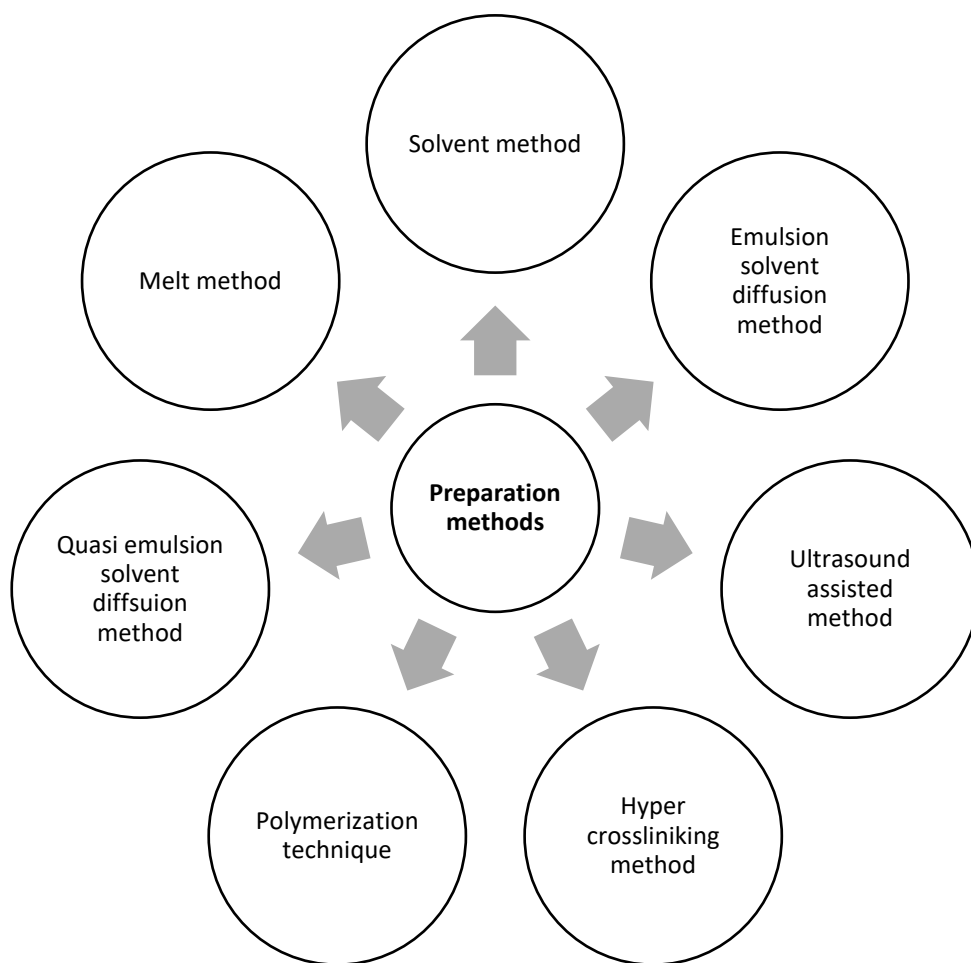## 7.1 Methods of preparing nanosponge [73]

Figure 8: Summarization of various preparation technologies of nanosponge

A. Solvent method

Mix the polymer with a suitable solvent, particularly with a polar aprotic solvent such as dimethyl formamide, di methyl sulfoxide. Then add this mixture to excess quantity of the cross-linker, preferably in cross linker/polymer molar ratio of 4:16. Carry out the reaction at temperature ranging from 10°C to the reflux temperature of the solvent, for a period of 1 to 48hrs. Preferred cross linkers are carbonyl compounds (di methyl carbonate and carbonyl di imidazole. Dry the product under vacuum and grind in a mechanical mill to obtain white homogeneous powder mass which is the nanosponge.
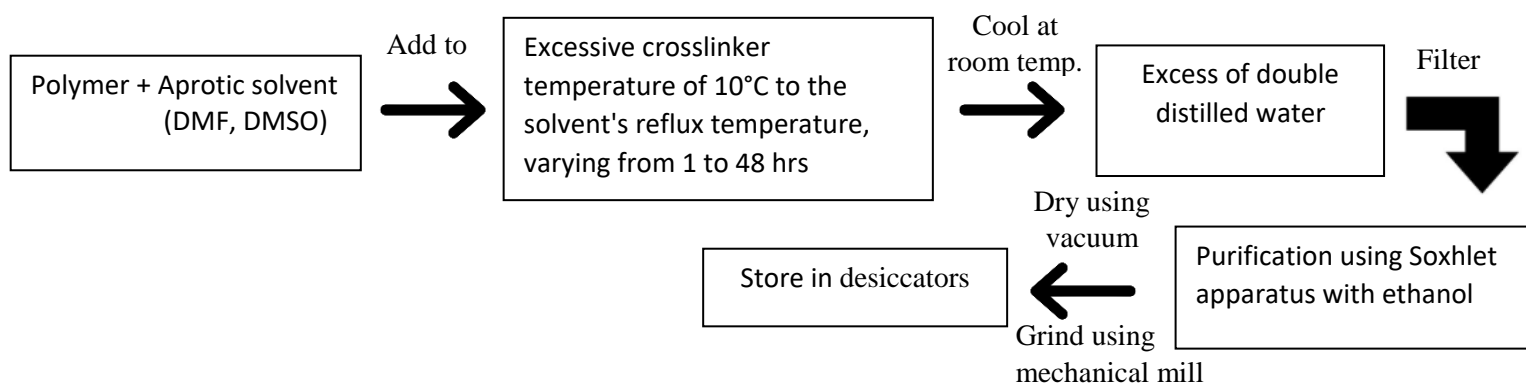
Figure 9: Flowchart depicting solvent method utilized for fabricating nanosponge.

B. Emulsion solvent diffusion method

Organic and aqueous phases are used in this method. The aqueous phase consists of the PVA and organic phase include the drug and polymer. The drug and polymer are mixed with the organic solvents (like dichloromethane) and it is added slowly to the aqueous phase and stirred for 2 hours or more. The Nano sponges are collected, filtered, washed and dried at room temperature or dried in an oven at 40°C for 24 hrs. Finally, products were stored in the vacuum desiccator to ensure the removal of residual solvent.
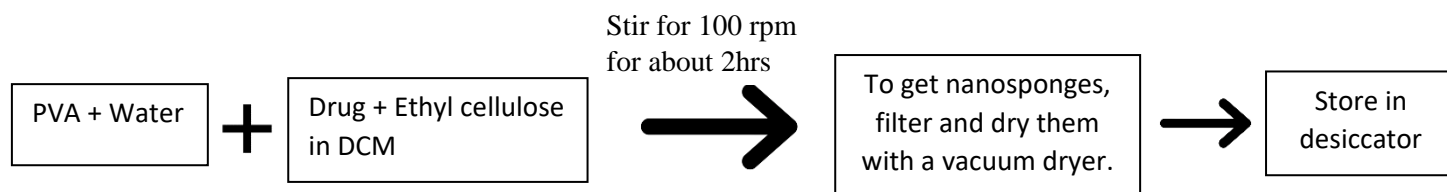

Figure 10: Flowchart depicting emulsion solvent diffusion method for preparing nanosponge.

C. Ultrasound assisted method

Mix the polymer and the cross-linker in a particular molar ratio in a flask. Place the flask in an ultrasound bath filled with water and heat it to 90°C. Sonicated the mixture for 5hrs. Then allow the mixture to cool and break the product roughly. Wash the product with water to remove the unreacted polymer and subsequently purify by prolonged soxhlet extraction with ethanol. Dry the obtained product under vacuum and store at 25°C until further use. The Nano sponges obtained by this method will be spherical and uniform in size.
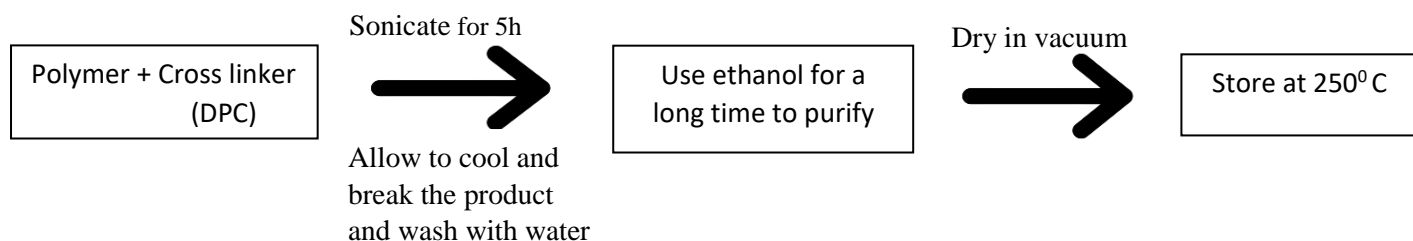
Sonicate for 5h

| Polymer + Cross linker (DPC) | → | Use ethanol for a long time to purify | → | Store at 250^0 C |

Allow to cool and break the product and wash with water

Dry in vacuum

Figure 11: Ultrasound assisted synthesis method for nanosponge.

D. Hyper crosslinking method

Nano sponge has been developed recently by hyper cross linked cyclodextrin polymers with Nano structured to form 3-dimensional networks. Due to this 3-d network the Nano sponge formed may be of a roughly spherical structure about the size of a protein having channels and pores in the internal part. They are obtained by reacting cyclodextrin with a cross-linker such as di isocianates, diaryl carbonates, Dimethyl carbonate, diphenyl carbonate, and carbonyl di-imidazoles, carboxylic acid dianhydrides and 2, 2-Bis (acrylamido) acetic acid. The surface charge density, porosity and pore sizes of sponges can be controlled to attach different molecules. Nano sponge with low cross linking gives a fast drug release. They are used in the enhancement of aqueous solubility of poorly-water soluble drugs mainly BCS class II drugs.
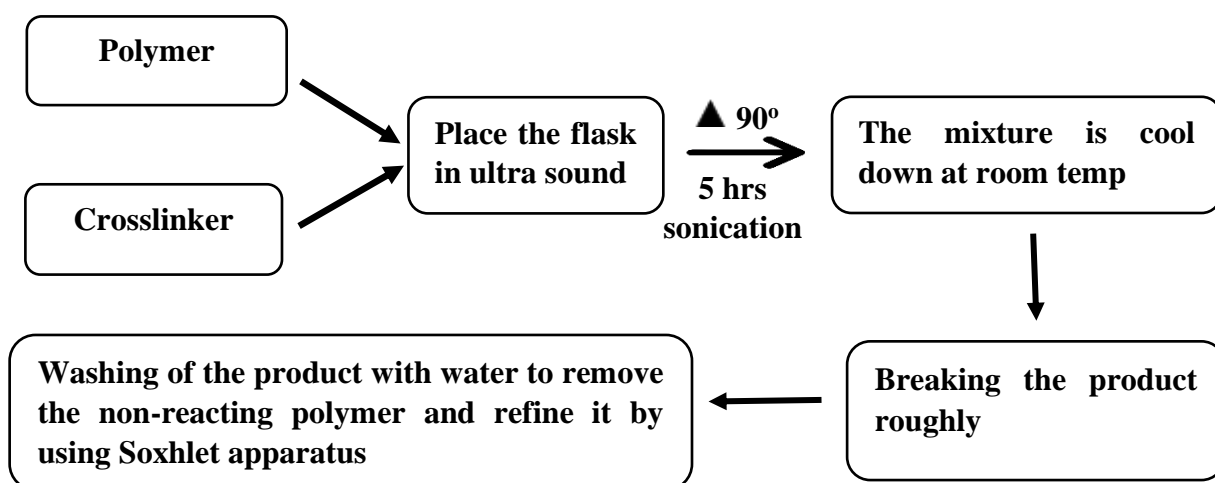

Figure 12: Flowchart depicting hypercrosslinking technique used in fabrication of cyclodextrin nanosponge.

E. Polymerization technique

The non-polar drug is first dissolved in the monomer, and then the aqueous phase (which typically includes surfactant and dispersant to aid in suspension) is added. Once the suspension with the desired-sized droplets has been created, polymerization can be affected by activating the monomers through catalysis or elevated temperature. The polymerization procedure creates a reservoir-style system with porous openings on the surface creating nanosponges.

F. Quasi-emulsion solvent method

It is a modified emulsion solvent diffusion type technique. Nanosponges are made by combining several polymers. The inner phase was prepared by dissolving Eudragit RS100 in a suitable solvent and then adding the drug, which was dissolved using ultra-sonication at 35°C. The inner phase was poured into the PVA solution in water which was the external phase. After 60 minutes of stirring, the nanosponges were extracted by filtering the liquid. The Nano sponges were dried in an air-heated oven at 40°C for 12hrs.
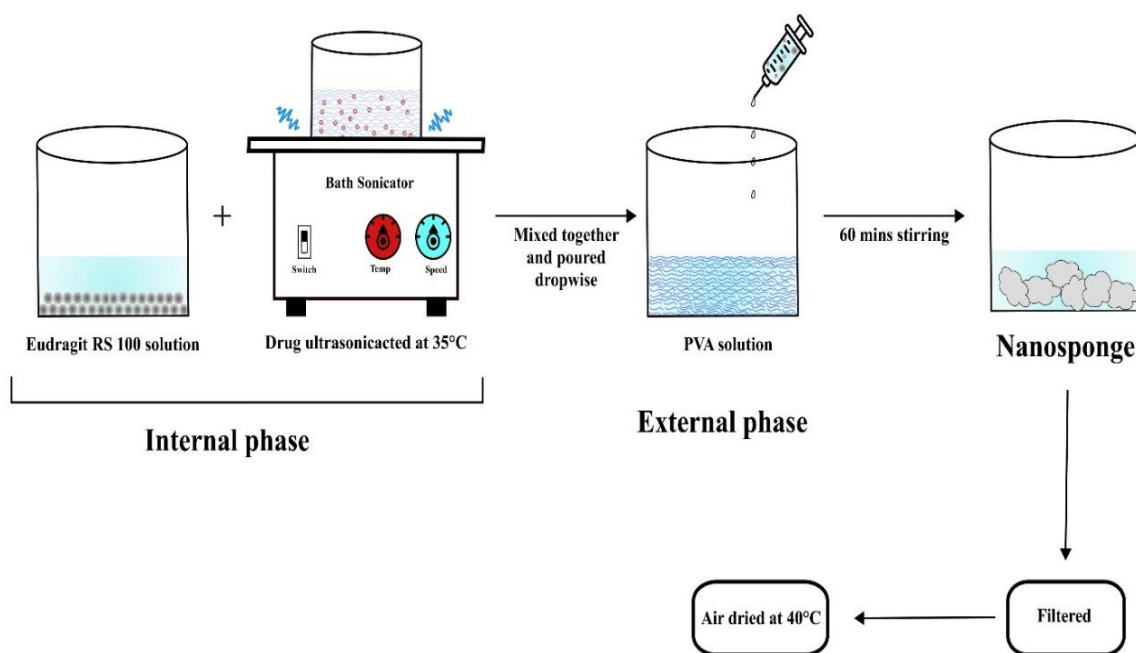

Figure 13: Pictorial representation of quasi-emulsion solvent method.

G. Melt method

In this method, cross linkers and polymers are heated to up to 100°C while the other materials are homogenised using magnetic stirring over the course of 5 hours. This solution is then cooled and washed continuously to remove any remaining unreacted.
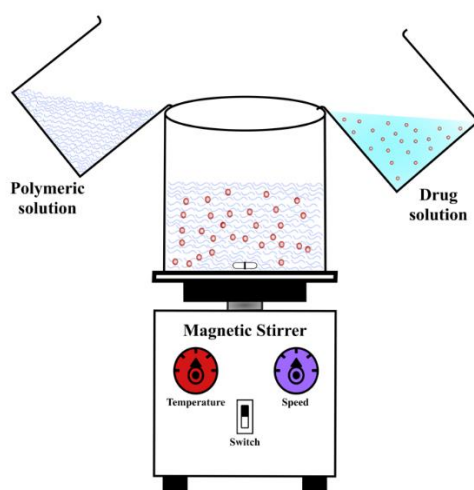
Figure 14: Melt technique for preparing nanosponge.

7.2 Loading of drugs into nanosponge

Drug loading in nanosponges can be achieved by a few simple steps:

Sonicate while suspended in an aqueous solution to break up any clumps. → Centrifugation yields the colloidal fraction. → Freeze-drying is used to remove the supernatant layer.

Centrifugation is used to separate the undissolved drug ← For a specified period of time, constant stirring is maintained to produce complex. ← Excess drug is dispersed in the aqueous solution.

Solvent evaporation or freeze drying → Solid crystals of Nanosponge are produced

Drugs can be either passively or actively (figure 15) loaded into nanosponges. Ideally, the mean particle size of the nanosponge used in the drug administration would be less than 500 nm, and this might be achieved through pre-treatment. Nanosponges are sonicated in water to break up any aggregates that could be present, and the resulting suspension is centrifuged to separate out the colloidal fraction. After removing the supernatant liquid, the sample is dried using a freeze dryer. Nanosponges' complexation with drugs is heavily dependent on their crystalline structure. Comparing crystalline and paracrystalline Nanosponges, the latter were shown to have higher loading capabilities. Crystalline Nanosponges display drug loading more clearly [74].

Apart from traditional approaches, one can also go for physical adsorption where the drug molecules are physically absorbed or attached to the surface of the nanosponges through weak interactions such as van der Waals forces, hydrophobic interactions, or hydrogen bonding. Electrostatic interactions where nanosponges can be functionalized with charged groups that can interact with oppositely charged drug molecules (for drugs with ionizable functionable groups). Supercritical carbon dioxide (SC-CO2) is also sometimes used as a solvent to load drugs into nanosponges [75].
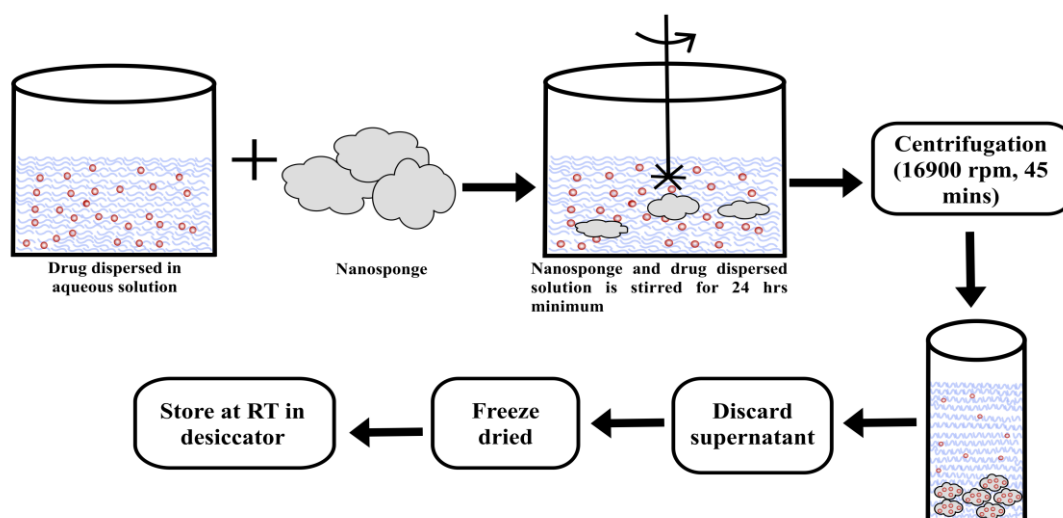

Figure 15: Active loading of drug in nanosponge (adapted from Ref no. 75)

7.3 Mechanism of action of topically delivered nanosponge

Topical delivery of nanosponges involves the application of a formulation containing nanosponges to the surface of the skin. Nanosponges have a porous structure [76]; thus, the active ingredient is supplied to vehicles in an enclosed form. The psychoactive chemical is free to travel in either direction from the particles into the vehicle until equilibrium is attained. When the product is used, the active ingredient in the vehicle will become unsaturated, which will throw off the balance. The nanosponge active ingredient is carried by the vehicles to the skin, where it lingers until the vehicle either dries out or is absorbed. Also, after drying, nanosponge particles persist on the surface of the skin and act on the fungal cell wall of the fungi on the skin (figure 16). This will ensure continuous release of the active ingredient, thereby providing a prolonged release of the medication [77].

The nanosponges are also designed to be biocompatible, meaning they do not cause any harmful effects on the skin or body. They are typically made of biodegradable materials, such as polysaccharides, that are naturally broken down by the body after they have served their purpose.
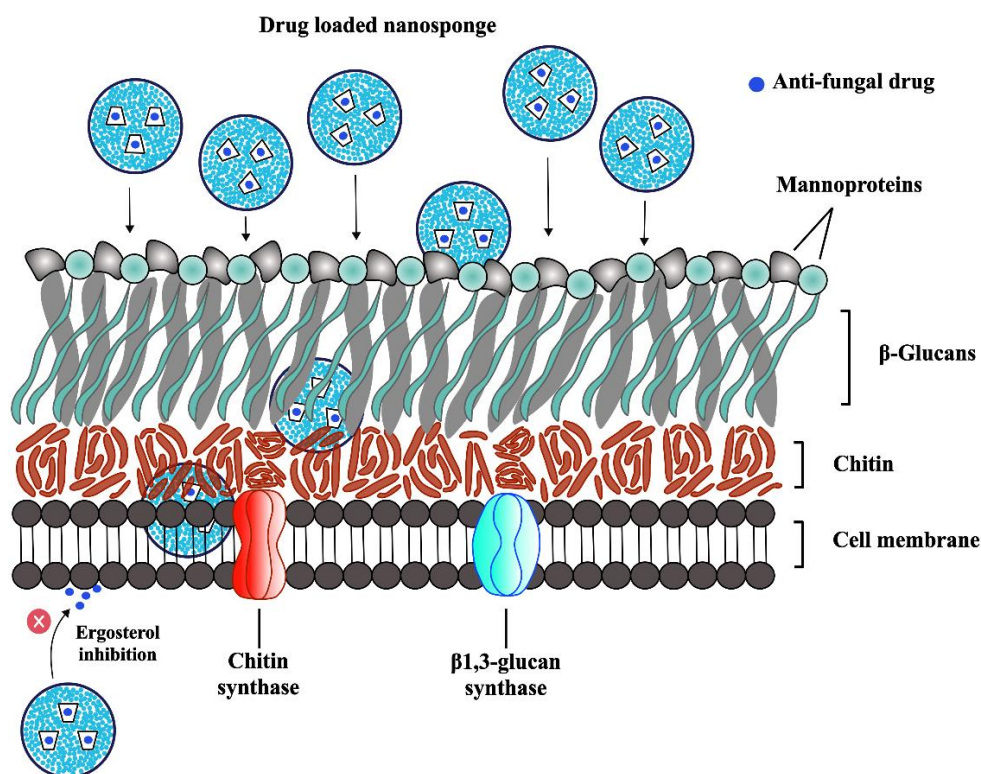

Figure 16: Nanosponge action on fungal cell wall after topical delivery on skin infected with Fungus (adapted from Ref no. 4).

In topical delivery, once the product containing nanosponge with drug is applied to the skin, the drug which is already present in the vehicle will be absorbed into the skin. This will decrease the concentration of drug in the vehicle until it reaches equilibrium. At that time flow of the drug from the sponge particle into the vehicle will starts into the skin and vehicle is either dried or absorbed. This will provides prolonged release of drug to the stratum corneum of the skin [78]. There are several steps involved in the mechanism of action of topical delivery of nanosponges. First, the nanosponges are applied to the skin, where they come into contact with the outer layers of the skin (the epidermis and dermis). The nanosponges are designed to be small enough to penetrate into the skin and reach the site of action. Once the nanosponges are in contact with the skin, they enter the cell mainly by endocytosis and begin to release the drug they are carrying. The drug is released through a process called diffusion, which involves the movement of molecules from an area of high concentration to an area of low concentration. The drug diffuses out of the nanosponges and into the surrounding skin tissue, where it can then act on its target cells, as depicted in figure 17 [79].
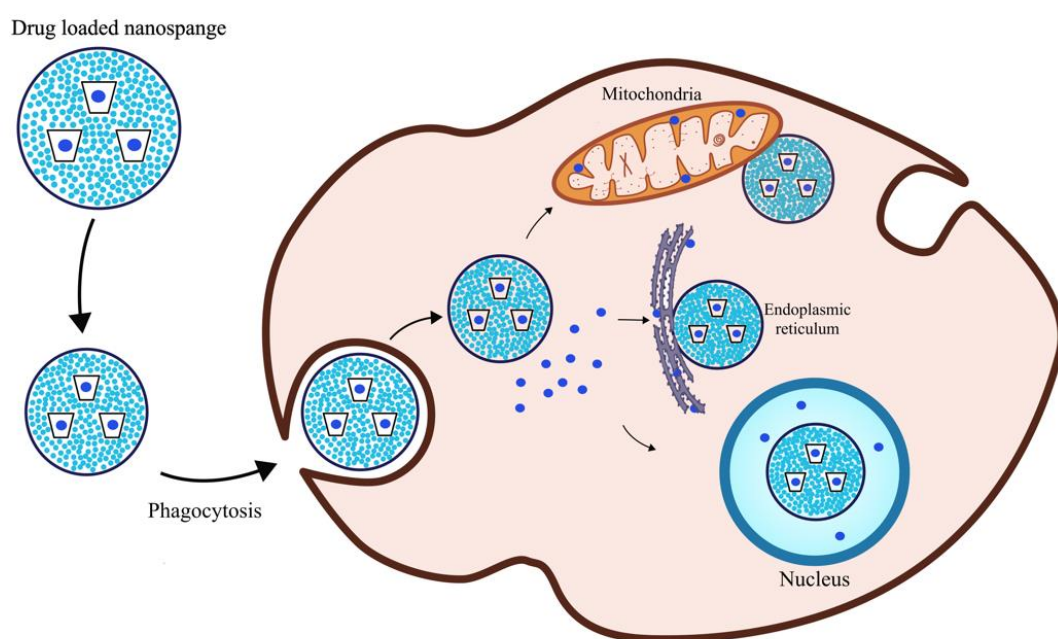

Figure 17: Nanosponge cell biology (adapted from Ref no. 73).

8.1 Characterization of nanosponge

The assessment of the formation of nanosponges and their complete characterization is not a straightforward assignment and requires employment of various sophisticated analytical methods in order to explore their features. Characterizing nanosponges involves various techniques to evaluate their physical, chemical, and biological properties. Each test gives an idea of the size, shape, morphology, crystallinity, encapsulation etc.

A. Loading efficiency and Production yield [80]

The loading efficiency of nanosponge complexes can be determined by dissolving them in a suitable solvent. Sonication is performed afterwards to break the complex and the resulting solution is diluted suitably for analysis by UV spectrophotometer & HPLC methods. The production yield of nanosponges can be determined by calculating accurately the initial weight of raw materials (theoretical weight) and dividing it with the production yield obtained (practical weight).

B. Microscopy studies [81]

Scanning electron microscopy (SEM) and Transmission electron microscopy (TEM) can be used to study the microscopic aspects of the drug, nanosponges and the product (drug/nanosponge complex). The difference in crystallization state of the raw materials and the product seen under electron microscope indicates the formation of the inclusion complexes, even if there is a clear difference in crystallization state of the raw material and the product obtained by co-precipitation.

C. Particle size and Polydispersity [82]

The particle size can be determined by dynamic light scattering using 90 Plus particle sizer equipped with MAS OPTION particle sizing software. From this the mean diameter and polydispersity index can be determined.

The polydispersity index (PDI) can also be measured from dynamic light scattering instruments. PDI is an index of width or spread or variation within the particle size distribution. Monodisperse samples have a lower PDI value; whereas higher value of PDI indicates a wider particle size distribution and the polydisperse nature of the sample.

D. Zeta potential [82]

Scientifically, the zeta potential (ZP) is used for measuring the electrokinetic potential of the colloidal systems. Simply, ZP is the potential difference between the stationary layer of fluid to dispersion medium and dispersed particle. In other words, it is applicable to quantify the magnitude of the charge. It can affect the phagocytosis of the nanoformulations as well as pharmacokinetic profile of the nanosystems in the body. To evaluate the charge conditions of the nanoparticles, the zeta potential should be measured by dispersing them in the original dispersion medium or distilled water. The experimental techniques for the determination of the ZP are microelectrophoresis and electrophoretic light scattering. This technique has been widely used in NS literature by various research groups.

E. Fourier Transform Infrared (FTIR) analysis [81]

Fourier transform infrared analysis was conducted to verify the possibility of interaction of chemical bonds between drug and polymer. Samples were scanned in the range from 400-4000cm^{-1} and carbon black reference. The detector was purged carefully by clean dry helium gas to increase the signal level and reduce moisture.

During the cross-linking, the vibrational modes of the polymers, cross-linkers and active molecule gets shifted from original positions leading to broadening or disappearance of the characteristic bands of the active moiety, cross-linker, and polymer. Fluctuation in peak intensity and displacement in their wave number may also take place indicating interaction of polymers either with itself or with cross-linker. The restriction of the stretching vibration in these molecules induced by cross-linking between polymer, cross-linker and drug, may lead to these changes. Additionally, inter atomic bond weakening takes place upon cross-linking and/or complexation in NS. Besides significant selectivity and sensitivity, other chief advantages of this analytical technique include affordable cost, extensive diffusion, rapid and easy acquisition time of spectrum.

F. Thin Layer Chromatography [83]

In thin layer chromatography, the Rf value of a drug molecule diminishes to considerable extent and those helps in identifying the complex formation between the drug and nanosponge. Inclusion complexation between guest and host molecule is a reversible process. Consequently, the complex may separate completely in guest and hst molecules during the chromatographic process and only the spots of the guest and host molecules are found on the TLC-plate.

G. Infra-Red spectroscopy [83]

Infra-red spectroscopy is used to estimate the interaction between nanosponge and the drug molecules in the solid state. Nanosponge bands often change only slightly upon complex formation and if the fraction of the guest molecules encapsulated in the complex is less than 25%, bands which could be assigned to the included part of the guest molecules are easily masked by the bands of the spectrum of nanosponges. The technique is not generally suitable to detect the inclusion complex and is a little bit less clarifying.

The application of IR-spectroscopy is limited to the drugs having some characteristic bands, such as carbonyl or sulfonyl groups. Infrared spectral studies give information regarding the involvement of hydrogen in various functional groups. This generally shifts the absorbance bands to the lower frequency, increases the intensity and widens the bands caused by stretching vibrations of the group involved in the formation of the hydrogen bonds. Hydrogen bond at the hydroxyl group causes the largest shift of the stretching vibration band.

H. Thermo-analytical methods [84]

Thermo-analytical methods determine whether the drug substance undergoes some change before the thermal degradation of the nanosponge. The change of the drug substance may be melting, evaporation, decomposition, oxidation or polymorphic transmission. The change of the drug substance indicates the complex formation. The thermogram obtained by DTA and DSC can be observed for broadening, shifting and appearance of new peaks or disappearance of certain peaks. Changes in the weight loss also can provide supporting evidence in the formation of inclusion complexes. Drug-excipient compatibility can also be determined by DSC. For DSC approximately 5mg samples can be accurately weighed into aluminium pans and sealed and can be run at a heating rate of 15°C/min over a temp range of 20-450°C

I. X-ray Diffraction techniques [81]

Powder X-ray diffractiometry can be used to detect inclusion complexation in the solid state. When the drug molecule is liquid since liquid have no diffraction pattern of their own, then the diffraction pattern of a newly formed substance clearly differs from that of uncomplexed nanosponge. This difference of diffraction pattern indicates the complex formation. When the drug compound is a solid substance, a comparison has to be made between the diffractogram of the assumed complex and that of the mechanical mixture of the drug and polymer molecules.

A diffraction pattern of a physical mixture is often the sum of those of each component, while the diffraction pattern of complexes are apparently different from each constituent and lead to a "new" solid phase with different diffractograms. Diffraction peaks for a mixture of compounds are useful in determining the chemical composition and complex formation. The complex formation of drug with nanosponges alters the diffraction patterns and also changes the crystalline nature of the drug. The complex formation leads to the sharpening of the existing peaks, appearance of few new peaks and shifting of certain peaks.

Single crystal X-ray structure analysis is used to determine the detailed inclusion structure and mode of interaction. The interaction between the host and guest molecules can be identified and the precise geometrical relationship can be established. This information obtained during the analysis leads to know about the formation of inclusion complexes.

J. Characterization of pore structure [85]

Pore volume and diameter are vital in controlling the intensity and duration of effectiveness of the active ingredient. Pore diameter also affects the migration of active ingredients from nanosponge into the vehicle in which the material is dispersed. Mercury intrusion porosimetry can be employed to study effect of pore diameter and volume with rate of drug release from nanosponges. Porosity parameters include intrusion-extrusion isotherms. Pore size distribution, total pore surface area, average pore diameters, shape and morphology of the pores, bulk and apparent density can be determined by using mercury intrusion porosimetry. Instrumental intrusion volume can be plotted against pore diameters that represented pore size distributions. The pore diameter of nanosponges can be calculated by using Washburn equation:

$$D = \frac{-4\gamma \cos\theta}{P}$$

Where, D is the pore diameter (μm); γ the surface tension of mercury (485 dyne cm^{-1}); θ the contact angle (130°); and P is pressure.

K. Polymer/Monomer composition [85]

Factors such as particle size, drug loading and polymer composition govern the drug release from nanosponges. Polymer composition of the nanosponge drug delivery system can affect partition coefficient of the entrapped drug between the vehicle and the nanosponge system and hence have a direct influence on release rate of entrapped drug. Release of drug from nanosponge systems of different polymer compositions can be studied by plotting cumulative

% drug release against time. Release rate and total amount of drug released from the system composed of methyl methacrylate/ ethylene glycol dimethacrylate is slower than styrene/ divinyl benzene system. Selection of monomer is dictated both by characteristics of active ingredient ultimately to be entrapped and by the vehicle into which it will be dispersed. Polymers with varying electrical charges or degrees of hydrophobicity or lipophilicity may be prepared to provide flexibility in the release of active ingredients. Various monomer combinations will be screened for their suitability with the drugs by studying their drug release profiles.

L. *In-Vitro* drug release study [86]

The release of the drug from the optimized nanosponge formulation can be studied using multi-compartment rotating cell with dialysis membrane using Franz Diffusion cell with a diffusional area of $2.26cm^2$. The donor phase consists of drug-loaded nanosponge complex in distilled water. The receptor phase also contains the same medium. The receptor phase is withdrawn completely after fixed time intervlas, suitably diluted with distilled water and then analysed by UV spectrophotometer.

M. Drug release kinetics [86]

To investigate the mechanism of drug release from the nanosponge, the release date can be analysed using zero order, first order, Higuchi, Korsmeyer-Peppas, Hixon Crowell, Kopcha and Makoid-Banakar models. The data can be analysed using graph pad prism software. The software estimates the parameters of a non-linear function that provides the closest fit between experimental observations and non-linear function.

N. Resiliency [87]

Resiliency (viscoelastic properties) of nanosponges can be modified to produce beadlets that is softer or firmer according to the needs of the final formulation. Increased cross-linking tends to slow down the rate of release. Hence resiliency of nanosponges is studied and optimized as per the requirement by considering release as function of cross-linking with time.

8.2 Applications of nanosponge [73,111]

The nanoporous nature of nanosponges makes them useful transport medium for water-insoluble drugs and/or agents (BCS Class-II pharmaceuticals). These complexes can be used to improve the rate of medication dissolution, the solubility of drugs, the stability of drugs, to

conceal off-putting odours, and to solidify liquids. By loading the Nano sponges with solubility-sensitive medications, it is possible to successfully administer these medications. Nanosponges can be taken orally, intravenously, topically, or inhaled. For oral dosing, the complexes can be encapsulated or formulated into tablets by dispersing them in a matrix containing excipients, diluents, lubricants, and anti-caking agents [9]. Aqueous solutions such as sterile water, saline, or others can be used to transport the complex for parenteral delivery. They can be easily integrated into topical hydrogel for topical delivery. Table 5 gives possible application of nanosponges. Table 6 provides a comprehensive list of all plant extracts encapsulated as nanosponges against mycotoxigenic fungus. Figure 18 cites other various applications of nanosponge.

Table 5: Application of nanosponges with respect to their possible advantages

Sl. No.	Application	Advantages
1.	Sunscreens	Long lasting product efficacy, with improved protection against sunburns and sun related injuries even at elevated concentration and with reduced irritancy and sensitization
2.	Anti-acne Eg: Benzoyl peroxide	Maintained efficacy with decreased skin irritation and sensitization.
3.	Anti-inflammatory Eg: Hydrocortisone	Long lasting activity with reduction of skin allergic response and dermatoses.
4.	Antipruritics	Extended and improved activity.
5.	Skin depigmenting agents Eg: Hydroquinone	Improved stabilization against oxidation with improved efficacy and aesthetic appeal.
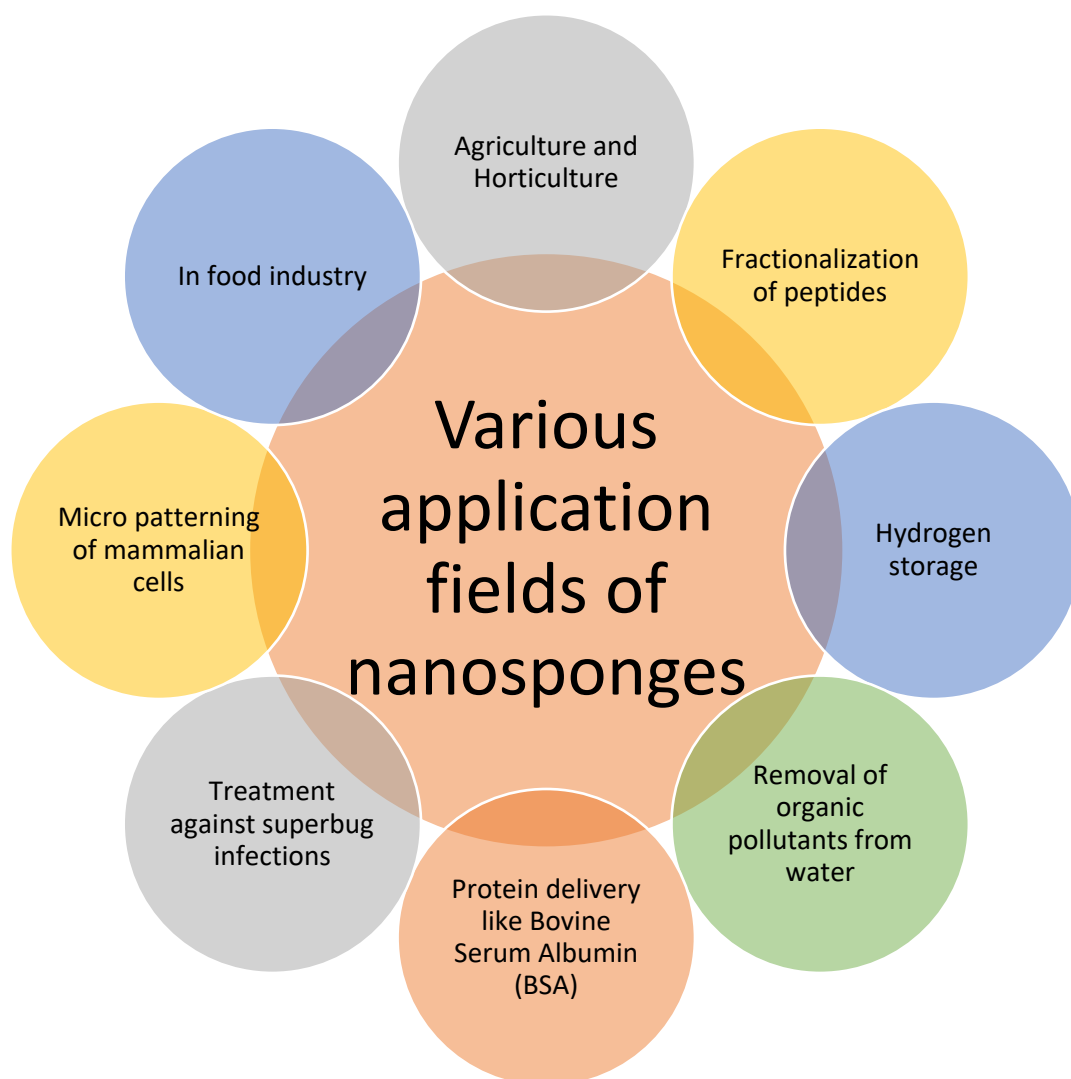
Figure 18: Versatile uses of nanosponges (adapted from ref no. 73)

1. Nanosponges for oral delivery

Drugs that aren't easily dissolved in water can benefit from being entrapped in the Nano sponge's pores and get administered orally. Nano size forms result in a greater surface area and a faster rate of solubilization. When formulated with Nanosponges, the solubilization efficiency of BCS class-II drugs is improved, and the dissolution rate is increased, leading to improved bioavailability.

2. Nanosponges for drug delivery

The nanoporous nature of nano sponges makes them useful transport medium for water-insoluble drugs and/or agents (BCS Class-II pharmaceuticals). These complexes can be used to improve the rate of medication dissolution, the solubility of drugs, the stability of drugs, to

conceal off-putting odours, and to solidify liquids. By loading the Nano sponges with solubility-sensitive medications, it is possible to successfully administer these medications. Nanosponges can be taken orally, intravenously, topically, or inhaled.

3. Nanosponges as chemical sensors

Metal oxides nanosponge titania, which is sensitive to H2 gas, is used to detect hydrogen with a high degree of sensitivity utilising nano sponge chemical sensors.

4. Solubility enhancement

Some recently released medications have low solubility in water, limiting their clinical utility. Nanosponges increase the solubility and dissolving rate of medications that are normally difficult to dissolve. The medications are gradually released from the Nano sponges. Complexation in nanosponges is strongly impacted by molecular structure and conformation. To improve drug solubility and therapeutic efficacy, the drugs can be molecularly disseminated inside the Nano sponge structure before being released as molecules.

5. Nanosponges as a vehicle for biocatalysts and release of enzymes, proteins, vaccines and antibodies

The operational drawbacks of many chemically transformed industrial processes include the need for high temperatures and pressures, which necessitate a great deal of energy and cooling water in the subsequent process. Enzymes can be used as biocatalysts to avoid these limitations because they function rapidly and gently. In the case of enzymes in particular, this allows for the conduct of continuous flow operations, the maintenance of activity, efficiency, and duration of operation, as well as an expansion of the pH and temperature ranges at which they are active. In addition, cyclodextrin Nanosponges can be used to transport proteins and other macromolecules by adsorbing or encapsulating them.

6. Protective agents against photo degradation

It was revealed by Sapino et al. that the antioxidant gamma-oryzanol (a combination of ferulic acid esters) is also used as a sunscreen in the cosmetics sector. However, due to its high instability and photodegradation, its usefulness is restricted. Encapsulating gamma-oryzanol in nanosponges has been shown to provide effective protection against photodegradation. The gammaoryzanol-loaded nanosponges are used to formulate a gel and an O/W emulsion.

7. Nanosponges as a carrier for a delivery of gases

The three gases 1-methylcyclopropene, oxygen, and carbon dioxide were utilised to generate inclusion complexes using Cyclodextrin-based carbonate Nano sponge. Many potential health benefits may be attained through the complexation of oxygen or carbon dioxide. The nanosponge infused with oxygen is used to treat hypoxic tissue. The highly porous characteristic of the nanosponge makes it a useful gas carrier. The ability to store and release oxygen was demonstrated in a nanosponge formulation. In the near future, nano sponges could be used to transport some critically important gases.

8. Nanosponges as oxygen delivery systems

An oxygen delivery device based on cyclodextrin nanosponges is being developed. Nanosponges of different types were fabricated using α, β, and γ cyclodextrin, and were then suspended in water, saturated with oxygen, and characterised for in vivo evaluation. the cyclodextrin Oxygen diffusion via a silicone membrane is achieved by a β-cyclodextrin nanosponge/hydrogel combination technology. To treat hypoxic tissues brought on by disease, nanosponges can be used to store and gradually release oxygen.

9. Nanosponges in cancer treatment

When treating cancer patients, doctors often find that the medications they inject into their bodies have little effect. This occurs for one of two major reasons: either they are unable to reach the tumour location, or the immune system attacks and destroys them. Nanosponge technology has enabled a partial removal of this barrier. By embedding the anticancer medicine in the Nano sponge, hydrophobic pharmaceuticals can be used in cancer treatment, but in the past, they have had to be combined with adjuvant reagents, which might impair the drug's efficacy or cause unwanted side effects. Nanosponges have potential as a medication delivery method for malignancies that are targeted by anticancer therapies. This approach is three- to five-times more successful than injecting the medications directly into the tumours themselves for halting growth. The sponges adhere to the surface of tumour cells and are triggered to release their medication when they come into contact with cancer cells. Targeted drug delivery has benefits like making treatment more effective at the same dose and causing fewer side effects.

10. Nanosponges as Topical agents

Nanosponge delivery system is a novel technique for topical medications that allows for sustained release of medication after topical application. Common dermatological and personal care treatments give relatively high concentrations of active chemicals; however, these compounds wear off quickly. This could start a vicious cycle of overmedication in the near term followed by undermedication in the long term. Active chemicals that are absorbed by the skin can cause rashes or more severe side effects. In contrast, this innovation enables a gradual and constant rate of release, which simultaneously lessens discomfort and maximises effectiveness. Formulated products like gels, lotions, creams, ointments, liquids, and powders can contain a wide range of substances.

11. Nanosponges in targeted drug delivery

Nanosponges travel throughout the body until they come into contact with a tumour cell's surface, at which point they adhere to the cell and begin releasing the medication in a controlled and predictable pace. The nanoparticle drug delivery technique used a targeting peptide that recognised a radiation-induced cell surface receptor. This targeting agent increased apoptosis and slowed tumour development by delivering paclitaxel-encapsulated nanoparticles exclusively to irradiation tumours. Nanosponges infused with anticancer drugs can slow tumour development by a factor of three to five compared to injection of the drug alone.

12. Nanosponges in antiviral therapy

The ocular, nasal, and pulmonary delivery routes can all benefit from the usage of nanosponges. Viruses like respiratory syncytial virus, influenza virus, and rhinovirus can be effectively treated by the selective delivery of antiviral medicines or small interfering RNA (siRNA) to the nasal epithelia and lungs using nanosponges. Their application extends to the treatment of AIDS, hepatitis, and herpes simplex virus. Zidovudine, saquinavir, interferon-α, and acyclovir are some examples of medications currently administered by Nano delivery (Eudragit based).

13. Greater efficiency compared to direct injection

The effectiveness of nano sponges in slowing tumour growth is five times greater. Chemical linkers that bind to a receptor on tumour cells are attached to virus-sized sponges containing an anti-cancer medication before being injected into the body. When the Nano sponges cling to the surface of the tumour cell, the medicine placed within is released in a predictable and regulated manner.

Table 6: Plant extracts encapsulated as nanosponge for anti-fungal use.

Plant	Active constituent	Fungal strains	Mechanism of action	References
Curucma longa L. (Turmeric)	Curcumin	*F. solani, C.albicans, P. expansum, A. flavus, A. parasiticus*	Works by eliminating the ERG3 desaturase gene leads to a decrease in ergosterol biosynthesis, which in turn leads to cell death due to increased levels of reactive oxygen species (ROS) generation. Reducing proteinase secretion and blocking H^+-ATPase activity increases acidification of extracellular and intracellular matrix, which in turn limits hyphae formation by blocking thymidine uptake 1. (TUP1) Curcumin is a photosensitizer (0PS) where the following reactions occur: $0PS + \gamma \rightarrow$ singlet excited state (1PS*) $\rightarrow$ triplet excited state (3PS*) $\rightarrow H^+$ to a biomolecule = radicals (anion superoxide (O_2^-), hydrogen peroxide (H_2O_2), hydroxyl radical, and singlet oxygen resulting in cell death by apoptosis, necrosis, or autophagy	[88], [89], [90], [91], [92], [95]
	Turmeric essential oil (*β*-pinene, camphor and eucalyptol)	*A. flavus*	Destruction of cellular integrity and induced modification in mitochondrial membrane potential are the two mechanisms that constitute fungicidal action	[93], [94]
	Curcumin and Quercitin	*A. niger, A. fumigates* and *Candida spp.*	Cuases the excess formation of lomasomes and plasmalemmasomes which results in cell wall and plasma membrane expansion and apoptosis.	[102], [103]
Curcuma amada (Ginger)	*α*-zingiberene, geranial, 6-gingerol and 6-shogaol	*A. flavus, A. parasiticus* and *F. verticilliodes*	Through an induction of a change in the potential of the mitochondrial membrane, anti-mycotoxigenic activity is produced. This results in a loss of membrane integrity, the release of cellular materials, and inhibition of ergosterol production.	[95], [96]
Syzygium aromaticum (Clove)	Eugenyl acetae, Eugenol	*A. flavus* and *A. niger*	Causes cell death by activating both early apoptosis (characterised by nuclear condensation) and late apoptosis (damage of plasma membrane) It also works by downregulation of metabolic genes (laeA, lipA,	[94], [97], [98]

			metP) responsible for fungal lipid and protein metabolism	
Clove essential oil	Eugenol	*Peronophythora litchi*	Damage is caused to the cell walls and plasma membranes of hyphae and sporangiophores, which results in the shrinking, wrinkling, and partial deformation of the cells.	[104]
Rosmarius officinalis L. (Essential oil)	Eucalyptol, camphor and α-pinene	*A. flavus*	Inhibits ergosterol production and reduces biomass of mycelium	[94], [99]
Punica granatum (Pomegranate)	Tannins	*A. niger, F. oxysporum, F. culmorum* and *P. digitatum*	Generation of reactive oxygen species (ROS) results in destruction of plasma membrane and cessation of mitochondrial function	[100]
Solanum lycopersicum (Tomatoes)	Lycopene	*C. albicans*	The primary mechanism is a rise in intracellular ROS, which causes a depolarization of the plasma membrane and an arrest of the cell cycle(G2/M)	[95], [101]
Piper nigrum L. (Pepper)	Limonene and β-caryophyllene	*A. niger* and *F. oxysporum*	Destruction of the cell wall and the plasma membrane, coagulation of the cytoplasm, damage to cellular organelles, and an increase in ergosterol production are all potential antifungal actions	[96]
Origanum majorana (Essential oil)	Chitosan	*A. flavus, A. parasiticus,* and *F. graminearum*	Inhibits the synthesis of ergosterol, which is then followed by the release of cellular ions, inhibition of methylglyoxal, and an inhibition of lipid peroxidation that takes place in situ.	[94], [105]
Camellia sinensis L. (green tea) and a variety of plants	Epigallocatechin	*Candida spp.*	It works by disruption of plasma membrane function and loss of cell membrane integrity which leads to lesion formation. Osmotic imbalance, brought on by the membrane's increased permeability, leads to cell death.	[95], [106]

8.3 Challenges associated with nanosponge

Like other nanoparticles, the fundamental issue with nanosponge usage in medicine is how slowly they are implemented. One of the main challenges in the field of nanosponges is the development of methods for their synthesis [107]. Nanosponges need to be produced in large quantities, with consistent size and shape, and in a manner that preserves their stability and functionality [. Although laboratory synthesis of nanoparticles has typically advanced to a very high level of perfection, "irreproducibility," or the inability of other laboratories to replicate a scientific study's published findings, and scale up upto production level remains a challenge

[108]. The nanosponge manufacturing process is not yet scalable enough to meet the needs of clinical applications because of irreproducibility of products caused by various physical factors such as phase change of emulsion globules during manufacturing and the problem in maintaining similar hydrodynamics in manufacturing liquid. They can only incorporate small molecules and the degree of crystallinity can also affect drug loading. The cost of producing nanosponges is currently quite high because of high running cost and product loss as fines, and this is a major barrier to their widespread use [109]. As with any new technology, there is concern about the potential toxicity of nanosponges. Studies are needed to evaluate the safety of nanosponges in different organisms and tissues. Pre-clinical studies with several *in-vivo* and *in-vitro* models are being used to evaluate the safety, efficacy, and biodistribution of nanosponges [110].

8.4 Future prospects [111]

Nanosponges are a type of nanomaterial that have a sponge-like structure and are made of biocompatible materials. They have a number of potential applications in a variety of fields, including drug delivery, tissue engineering, and environmental remediation.

One potential future application of nanosponges is in drug delivery. Nanosponges can be loaded with a drug and used to target specific cells or tissues in the body, allowing for more precise and effective delivery of the drug. They can also be used to release drugs over a longer period of time, reducing the need for multiple doses. In tissue engineering, nanosponges could be used to support the growth of new tissues or to repair damaged tissues. They could also be used in combination with stem cells or other growth factors to promote tissue regeneration. Nanosponges could also have environmental applications, such as the removal of pollutants from water or air. They have a large surface area and high adsorption capacity, which makes them effective at capturing and removing contaminants. Overall, the future perspective for nanosponges is very promising, with a wide range of potential applications in various fields. As research and development in this area continues to advance, it is likely that we will see even more innovative and practical uses for nanosponges in the future.
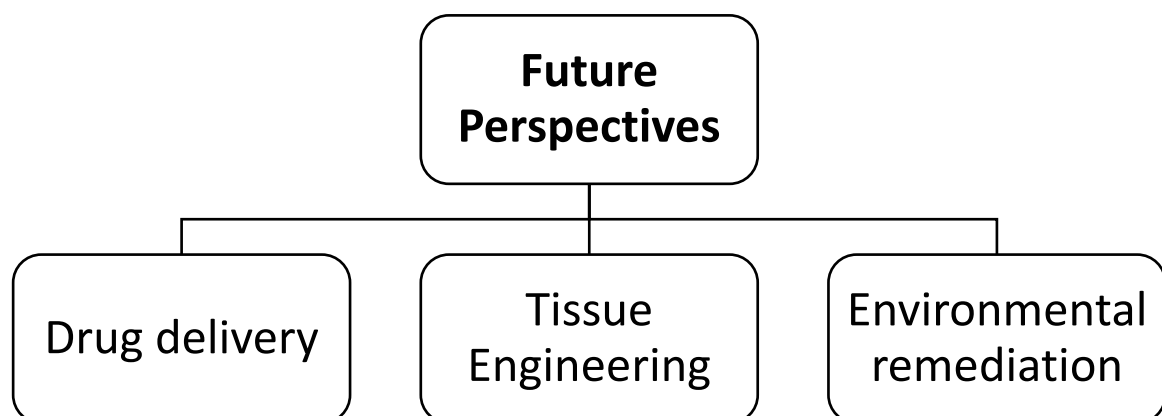
Figure 19: Future perspective of nanosponge (adapted from Ref no. 111)

Chapter 2
Literature Survey

A. Butenafine loaded nanosponge-based gel

In recent years, the frequency of superficial fungal infections (SFI) has grown, impairing immunological processes. Antifungal medications' activity is quadrupled when they are added to nanocarrier systems. The manufacture and assessment of butenafine-loaded nanosponges for the treatment of SFI of the skin are exploited by *Ahmed et al* in 2021[46]. Butenafine offers a potential for topical delivery through skin despite being a BCS class II medicine with limited water solubility because its molecular weight is under 400Da. Butenafine HCL (BTF), is a potent new generation antimycotic antifungal compound showed fungicidal activity by inhibiting the sterol synthesis [112]. Butenafine-loaded nanosponges with varied quantities of ethylcellulose and polyvinyl alcohol were made using the emulsion solvent diffusion method. BTF and various quantities of polymer in DCM made up the internal phase. PVA at 0.3 % concentration, in 100 ml water made up the external phase. The generated nanosponges were stabilized by PVA after the organic phase was emulsified dropwise into the aqueous phase using ultrasonication. The organic solvent was then removed from the dispersion by allowing it to sit on a magnetic stirrer for 24 hours in a temperature-controlled incubator. After that, it was centrifuged at 16,900 rpm for 30 minutes at 4°C.

The generated nanosponges were evaluated for their particle size (PS), polydispersity index (PDI), zeta potential (ZP), entrapment efficiency (EE), and drug loading (DL). Formulation containing 100 mg BTF, 200 mg EC, and 0.3% PVA was chosen for incorporation into carbopol gel after being optimized. Additional physicochemical characterizations, including FTIR, DSC, XRD, and SEM, were carried out on the optimized formulation. The physicochemical characterization findings for optimized formulation were all in acceptable ranges. In FTIR spectra of pure BTF and the optimized nanosponge formulation, broadening and disappearance of fingerprint region of drug was observed indicating good drug encapsulation. The optimized formulation exhibited a broad endothermic peak in DSC showing drug encapsulation. All nanosponges via SEM images depicted spherical smooth surfaces with uniform porosity [113]. Experiments were performed on the carbopol gel loaded with optimized butenafine nanosponge to measure its pH, viscosity, spreadability, drug content, flux, drug diffusion, antifungal activity, stability, and skin irritancy. Topical gels showed anomalous non-Fickian drug release, with a flux rate of 0.18 (mg/cm^2/h) as anticipated by the Higuchi models. The authors compared the relative rates of medication release between an FDA-approved Butenafine cream and optimized nanosponge based gel. However, Butenafine release from the

commercially available preparation was 92.88 ± 0.22% after 3 hours, whereas drug release from the carbopol gel was 89.9 ± 0.15% after 24 hours. The release profiles showed that optimized nanosponge based gel released the medication slowly and steadily. Using A. niger, fungicidal efficiency was assessed in vitro. It was discovered that butenafine loaded nanosponge gel was most effective, followed by commercially available butenafine cream, and finally pure butenafine.
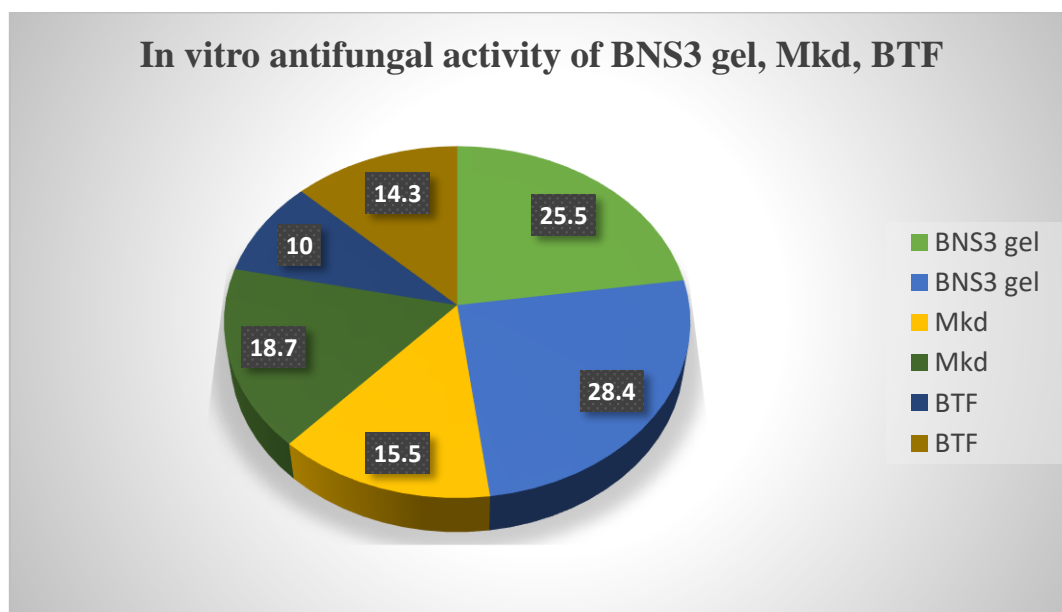

Figure 20: In-vitro antifungal activity assessed for BTF, BTF loaded Nanosponge gel and Marketed preparation (adapated from Ref no.46)

Drug delivery systems (DDSs) containing nanocarrier based antifungal agents are promising for the therapeutic treatment of fungal infections, and the results suggest that butenafine-loaded nanosponges inserted in a carbopol polymeric gel system may be a such DDS.

B. Lemongrass loaded topical based nanosponge hydrogel

Citing its many pharmacological and therapeutic benefits, the pharmaceutical industry has long recognised Lemongrass oil's (LGO) significance. As a result of the high citral concentration, LGO, which is isolated from the Cymbopogon citratus plant, has been shown to have potent antibacterial, antifungal, and insect repellent properties [114]. However, it is unstable because of exposure to heat, oxygen, and light, which can cause it to vaporise, oxidise, or react with other compounds in the formulation, resulting in skin irritation. Another difficulty in formulation development is its low aqueous solubility. To address these limitations, the researchers [115]

have created LGO-loaded nanosponges with topical hydrogel, resulting in a more potent antifungal action with less associated inconvenience.

Two independent variables; EC: PVA ratio (X1) and stirring rate (X2) were estimated using a 32 full factorial design. Particle size (Y1) and percentage LGO released after 6 hours (Y2) were the dependent variables. ANOVA was applied to evaluate the level of significance of the independent variables on the response variables as well as the interaction between them. Varying X1 and X2, different formulations were made. For internal phase, defined amount of EC and 200µL LGO were dissolved in 10 ml DCM. External phase was 15 ml deionized water with required amount of PVA. Internal phase was slowly added to exterior phase while stirring and left for 30 mins under controlled heating. The dispersion was then centrifuged in 4°C for 30 minutes at 20,000 rpm. To develop a hydrogel, specific amount of carbopol 934 diluted in 5 ml distilled water was mixed with the optimized nanosponge. Particle Size (PS) determination by dynamic light scattering (DLS) study and SEM studies were performed on the nanosponges to determine their surface morphology. The citral content of LGO Nanosponges was determined by high-performance liquid chromatography (HPLC) on a reverse-phase column operating at 240 nm. Hydrogels with optimized nanosponge were tested for LGO release in-vitro using a cellulose dialysis bag. Six albino rats were subjected to a Draize patch test to determine the gel's irritant potential. Hydrogel antifungal activity was measured in male albino rats. Minimal inhibitory concentration (MIC) and minimal fungicidal concentration (MFC) of LGO were calculated against C. albicans using a broth macrodilution technique.

DLS showed every formulation was in the nano range. Linear model was used to evaluate PS and it was observed to increase with increment of EC:PVA ratio (X1) and decrement in stirring rate (X2). SEM showed that nanosponges were all uniformly spherical in shape and had smooth, porous exteriors. Nanosponge integrity was shown by TEM to have been unaffected by their incorporation into hydrogel. The in-vitro release profiles of several formulations showed substantial heterogeneity. The proportion of LGO released after 6 h decreased with increasing values of X1 and X2, perhaps due to longer diffusional routes and decreased porosity respectively. The plastic and hydrophobic properties of EC led to the observation of an early burst effect. Rats showed no signs of skin irritation after 24h, 48h, or 72h. Antifungal activity was shown below.
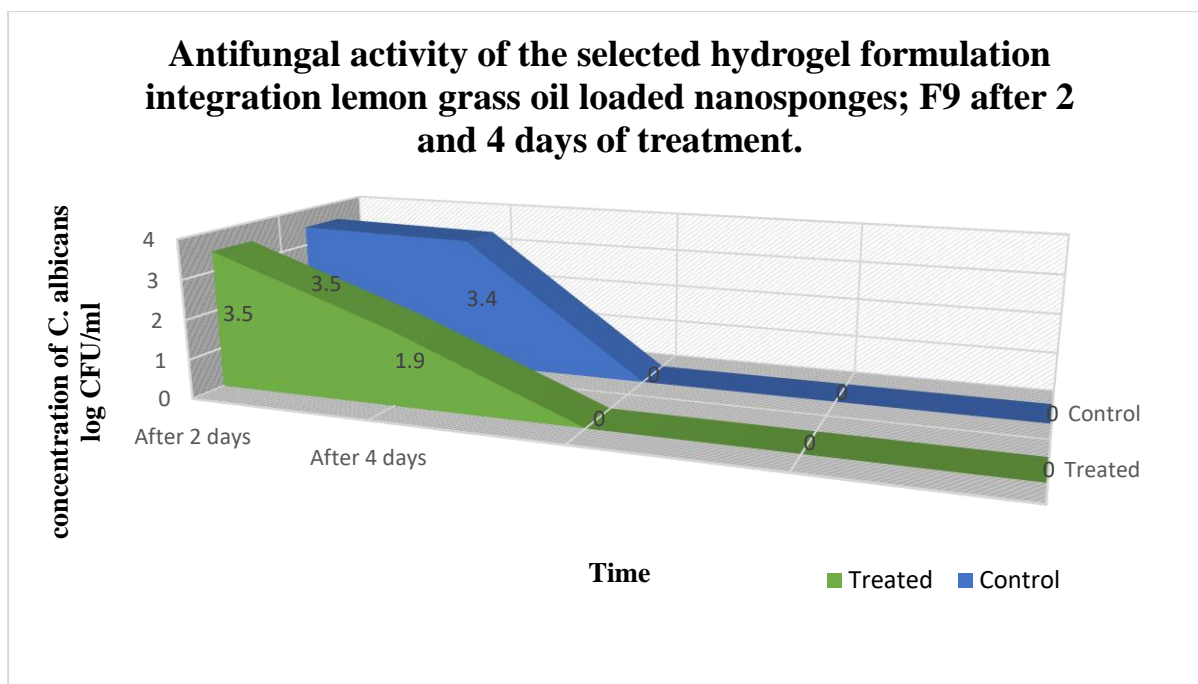
Figure 21: Antifungal activity of F9 hydrogel formulation after integration with lemongrass loaded NS, after 2 and 4 days (adapted from Ref no. 115)

These results have proved a successful incorporation of LGO into nanosponge via emulsion solvent evaporation technique. To reduce the risks associated with using LGO in conventional pharmaceutical delivery systems, nanosponge strategy holds great promise for introducing LGO into a wide range of pharmaceutical formulations bolstering its antifungal effect and decreasing irritation on the skin.

C. Ciprofloxacin and its binary mixture nanoassemblies

Medication combination treatment increases therapeutic efficacy in numerous clinical studies [116]. Nanosponges have been used to solve the problem of microbial resistance to some drugs, improving the pharmacodynamics and pharmacokinetics of antibiotic agents. In this study, Ciprofloxacin (CIP) and a 1:1 binary combination of CIP and N-acetyl cysteine (NAC) were loaded onto nanosponges to increase loading capacity, drug release, antibacterial and antifungal action [117].CIP is a broad-spectrum fluroquinoline antibiotic which has properties intermediate between BCS Classes II and III, making it a good candidate for nanosponge delivery. NAC is a free radical scavenger and can protect against lipid peroxidation of cornea. To make the nanosponge, HPβ-CD and Diphenyl carbonate were mixed in different molar ratios and then sonicated. Nanosponges were weighed, sonicated, and then stirred for 24 hours in drug

solution. Centrifuging suspensions at 9000 rpm for 15 minutes separated the free drug from the colloidal supernatant. Drug-loaded nanosponges were lyophilized at -20°C and 13.33 mbar.

The prepared Nanosponges were characterized for particle size (PS), polydispersity index (PDI) and entrapment efficiency (EE %). EE % of CIP or its binary mixture with NAC in nanosponges was found to be significantly high suggesting a good amount of crosslinking. Particle size and PDI were measured by dynamic light scattering instrument and were in acceptable ranges. Further physicochemical characterizations were performed such as FTIR, DSC, XRD, SEM, and TEM. Thermograms of DSC indicated a shifting in the sharp peaks of CIP, proving its inclusion in nanosponge formulation. FTIR data suggested definite interactions between drugs and nanosponges as the characteristic peaks of CIP/NAC were masked and undistinguishable in the fingerprint region (3524, 3237 and 3049cm-1). Broadening and disappearance of CIP and NAC were observed showing their inclusion nature in nanosponge. Comparative analysis of diffractograms [118] of nanosponge formulation and HPβ-CD indicate identical and broadened peaks proving complete inclusion of the drug within the complex. The release pattern of drug from nanosponges followed Korsmeyer-Peppas model and it was biphasic (n<0.5, obeyed Fickian diffusion). There was continuous release for up to 96 h (figure 22).

In-vitro antibacterial activity and in-vitro antifungal activity of the formulations were performed by well diffusion method. Ex vivo and in vivo study results revealed that the antibacterial impact was boosted by incorporation of drugs in the nanosponge system, hence inventing a new promising therapeutic activity for both drugs. All Nanosponges formulations showed strong fungicidal action, however the free drug had no effect on *C. albicans*. As it is well known, neither CIP nor NAC had any indication of antifungal action when used separately, but their binary combination and subsequent loading into nanosponges enabled a brand-new activity. Thus, this study has innovated a new promising therapeutic course for both drugs.
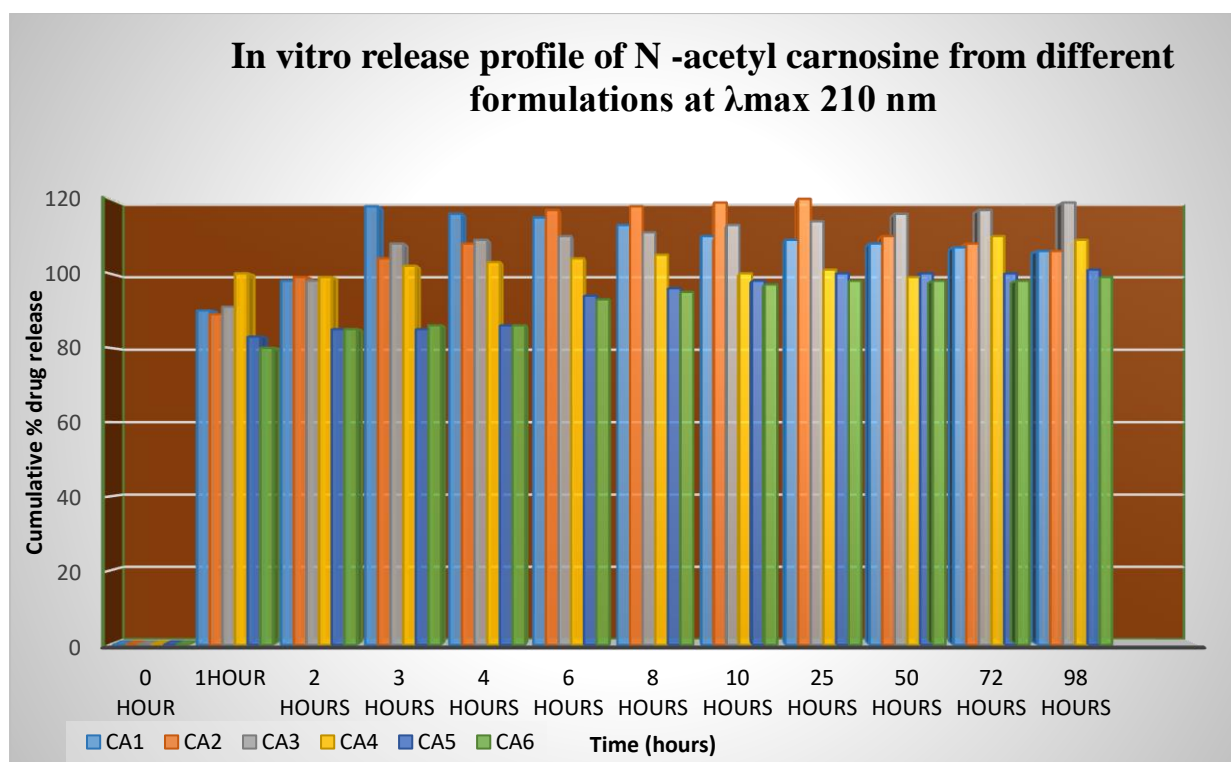
Figure 22: In-vitro release profiles of six formulations CA1, CA2, CA3, CA4, CA5 and CA6 at λmax 210 nm (adapted from Ref no. 117).

D. Topical Terbinafine hydrochloride nanosponges

Amer et al. in 2020 [119] produced terbinafine hydrochloride (THCL) nanosponge hydrogel for topical fungal infection treatment. THCL, a BCS Class II broad-spectrum antifungal inhibits fungus ergosterol production. Due to its low absorption, dose frequency increases, causing systemic side effects. THCL Nanosponges can minimize hepatotoxicity, anorexia, vomiting, and fatigue and also enhance solubility [120]. The study involved 45 female Wistar rats for in vivo study. THCL Nanosponges were made by emulsion solvent evaporation. The two independent variables; Drug: EC ratio (X1) and stirring rate (X2) were estimated using a 3^2 full factorial design. Particle size (Y1) and entrapment Efficiency (Y2) were the dependent variables. Varying X1 and X2, different formulations were made. For Internal phase, THCL and EC were dissolved in 10 ml dichloromethane (DCM). External phase was 20 ml deionized water with 1% PVA. Internal phase was slowly added to exterior phase while stirring and left for 15 mins. THCL nanosponges were made by homogenising the mixture at varying speeds and filtering. To develop nanosponge entrapped hydrogel, carbopol 934 diluted in 100 ml distilled water was mixed with an equivalent weight of tailored THCl Nanosponges. Additionally, conventional THCl gel was created.

The nanosponges were assessed for particle Size (PS), entrapment Efficiency (EE), production yield (PY) and scanning electron microscopy (SEM) analysis for surface methodology. Nanosponge hydrogel underwent DSC, TEM, drug content investigations, pH, and release studies to characterise its physical properties. When the polymer ratio was raised, the PY was found to rise. The influence of the stirring rate (X2) was quantified using a quadratic model and shown to be significant in the overall assessment of PS. Almost all formulations fell inside the nanosize range. Linear model was used to evaluate EE and it was observed to decrease with increase in stirring rate. All nanosponges depicted spherical smooth surfaces with uniform porosity. According to DSC results, both THCL nanosponge and THCL nanosponge hydrogel exhibited a reduction in endothermic peaks of drug due to its encapsulation within nanosponge and hydrogel. pH and drug concentration were also within therapeutic ranges for topical application.In-vitro release studies of THCL Nanosponge, THCL Nanosponge Hydrogel and marketed cream were done with a Franz Diffusion cell [26] and samples were analyzed by a spectrophotometer at λ_{max}=222nm. The drug slowly released from the hydrogel for 8 hours, which showed that more THCL was released as entrapped form than as unentrapped form. Using Sabouraud dextrose as a culture medium, the Cup-plate method was used to measure the activity of hydrogel against *C. albicans*. In comparison to commercial cream and THCL hydrogel, it was shown that the mean growth inhibition zone around THCL Nanosponge hydrogel was significantly larger.
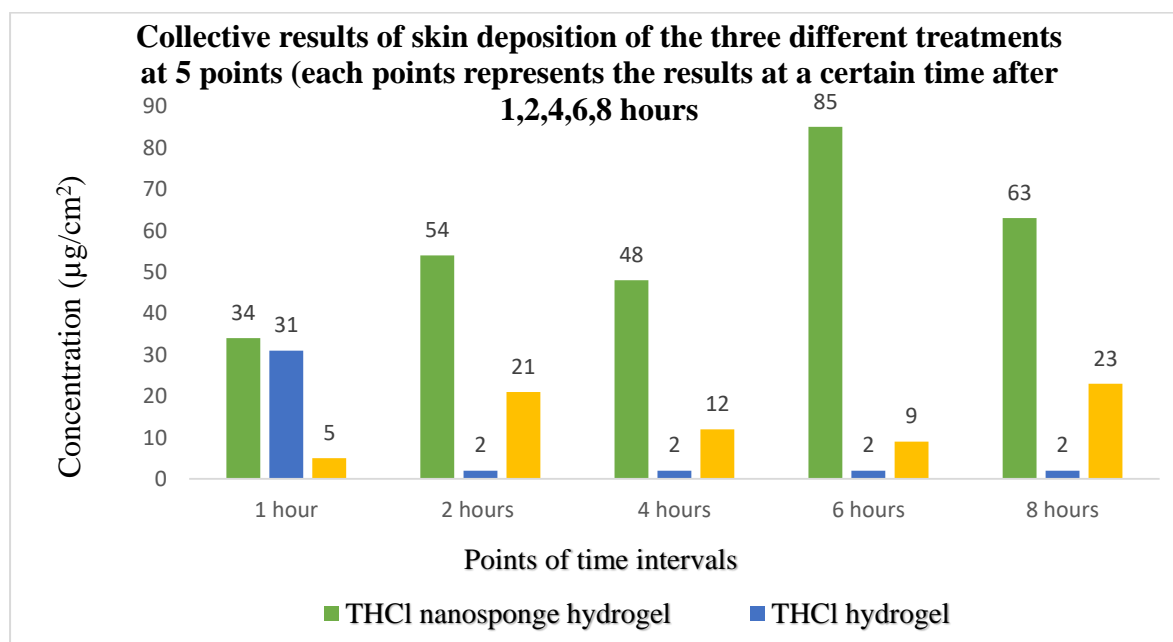

Figure 23: Skin deposition of THCL nanosponge, THCL hydrogel and Marketed Cream (adapted from Ref no. 119).

Sustained release from the hydrogel formula was observed for 8h, even superior antifungal activity and skin deposition were demonstrated than that of marketed THCL cream . The results of the study undoubtedly demonstrated that nanosponge hydrogels are a promising therapeutic strategy for treating fungal infections.

E. Babchi oil loaded beta-cyclodextrin nanosponge

The essential oils have long been acknowledged for their use in the pharma industry. Some examples of such phytoextracts include the oil of the *Psoralea coryfolia* plant, known as babchi oil (BO), which has antimicrobial, antifungal, antioxidant, anti-inflammatory, immunomodulatory, and anticancer properties [121]. However, its instability, low solubility, and volatility prevent it from being widely used in the pharmaceutical industry. In this study, the authors set out to find a way around the shortcomings of BO by encasing the molecule in beta-cyclodextrin (β -CD) based Nanosponges. Cyclodextrins are biocompatible and biodegradable, and they have the ability to encapsulate molecules at a cheaper cost. Due to complexation, the produced Nanosponges facilitate BO solubilisation and enhance the compound's stability [122]. Peak measurement in GC-MS was used to quantitatively analyse the main components of the oil (Furocoumarins). To create the nanosponges, β-CD was crosslinked with diphenyl carbonate (DPC) at varying molar ratios, and the mixture was heated with a magnetic stirrer for 6 hours. After cooling, the liquid was filtered through Soxhlet extraction to get rid of any residual DPC and phenol. The formed nanosponges were dried at 40°C and loaded with BO by freeze drying technique. Effectiveness of BO solubilisation among formulations was examined by UV spectrophotometer readings (λ_{max}265nm).

The prepared Nanosponges were characterized for particle size (PS), polydispersity index (PDI), zeta potential (ZP) and entrapment efficiency (EE). Solubilisation efficiency of BO rose by a factor of 4.95 after incorporation with β-CD Nanosponge [123]. Formulation with (4.548g β -CD and 3.424g DPC was chosen for medicinal oil loading as it showed highest encapsulation and further tested with FTIR, TGA, XRD, SEM, and TEM study. The MTT assay was used to test the optimised nanosponges for toxicity against a human epidermal keratinocyte cell line. In-vitro antibacterial tests were performed to compare optimised nanosponges to BO. Researchers also tested the photo-degradation of BO and BO loaded nanosponge in the presence of UVA irradiation. All formulations had 61–93% EE. All Nanosponges were in the nano range, with a high zeta potential but a low PDI. FTIR spectra of BO, blank nanosponge, and optimized nanosponge showed BO peaks shifting in the formulation, suggesting oil-

nanosponge interaction. β-CD and DPC mixture's TGA curve matched with that of blank Nanosponge, demonstrating crosslinking between them. DTG results strengthened the findings in TGA. XRD peaks showed that BO-encapsulated β-CD Nanosponges had less crystallinity. SEM showed that all nanosponges had smooth spherical surfaces with consistent porosity. TEM showed consistent size distribution in melt-prepared nanosponges. IC50 values from MTT test showed that the nanoformulation was safer on human skin cells than BO alone. Loading of the essential oil in nanosponge also significantly reduced the photo oxidation process. The inhibitory impact of BO-loaded Nanosponges against *P.aeruginosa*, *E.coli*, and *S.aureus* was evident and significantly more effective than that of traditionally given BO.

These results have proved that nanosponge can be a successful delivery system for encapsulating BO and also help in bypassing the negative effects of conventional delivery techniques by showing improved solubility, photo-stability and therapeutic activity.
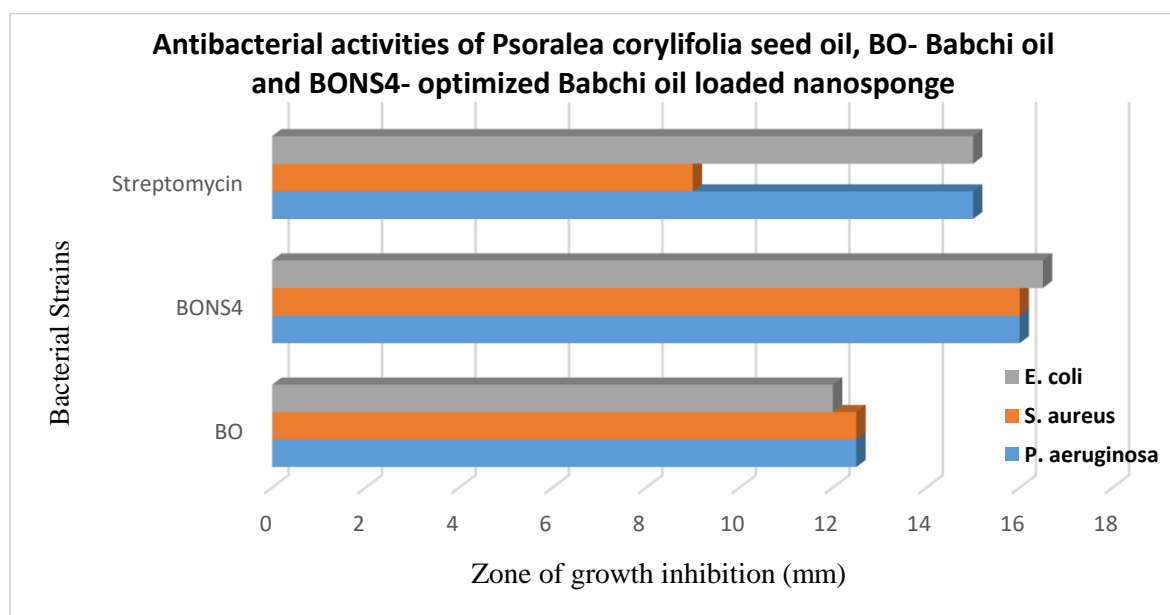
Figure 24: Zone of Inhibition of Babchi Oil and BONS4: optimized Babchi Oil loaded NS (adapted from Ref no 122).

.

F. Nanosponge loaded with Clotrimazole based in situ gel

Vaginal candidiasis affects about 75% of women, and while it can be treated locally with antifungal medications, patients prefer shorter treatment regimens. Recurrent vaginal infections caused by *candida albicans* require long-term treatment [124]. In vaginal candidiasis, clotrimazole (CTZ) is the treatment of choice. Conventional CTZ preparations have limited

action owing to short residence time in genitourinary tract. Moreover, CTZ, a BCS class II entity must be administered often due to its short half-life and limited water solubility. These worsen its negative effects and reduce antifungal therapy. This investigation developed a dosage form by entrapping CTZ into β-Cyclodextrin (β-CD) based hyper-crosslinked nanosponges and made *in situ* gel formulation for effective candidiasis treatment [125].

To create the nanosponges, hydroxylpropyl β-CD was crosslinked with dimethylcarbonate (DMC) at varying molar ratios, and the mixture was heated with a magnetic stirrer for 5h. After cooling, the liquid was refined through soxhlet extraction to get rid of any residual DMC and other impurities. The formed nanosponges were dried and loaded with CTZ by freeze drying technique. UV spectrophotometer readings at 264 nm were used to examine CTZ solubilization effectiveness among formulations. The prepared nanosponges were characterized for particle size (PS), polydispersity index (PDI), zeta potential (ZP) and entrapment efficiency (EE). Solubilisation efficiency increased with increasing β-CD ratio. To develop the *in situ* gel system, pluronic F-127 (PF-127) and pluronic F-68 (PF-68) were used to incorporate specified amount of CTZ nanosponges using 'cold method'. Additionally, a conventional CTZ gel was created. To examine the interaction between independent and dependent variables, a 3^2 full factorial design was utilised and *in situ* gels based on CTZ nanosponge were optimised. The sol-gel transition, gelation temperature, gelation time, in-vitro drug release, pH, drug content, viscosity, and spreadability of nanosponge loaded gel formulations were characterised. On rats, the in-vitro bio adhesion, in-vivo irritation, and antifungal efficacy were also evaluated. All nanosponges were in the nano range, indicating a stable colloidal system with a high zeta potential and low PDI. In CTZ-loaded β-CD nanosponge FTIR spectrum, all peaks were sharp but moved to high and low wave numbers, and only a few typical CTZ peaks were found, confirming interaction between CTZ and nanosponge. Pure CTZ and blank nanosponge thermograms showed peaks at 147.47 and 95.27°C respectively. Drug's DSC peak was absent due to encapsulation. CTZ based nanosponges demonstrated lower crystallinity as confirmed by XRD peaks. All nanosponges exhibited smooth spherical surfaces with consistent porosity by SEM [126]. Melt-prepared nanosponges had uniform TEM size distribution. The optimised formulation's gelation temperature, gelation time, and in-vitro drug release were concentration dependant of polymer. Concentration of PF-127 and PF-68 concentrations decreased drug release, prolonging its action for up to 15h. Bioadhesion and antifungal activity were higher

than that of conventional *in situ* gel. Optimized formulation reduced inflammation and improved animal tolerance.
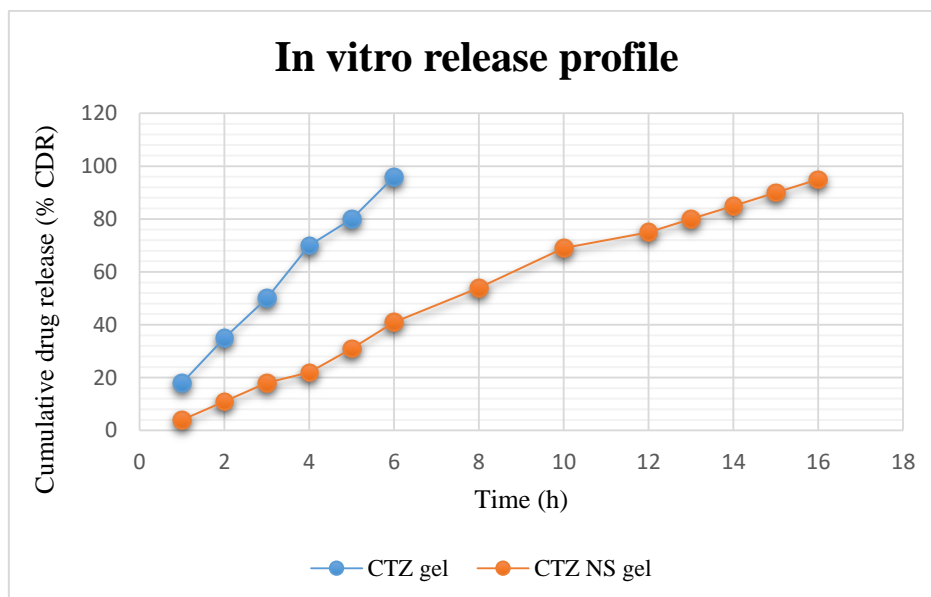

Figure 25: In-vitro release profile of marketed CTZ gel and CTZ loaded hydroxylpropyl β-CD NS- based in situ vaginal gel (adapted from Ref no. 125)

The results of the study undoubtedly demonstrated that nanosponge based *in situ* gels loaded with CTZ are a promising therapeutic strategy for treating vaginal candidiasis. When incorporated as *in situ* gel CTZ displayed a higher residence time and a greater potential to effectively alleviate vaginal infection, more than any present conventional formulation in market.

G. Luliconazole loaded nanosponge

Dermatophyte-induced superficial fungal infections (SFI) have long posed a significant threat to health. BCS class II agent Luliconazole inhibits dermatophytes both in-vivo and in-vitro [127]. However, its limited water solubility and low cutaneous availability reduce its topical delivery potential. Localization in the dermal and epidermal layers of the skin is important for topical fungal infection treatment. Commercial formulations have minimal skin penetration and drug retention. This drawback is overcome by entrapping drugs in nanosponges. For a novel SFI treatment, researchers created luliconazole-loaded nanosponges and incorporated an optimised formulation within a carbomer-based hydrogel [128].

Luliconazole-loaded nanosponges with varied quantities of ethylcellulose and polyvinyl alcohol were made using the emulsion solvent diffusion method. Drug and various quantities

of polymer in 20 ml DCM made up the internal phase. Specified amount of PVA, in 150 mlwater made up the external phase. The generated nanosponges were stabilised by PVA after the organic phase was emulsified dropwise addition of internal phase into the aqueous phase using ultrasonication. After that, it was centrifuged at 3000 rpm for 10 minutes and dried. To examine the interaction between independent and dependent variables, a 2^3 full factorial design was utilised. Different formulations were created by combining various levels of each variable in the formulation process. Using carbomer 934, prepared nanosponges were mixed into a gel base. The generated nanosponges were evaluated for their PS, polydispersity index (PDI), zeta potential (ZP), EE, SEM and high resolution TEM for surface morphology. FTIR, DSC and XRD investigations and in-vitro release were also carried out. The gel system was evaluated for viscosity, swelling behaviour, and in vitro diffusion experiments. Finally, an optimised formulation was chosen for the study of stability, antifungal activity, skin irritancy, and permeation experiments using rat skin membrane. All the nano-sized sponges indicated a stable colloidal system with a high zeta potential and a low PDI. The formulation's EE improved as its polymer concentration increased. FTIR spectrum of optimised formulation exhibited no distinctive peaks of pure drug luliconazole, indicating drug entrapment. Drug inclusion in luliconazole nanosponges was confirmed by reduced crystallinity visible in XRD peaks and absence of DSC peaks. SEM and TEM studies verified that all of the nanosponges had uniformly porous, spherical surfaces. The kinetic data on drug release showed a sustained release of up to 8 hours. The diffusion-controlled nature of the release pattern was validated by Higuchi's plot. Better drug penetration and retention over a longer period of time (10 hours) in animals was seen with the modified hydrogel formulation. The inhibitory zone of the optimised hydrogel was likewise greater than that of the pure medication and the commercially available cream when tested against *C. albicans* [129].

The results of the study undoubtedly demonstrated that nanosponge based hydrogel of Luliconazole are a promising therapeutic strategy for treating SFI, more than any present conventional formulation in market. The formulation of nanosponge gel accomplished the goals of increasing availability of drug in cutaneous and maintaining the release of medication for efficient fungal therapy.

H. Beta-cyclodextrin based Itraconazole nanosponge

Itraconazole, a popular broad-spectrum antifungal drug, inhibits cytochrome P450-dependent fungal enzymes, but as a BCS class II agent, it has significant formulation challenges. Low solubility and poor oral bioavailability lead to increased dose frequency, which in turn increases the risk of unwanted side effects.

In this study *Swaminathan et al*, encapsulated Itraconazole in β-cyclodextrin (β-CD)-based nanosponges to improve its solubility and examined the influence of copolyvidonum on the drug's solubility. In the past, β-CD has been fortified by the addition of hydrophilic polymers to increase its complexation efficiency. Researchers included copolyvidonum for similar reasons. Using solid dispersion, the drug was integrated into the prepared nansoponges. Dichloromethane was used to dissolve the itraconazole, and this solution was then mixed with nanosponge and copolyvidonum in a specific ratio and triturated until the organic solvent dissipated. Phase solubility studies were performed to examine the solubilization efficiency of the drug-nanosponges system, the drug-copolyvidonum system, and the drug-nanosponges-copolyvidonum ternary system [130]. Studies on solution state interaction and saturation solubility were also conducted on binary and ternary systems. Dispersions were analysed for a number of different properties, including particle size, polydispersity index, DSC, XRD, and in-vitro dissolution.Phase solubility plots demonstrated that nanosponges or copolyvidonum concentration increased drug solubilization proportionally. Maximum drug solubilization was achieved in the ternary system, suggesting that copolyvidnoum's inclusion was beneficial. The wavelength shift increased with nanosponge concentration in solution state interaction data. The drug was foundd to absorb UV at wavelengths 260 and 222.4nm. Masking of Itraconazole's hydrophobic group increased solubility. Nanosponges increased solubility 55-fold in ternary complexes and 27-fold in binary complexes. The ternary system's average particle size was 645–675 nm, compared to nanosponge's 1,300–1,400 nm. The colloidal system was stable as evidenced by the small particle size and low polydispersity index. DSC thermograms showed complexation in nanosponges and considerably more in ternary complex. In ternary complex, the drug displayed maximal amorphousness, as shown by area and enthalpy values and reduced peaks in XRD examinations further confirmed it. In the ternary system, dissolution was shown to be accelerated. Possible explanations for the ternary system's enhanced solubility of itraconazole include: decreased crystallinity; decreased particle size;

increased wetting; surfactant action of copolyvidonum; and nanosponge masking of itraconazole's hydrophobic groups [72].
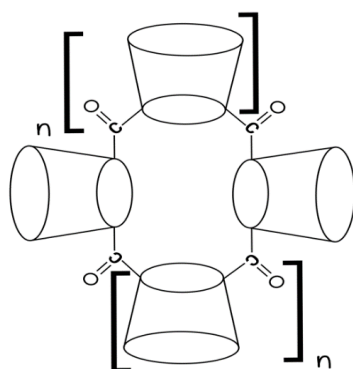

Figure 26: Proposed nanosponge structure of β-CD (adapted from Ref no. 72)

Based on the findings, it is evident that the addition of β-CD nansoposnges and copolyvidonum significantly increased the solubility of Itraconazole. If the medicine is more soluble, more of it will be absorbed by the body, making it a more effective antifungal treatment.

I. Cyclodextrin based Resveratrol nanosponge

In the year 2011, Ansari *et al* prepared a complex of resveratrol, a polyphenolic phytoconstituent with cyclodextrin-based nanosponges (NS) to increase the stability, solubility and permeation. Resveratrol, a BCS class II agent, is poorly water soluble and less bioavailable [43]. Moreover, increased frequency of dosing leads to unwanted side effects. Nanosponges can greatly enhance their in-vivo absorption. Carbonyl diimidazole was used as a cross-linker which reacted with cyclodextrin. At first, different molar ratios of β-cyclodextrin nanosponges (β-CD NS) were formulated by varying the crosslinker amount using a condensation polymerization technique. Second, the β-CD NS were suspended in sufficient purified water, followed by the addition of calculated amounts of drug and sonicated to obtain the drug-loaded nanosponges [26].

Particle size, Zeta potential and polydispersity index (PDI) were determined using dynamic light scattering techniques. Studies using characterization methods like DSC, FTIR, and X-ray powder diffraction (XRPD) technology validated resveratrol's interaction with NS. The interaction was observed between the OH groups of the nanosponges and the resveratrol, as evidenced by the shift in the peak at 3,273 cm^{-1} in the FTIR spectrum of NS due to the O-H stretching typical of carbohydrates in the presence of the complex. According to the XRPD study, Resveratrol's crystallinity decreased following encapsulation. A stable colloidal

nanosuspension was obtained due to sufficiently high Zeta potential and low PDI. The TEM study showed NS complexes' particle size was around 400 nm. SEM experiments have shown uniformly porous structures with ability to form clusters in water. It was discovered via in vitro release that the complex demonstrated a significantly higher release rate than the pure drug. It became evident from the degradation testing that NS complex was more photostable than that of simple drug. This could be as a result of resveratrol being strongly encapsulated with NS. The improved activity of resveratrol against HCPC-I cell cultures may be ascribed to its increased solubility due to complexation as opposed to that of plain drug. Comparing NS complex in water to the resveratrol plain in the ethanol-water mixture (50/50 v/v), permeation studies revealed that NS complex in water gave good penetration results. The increased solubility of resveratrol brought on by the inclusion as well as the non-inclusion occurrence of NS with resveratrol, may account for the improved penetration through pigskin. Resveratrol formulations were more cytotoxic than pure resveratrol, according to cytotoxic experiments on the HCPC-I cell. The rabbit mucosal accumulation study revealed that resveratrol NS formulation accumulated better than plain drug.
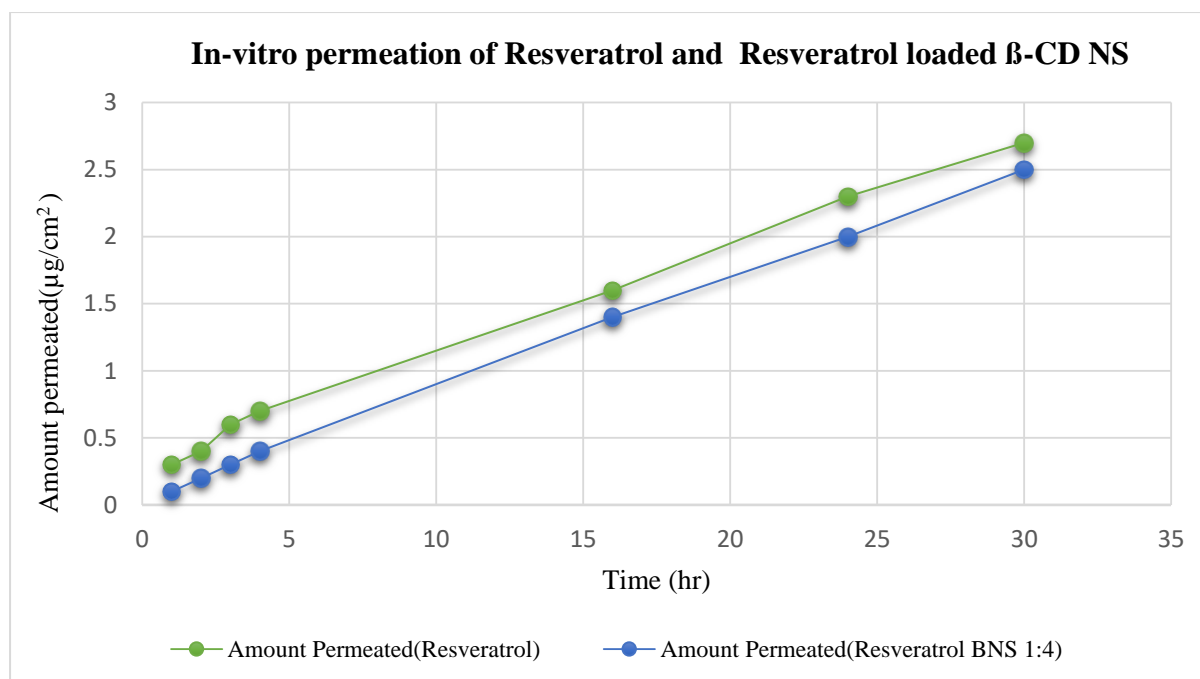

Figure 27: Permeation study of Resveratrol and Resveratrol BNS 1:4 (adapted from Ref no. 26).

These results lead to the conclusion that particles of resveratrol-loaded NS as produced using traditional inclusion complexation procedures are of appropriate particle size in nano range.

This nanosponge-based formulation greatly improves HCPC-I cell cytotoxicity [131], permeability, and stability. The results of the penetration and accumulation experiments demonstrated that the NS resveratrol complex could be applied topically and buccally, and greatly enhance its pharmacological effects overcoming all the limitations of pure drug alone.

J. Thyme loaded beta-cyclodextrin nanosponge

In recent years, natural preservatives' popularity has risen due to their potent antibacterial and antifungal effects [132]. Essential oils are a fascinating field. The hydrophobic nature of most essential oils, however, severely restricts their application in the pharmaceutical industry. They are easily disrupted by changes in temperature or pressure and have low water solubility and bioavailability. The researchers hoped to improve the preservation properties of Thymol essential oil (TEO) by encapsulating it in a β-cyclodextrin (β-CD) nanosponge (NS), and they found that nanoencapsulation is a promising method for overcoming these shortcomings [133].

The optimal conditions for synthesising TEO-NS were found by analysing the solubility, loading capacity, and encapsulation efficiency of TEO. Nanosponges were made using the melt method with varying molar ratios of β-CD and a suitable cross-linker like diphenylcarbonate (DPC). After an overnight incubation for intensive crosslinking, the resulting preparation was washed with water and refined using Soxhlet extraction with ethanol. This was mixed with TEO in various amounts, and freeze-drying was used to create TEO-loaded nanosponges. Solubility of TEO and TEO-NS was analysed separately using UV spectrophotometer at wavelength of 274nm. The produced Nanosponges were subjected to FTIR, XRD, thermal analysis, and morphological characterisation. Antibacterial activity was assessed on *Shigella*, *E.coli* and strains of *Staphylococcus aureus*. Nanosponges were also dispersed in suitable phosphate buffer solution and sealed in dialysis membrane to determine their in-vitro release profile. The solubilities of all TEO-NS batches were up to 41% more than the solubility of the free drug. Although solubility improved with lower β-CD:DPC ratios, but this effect was lost at higher ratios because to the substantial crosslinking that prevented drug contact with the NS cavity. With a mean particle size of less than 326 nm, solid porous structures were inferred from the morphological study. At 1700 to 1200 cm^{-1}, the FTIR spectrum revealed several interactions between TEO and NS. Changes in the absorption band at 1760cm-1 and the lack of weight loss phases in TGA analysis were indicative of successful encapsulation. The crystalline nature of TEO was also shown to diminish after being encapsulated in XRD

pattern. Encapsulated TEO had a lower minimum inhibitory concentration (MIC) and minimum bactericidal concentration (MBC) than free drug. Adding TEO to NS shielded it from the environmental conditions and reduced its volatility, both of which contributed significantly to its enhanced antibacterial potential. The notion that TEO-NS can be used as a preservative without posing any safety concerns which is supported by in vitro research showing a slow sustained release of 67% after 24h.

By making an inclusion complex between TEO and NS the researchers were able to overcome all the drawbacks associated with free TEO. The results undoubtedly demonstrate that TEO-NS have enhanced solubility and antibacterial activity allowing Thymol to be used as a natural preservative in food industry.

K. Econazole nitrate based polymeric nanosponges

Traditional topical treatments for superficial fungal infections (SFI) have relied on creams and ointments for years, but their low efficacy and unregulated drug input have severely limited pharmaceutical utilisation. Such flaws can be fixed by nanocarrier systems like nanosponge, which also improves the drug's antifungal effectiveness. These porous dosage forms can be combined into hydrogel systems for longer release and skin retention, lowering toxicity. A popular imidazole antifungal [134] used in several SFIs is econazole nitrate (EN). As a BCS class II agent, it doesn't mix well with water and has limited dissolving properties. Thus, a delivery mechanism is needed to optimise API's duration on the skin while maximising its body absorption. This study aimed to create EN-loaded nanosponges and incorporate them into hydrogel to improve antifungal topical action.

The emulsion solvent diffusion method was used to create EN-loaded nanosponges with various concentrations of polyvinyl alcohol and ethylcellulose (EC). The internal phase consisted of EN and different amounts of polymer in 20ml DCM, while the exterior phase was PVA in 150 ml water. The organic dispersed phase was introduced gradually to the aqueous continuous phase and agitated at 1000rpm for 2h on a magnetic stirrer. Nanosponges were examined for rheology, entrapment efficiency, particle size, PDI, and in-vitro drug release. The improved formulations were also subjected to further physicochemical characterizations as FTIR, DSC, and SEM. The resulting nanosponges were distinct, roughly spherical particles in the nano range. It was found that mean particle size is affected by drug:polymer ratio. SEM investigation showed perforated orange peel-like features during nanosponge production. Low

PDI and high zeta potential suggest colloidal stability. All nanosponges had satisfactory Carr's index and Hausner's ratio. In-vitro release was higher at pH 6.8 (normal skin pH) than 7.4 (simulated physiological pH). Polymer concentration lowered EN release. The PVA:EC (3:2) nanosponge showed the maximum in-vitro release after 12h. The chosen nanosponge was formulated as a Carbopol 934 NF hydrogel with different concentrations of permeation enhancers like propylene glycol [135] and N-methyl-2-pyrollidone. Hydrogel formulations were tested for viscosity, swelling index, in-vitro permeation, and histology. The pH of all hydrogels was within normal skin ranges, preventing irritation. At pH 6.8, the equilibrium swelling after 4 hours for all formulations was between 0.845 and 0.944g/g. The formulations demonstrated the desired textural properties of low hardness and high adhesiveness, making them suitable topical delivery systems. Permeation profiles fitted zero model, showing regulated drug release. Skin histology revealed no lesions. FTIR of EN showed peaks at 1091 and 1174 cm^{-1} due to C-N stretching. DRS and DSC spectra revealed drug stability and no drug-polymer interaction in nanosponge.

The outcomes unquestionably showed that EN loaded nanosponge could effectively address all the drawbacks of the drug alone and treat SFI more effectively with better patient compliance. The superior efficacy and prolonged retention time of nanosponge-based hydrogels make them a viable alternative to conventional creams and ointments.

L. Griseofulvin based cyclodextrin nanosponge

Griseofulvin (GRI) is a well-known antifungal medication with a proven efficacy and safety profile. However, its water solubility is only 8.64 mg/L, which limits GRI formulation development [136]. Apart from the disadvantages of being a BCS class II agent, it also has a bitter taste, which severely limits its use in children. To overcome this drawback, the strategy of solubility augmentation of GRI has been applied in the past as for example, complexation with β-CD. In addition, cyclodextrin-based nanosponges are on the rise as a result of their superior encapsulating properties. In this study, researchers investigated on GRI cyclodextrin-based nanosponges with the goal of increasing GRI solubility and bioavailability while disguising its bitter taste and providing a new treatment method for paediatrics [137].

Using ultrasonic aided synthesis, three blank nanosponges (NS) were made. β-CD and diphenyl carbonate (DPC) were ultrasonically reacted for 5 h at 100°C. After the reaction, the product was repeatedly washed with ethanol to eliminate any by-products. The nanosponges were

recovered as a whitish powder. Percentage yield and phase solubility diagrams were determined. Drug was loaded in NS at varying NS:drug weight ratios in presence or absence of PVP k30. Percentage drug loading was calculated; Optimized formula was selected on the basis of product,s excellent EE and loading capacity, and it is subjected to the additional characterisation tests like SEM, particle size, PDI, zeta potential, DSC, FTIR, NMR due to its excellent entrapment efficiency and loading capacity. Healthy human volunteers were also tested for GRI NS's taste masking capabilities. Rats were used for in vivo bioavailability tests, and release profiles were compared using difference factor (f1), similarity factor (f2), and dissolution efficiency. Using Resveratrol as a point of reference, a molecular docking study was done to predict the possibility of complex formation [138] and the way GRI would bind to the structure of -CD NS. Higher molar ratios of -CD to DPC led to a higher % yield. The SEM pictures showed that the structures of NS were very porous. High PDI and low zeta potential showed that the suspension was stable and in the nano size range (665.9 nm). The DSC thermograms showed that the medication was no longer crystalline after being encapsulated. Changes in the fingerprint areas (1222, 1176, 1138, and 1049 cm^{-1}) and peak intensity in the FTIR spectrum of GRI-loaded NS indicated a successful complexation. The complexation was also shown by chemical shifts in NMR data. When compared to plain GRI, the dissolution efficiency of GRI-loaded nanosponges was 3.19 times better. The in-vitro release data (figure 10) fit best with Higuchi's release kinetics, which followed a non-Fickian model (n=0.546). Human panel experiments verified GRI nanosponges' ability to mask medication bitterness. Moreover, in rats, C_{max} and AUC_{0-48} went up by 2.13 and 3.78 folds, respectively, compared to plain GRI which showed improved bioavailbility.
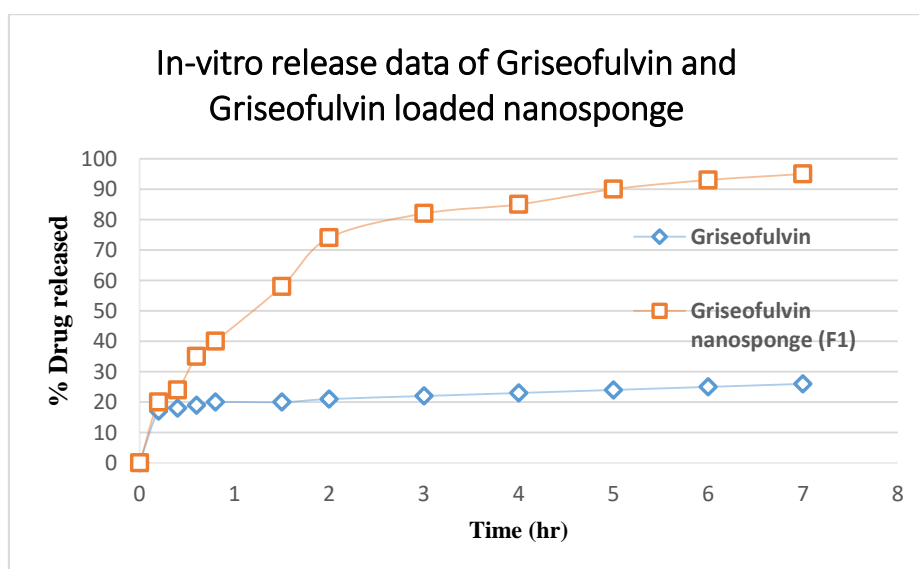
Figure 28: In-vitro release profiles of GRI and GRI loaded NS (adapted from Ref no. 137).

The results unequivocally revealed that this particular formulation has the potential to be utilised as an effective GRI dosage form for administration to paediatric patients in the form of a dry suspension that requires subsequent reconstitution. Researchers were able to use GRI-loaded NS to hide the bitter taste, speed up the rate at which the drug dissolves, and increase the drug's oral bioavailability. To validate the findings and allow for commercialization of this dosage form, additional clinical trials may be required.

Chapter 3
Drug and polymer profile

Griseofulvin

Drug class: Antifungal (Benzofuran derivatives)

Chemical formula: C17H17ClO6

Molecular weight: 352.76

Chemical structure:
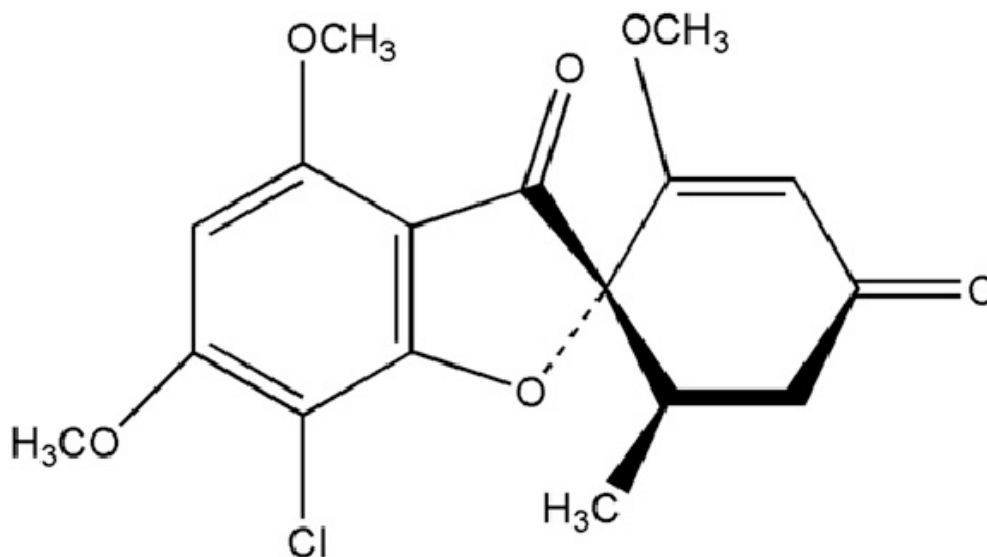
IUPAC: (2*S*)-7-chloro-3',4,6-trimethoxy-5'-methylspiro[1-benzofuran-2,4'-cyclohex-2-ene]-1',3-dione

Melting point: 220ºC

Log P: 2.18   **Log S:** -4.61

Physical state: Solid

Colour: White

Odor: odorless

Generic name: Griseofulvin

Brand name: Gris-peg

Stability: Stable when exposed to air

Storage: Store in 2-5ºC cool temperature.

Absorption: Poorly absorbed from GI ranging from 25 to 70% of an oral dose. Absorption is significantly enhanced by administration with or after a fatty meal.

Metabolism: Primarily hepatic with major metabolites being 6-methyl-griseofulvin and its glucuronide conjugate.

Half-life: 9-21 hours

Solubility: At 25°C, highly soluble in N,N-dimethylformamide (12-14g/100ml) , slightly soluble in ethanol, chloroform, methanol, acetic acid, acetone, benzene, ethyl acetate, practically insoluble in water (<1 mg/ml) and petroleum ether.

Stability: Preparations of griseofulvin have expiration dates of 2-5 years following the date of manufacture.

Uses: Employed in the treatment of ringworm infections of the skin, hair, and nails, namely: tinea corporis, tinea pedis, tinea cruris, tinea barbae, cradle cap or other conditions caused by *Trichophyton* or *Microsporum* fungi.

Mechanism of action: Although griseofulvin is fungistatic, the precise method by which it prevents dermatophytes from expanding remains unknown. Mitosis and the production of nuclear acids in fungal cells may be blocked by this compound. In addition, it attaches to alpha and beta tubulin, which prevents them from performing their normal roles in spindle and cytoplasmic microtubules. After binding to keratin in human cells, it travels to the fungal site of action, where it attaches to fungal microtubes and disrupts mitosis in fungi. Major targets are Tubulin beta chain and Keratin, type 1 cytoskeletal 12.

Adverse effect: Overall, griseofulvin has few adverse effects. It most commonly causes gastrointestinal issues of nausea, vomiting, and diarrhea, as well as headaches and allergic reactions. Other adverse effects include photosensitivity, fixed drug eruption, petechiae, pruritus, and urticaria. It may cause a worsening of lupus or porphyria.

Administration: Griseofulvin is an oral medication. It comes in microsize (250 and 500 mg tablets) and ultra micro-size (125 and 250 mg tablets) forms. The duration of therapy is long (e.g., 6 to 12 weeks for tinea capitis), potentially leading to non-compliance. It is also available in a liquid suspension formulation. Each of these medications should be taken daily for the indicated duration and continued until the patient is clinically asymptomatic.

Ethyl cellulose

Synonyms: Cellulose, ethyl ether, ethylated cellulose.

Chemical structure:
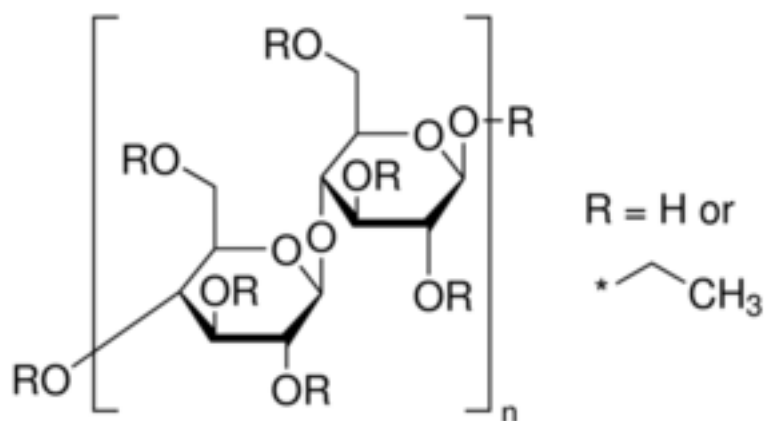
Physical state: Solid

Colour: White to light tan

Odor: Odorless

Melting point: 240ºC **Density:** 1.07-1.18 g/cm^3

Solubility: Soluble in organic solvents like methanol, ethanol, and dichloromethane. Sparingly soluble in hot water. Insoluble in cold water.

Toxic effects: In rat LD50 = 5mg/kg, skin rabbit LD50 = 5mg/kg

Uses: Used as a food additive.

Eudragit RS 100

Eudragit polymers are copolymers derived from ethyl acrylate, methyl methacrylate and a low content of methacrylic acid ester with quaternary ammonium groups. The ammonium groups are present as salts and make the polymers permeable. Their physicochemical properties are determined by functional groups (R). Eudragit polymers are available in a wide range of different physical forms (aqueous dispersion, organic solution, granules and powders).

Chemical structure:
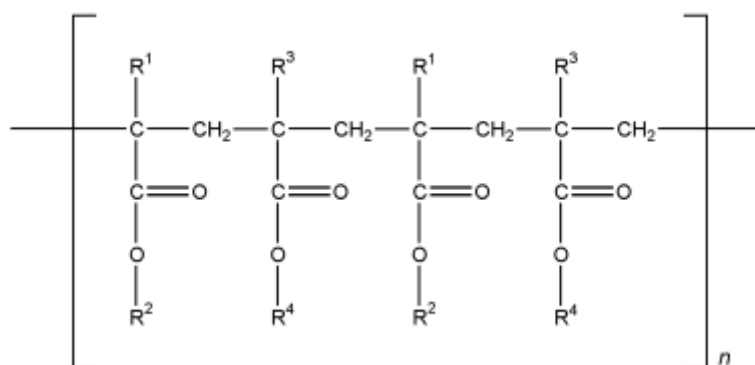
Appearance: Colorless to transparent crystals

Melting point: 394.91°C

Solubility: Miscible with methanol, ethanol, acetone, dichloromethane, ethyl acetate and methylene chloride.

Chapter 4
Aims and Objectives

Aims and Objectives

A well-known way to make polymeric nanoparticles is with the emulsion solvent diffusion process. The process entails adding a diffusing agent to a solution of hydrophobic polymer in an organic solvent, and then homogenising the mixture at high speed. Thermodynamic principles are used, and a solvent that is only partially miscible with water is used in equilibrium with a solvent that is not miscible with water. Once a stable emulsion has been created, the organic solvent can be evaporated by either raising the temperature or by swirling the mixture constantly.

Following are the aims and objectives to be implemented in my M.Pharm dissertation work.

1. To develop griseofulvin loaded nanosponges by using emulsion solvent diffusion technique for its sustained release.
2. Characterization of the prepared nanosponges in order to evaluate its efficacy against commercially available griseofulvin when administered topically.

Plans of work:

i. To identify various physical and chemical properties of drug (griseofulvin) required for the formulation of nanosponge drug delivery system as part of pre-formulation study.
ii. Understand the various physicochemical controlling parameters to formulate stable nanosponges by emulsion solvent diffusion method. Eg: Maintaining the correct room temperature, setting the correct speed of mechanical stirrer, attempting proper centrifugation rpm speeds and so on
iii. Attempt to develop a scale-up method for the optimized formulation of GRI nanosponge in laboratory scale.
iv. Check different properties of nanosponge (characterization) and study of *in vitro* drug release from this delivery system.
v. Perform an antifungal assay and check the efficacy of griseofulvin loaded nanosponges.

Chapter 5
Materials and Methods

1.1 Materials and Reagents

Pure Griseofulvin was purchased from Yarrow Pharma Ltd. Ethylcellulose, dichlormethane and Tween 80 was obtained from Merck India. Sodium alginate was purchased from Sisco Research Laboratories Pvt. Ltd. Eudragit RS 100 was procured from Evonik Industries Germany and 95% Ethanol was purchased from Standard Pharmaceuticals Ltd. All the chemicals used were of analytical reagent grade.

1.2 Pre-formulation studies

1.2.1 Physical Characterization

By visual examination, the drug was identified for physical characters like colour, texture.

1.2.2 Melting point determination

The capillary tubes used for the melting point study were sealed on one end by heating one of the ends over spirit lamp. Griseofulvin was filled into the capillary tubes and after filling some amount of drug inside the capillary tube it was gently tapped on the sealed end to fill the capillary tube for up to 1-2 mm. Then the capillary tube was kept in the tube holder of the melting point apparatus (SUNBIM®). The temperature adjuster knob was adjusted. When the drug started to melt the temperature was noted. At the time when the drug had completely melted the temperature was again observed and noted. The melting point of the drug was the average of both the temperatures noted above. The process was repeated for three times to obtain an optimum result.

1.2.3 Solubility study

Solubility of Griseofulvin was studied in distilled water, organic solvents and phosphate buffer. According to standard specified; Griseofulvin is very slightly soluble in water (0.2 g/L at 25°C); sparingly soluble in ethanol and methanol; soluble in acetone, chloroform and dimethyl formamide and dimethyl sulfoxide.

1.2.4 Preparation of standard curve of griseolfulvin

1.2.4.1 Preaparation of 1N phosphate buffer pH 7.2

Dissolve 6.8g of potassium dihydrogen orthophosphate and 1.56g of sodium hydroxide in 900ml of water. Record the pH in a suitable pH meter. Add 1N concentrated hydrochloric acid dropwise until the pH is adjusted to 7.2.

1.2.4.2 Determination of absorption maxima

Determination of UV absorption maximum was done by scanning 10μg/ml solution of Griseofulvin dissolved in phosphate buffer pH (7.2) in the range between 200-400nm by using UV Spectrophotometer (UV-1800, Shimadzu, Japan).

1.2.4.3 Determination of standard curve of Griseofulvin

Primary stock solution was prepared in a 100ml volumetric flask by dissolving 100mg of accurately weighed Griseolfulvin in phosphate buffer and the concentration was found to be 1000ppm. From this 10ml of solution was pipetted out in a 100ml volumetric flask and the volume was made upto 100ml with phosphate buffer to obtain a secondary stock of 100ppm. From the secondary stock distinct aliquots were made of different concentrations like 2, 4, 6, 8, 10, 12, 14, 16, 18 and 20μg/ml which were scanned at 295nm (λmax) by using UV Spectrophotometer (UV-1800, Shimadzu, Japan) with spectral bandwidth of 1 nm ± 0.3 nm wavelength accuracy. 10 mm pair of quartz cells were used to record the absorbance readings. All samples were analyzed for three times to minimize the error.

1.3 Preparation of nanosponge

Four different nanosponge formulations are prepared using a modified quasi emulsion solvent diffusion technique. Firstly the internal phase is prepared using varied cocnentrations of ethylcellulose and eudragit RS 100, dissolved in 7ml ethanol and 7ml of dichloromethane (co-solvent). To this 100 mg of Griseofulvin is added and agitated using a magnetic stirrer until the internal phase completely dissolves. In a second setup, 100mg of sodium alginate is dissolved in 100 ml of de-ionized water and agitated on a magnetic stirrer, which makes up the external phase. When the contents readily dissolved, 1 drop of Tween 80 is added as a surfactant on the external phase. This is followed by adding the internal phase drop by drop using a 25ml syringe on the external phase which is constantly stirred at 500 rpm for 2 hours using a mechanical stirrer (Remi RQ 121/D) at room temperature. Following stirring, the obtained product is heated for a few seconds to volatilize out any remaining organic solvent. Afterwards cold centrifuge is carried out (Sigma 3K30, laboratory centrifuge) at 16,900 rpm for 30 mins and the supernatant is carefully separated and stored. The rest of the centrifuged product is collected and lyophilized (Scanvac coolsafe) for 12 hours. The resultant white dried mass is used for further characterization studies.

Table 7: Formulation chart of Griseofulvin loaded nanosponges

Ingredients (mg)	Formulations			
	F1	F2	F3	F4
Ethylcellulose	350	525	700	0
Eudragit RS 100	350	175	0	700
Sodium alginate	100	100	100	100
Griseofulvin	100	100	100	100
Dichloromethane (ml)	7	7	7	7
Ethanol (ml)	7	7	7	7
De-ionized water (ml)	100	100	100	100
Nanosponge formation	+	+	+	-

1.4 Characterization of nanosponge

1.4.1 Percentage yield

The percentage yield of nanosponge was determined by measuring the end weight of nanosponges and the initial weight of drug with excipients used in the preparation of nanosponges, i.e. the weight of drug, polymer, and other excipients. Percentage yield of nanosponges were calculated using formula:

$$\%yield = \left\{ \frac{Actual\ weight\ of\ nanosponge\ prepared}{Weight\ of\ drug + Weight\ of\ polymer + Weight\ of\ crosslinker} \right\} * 100$$

1.4.2 Entrapment efficiency

The drug loaded nanosponges have been centrifuged at a high speed of 16,900 rpm for 30 min and the liquid remaining after removing the drug-loaded nanosponges was analysed in a UV spectrophotometer at 291 nm for unbound drug. Then percentage encapsulation efficiency was calculated using the formula:

$$\%EE = \left\{ \frac{Drug\ added - Unbound\ drug}{Drug\ added} \right\} * 100$$

1.4.3 Optical microscopy

Compound light microscope was used to study the appearance of nanosponges. The purpose of performing an optical microscopic analysis is to obtain a magnified view of the substance that is placed in it so that a thorough examination of the substance can be carried out. A small

amount of sample from three formulations F1, F2, F3 was taken and placed on a glass slide to analyze the structure further under microscope.

1.4.4 Particle size, Polydispersity index and Zeta potential

The average particle size and polydispersity index (PI) of the formulated nanosponges was determined by dynamic light scattering. Using Litesizer 500, Anton Paar GmbH, the experiment was performed at 25 °C using clear glass cuvette, and water as a dispersant which has refractive index (RI) - 1.330 and viscosity of 0.88 Cps. Zeta potential of the samples were measured in a disposable Zeta cell. All the samples were analyzed using Kalliope software and for three times to minimize the error.

1.4.5 Fourier Transform Infrared Spectroscopy

To determine if there is a drug-polymer relationship, FTIR was used. To better understand the relationships, individual IR spectra were obtained of blank nanosponge, drug, F1, F2, and F3. Scanning was performed over a range of 4000-400 cm^{-1} for a duration of 3 minutes. Using attenuated total reflectance (ATR) method the samples were pressed against a high refractive-index prism and infrared spectrum was measured using infrared light that is totally internally reflected in the prism. The infrared radiation interacts with the sample, causing the chemical bonds in the drug and nanosponge to vibrate at different frequencies. The resulting absorption spectrum is recorded and analyzed to identify the functional groups present in the sample and to provide information about the drug-nanosponge interaction. Analysis were done on Spectrum Two FT-IR Spectrometer (Perkinelmer) using Perkinelmer spectrum software.

1.4.6 Powder X-ray Diffraction

Powder X-ray diffraction (PXRD) study for drug-loaded nanosponge was performed using SmartLab X-ray Diffractometer, Rigaku. Small amounts of blank nanosponge, F1, F2, F3 and Griseofulvin were pressed on a glass plate and placed inside the XRD instrument. The X-rays are diffracted off the atoms in the sample, producing a diffraction pattern that is captured by a detector. The diffraction patterns were analysed using X'pert Highscore XRD software. Samples were scanned at range of 2 θ from approximately 5° to 40°. The scanning speed used for the recording was 5/min with step size of 0.02.

1.4.7 Differential Scanning Calorimetry

To conduct Differential Scanning Calorimetry (DSC) for drug-loaded nanosponge, a small amount of the sample is taken and placed in a hermetically sealed aluminum pan. The pan is then placed in the DSC instrument (NETZSCH STA 449 F3 Jupiter), which exposes the sample to a controlled temperature program of 20 to 300°C. The samples were purged using inert Argon gas at a flow rate of 20 ml/min. The thermograms obtained from the DSC analysis are then analyzed using NETZSCH-Proteus 61 software to identify the phase transition temperatures, enthalpy changes, and other thermal properties of the drug-loaded nanosponge. These were compared with the thermogram of pure drug to identify any interactions between the drug and the nanosponge matrix.

1.4.8 Scanning electron microscopy

Morphology and size of drug-loaded nanosponges were studied using Scanning Electron Microscopy (SEM). To conduct SEM study, a small amount of the sample is mounted onto stubs using double sided carbon tape, and sputter-coated with platinum-palladium (80:20) in an argon atmosphere to minimize charging effects. The sample is then placed in the SEM instrument, and examined at 3 kV accelerating voltage. The electrons interact with the sample, producing secondary electrons that are captured by a detector. The resulting image provides a three-dimensional view of the surface morphology of the drug-loaded nanosponge, revealing information about its size, shape, and surface texture. SEM studies were performed using GeminiSEM 300, Carl Zeiss Microscopy GmbH.

1.4.9 Transmission electron microscopy

Transmission Electron Microscopy (TEM) is another widely used technique for studying the morphology and internal structure of drug-loaded nanosponge. For TEM study, a small amount of F1 sample is dispersed in deionized water. It is diluted and deposited on a carbon-coated copper grid with micropipette. The solvent is then allowed to evaporate, leaving behind a thin film of the drug-loaded nanosponge on the grid. The grid is then placed in the TEM instrument (JEM 2100F), which is exposed to a beam of electrons at an accelerated voltage of 200 kV. The electrons interact with the sample, producing an image that reveals the internal structure of the drug-loaded nanosponge at a high resolution.

1.4.10 *In-vitro* drug release

In-vitro drug release study was carried out on a jacketed modified type of Franz diffusion cell using dialysis membranes (mol. wt. 12000-14000) with effective surface area of 3.14 cm^2. The procedure involved placing a solution of drug-loaded nanosponges (F1, F2 and F3) inside dialysis membrane and kept in the donor compartment. In a separate receiver compartment, 100 ml of phosphate buffer solution (pH 7.4) was kept at 37 ± 1°C while being stirred with a teflon-coated magnetic bar at a steady rate of 50-70 rpm, so that the surface of the dialysis membrane barely flushed out the solution. To prevent test sample leakage, a circular rubber gasket was placed above the permeation barrier, between the acceptor and donor compartments, and held by clips at the compartments' rims during membrane installation. After 15 minutes of stirring on a magnetic agitator, the membranes in both containers had reached a stable state. In the donor compartment, stabilized nanosponges (equivalent to 10 mg griseofulvin) had been added after 15 minutes. The drug diffusion is monitored by collecting samples from the receiver compartment at regular time intervals for up to 16 hours. To keep the sink condition maintained, 100 ml of phosphate buffer solution (pH 7.4) was replaced by fresh 100ml buffer after every sample collection. The drug release was checked with a UV Visible Spectrophotometer (Shimadzu UV-1800) at 291nm. All samples F1, F2, and F3 have been studied for 12 hours in triplicate.

1.4.11 Kinetics of release

The pharmacokinetics of a medication delivery system can be understood with the use of a kinetic model. Solubility, particle size, crystallinity, and amount of drug, as well as the nature of the vector that encapsulates the drug, all play a crucial role in the release pattern of the drug from the vector. Different kinetic models such as zero-order ($Q_t = K_0 t + Q_0$), first-order ($Q_t = Q_0 e^{-K_f t}$), Higuchi ($Q_t = K_H \sqrt{t} + Q_0$), Korsmeyer-Peppas ($Q_t/Q_\infty = K_k t^n$) and Hixon-Crowell ($Q_0^{1/3}/Q_t^{1/3} = K_s t$) have been used to describe the kinetics of drug release. For these equations, Q_t is the amount of drug released at time t, Q_0 is the initial amount of drug, K_0, K_f, K_H, K_s, K_k are release rate constants for Zero-order kinetics, First-order kinetics, Higuchi model, Hixon-Crowell model and Korsmeyer-Peppas model, respectively.

1.4.12 Antifungal sensitivity assay

The antifungal activity of the drug loaded nanosponges (F1, F2 and F3) and griseofulvin were determined by performing agar well diffusion method. An overnight culture of the test organism (*Candida albicans* MTCC 227) was allowed to grow in sterile Sabouraud dextrose

broth (HiMedia). Sabouraud Dextrose agar plates were prepared, and the cell density of test organism was adjusted using the 0.5 McFarland standard, then the inoculum was streaked on the plates using a sterile cotton swab to develop a lawn culture. For the assay, nanosponges having 10 mg equivalent drug were weighed. 69 mg of F1, 70.5 mg of F2 and 67 mg of F3 were taken. The test compounds were suspended in DMSO. The test samples were allowed to stand for 72 hours, and samples were withdrawn every 24 hours to check the effect of the release of the test compound on activity. With the help of a sterile cork-borer, wells of 8-10 mm diameter were made on the agar plates, and 100 µL of the solution of the test compounds withdrawn at different time frames were added in the respective wells. A solution of griseofulvin (10mg/mL) in DMSO was prepared and kept as standard and from there 100 µL of DMSO was kept as a solvent control. The plates were then kept at a low temperature for 3–4 hours for the compounds to diffuse properly, and then they were incubated at 33± 0.5°C for 16-20 hours. After the incubation period, the zone diameters were measured and recorded using an antibiotic zone reader scale.

Chapter 6

Results and Discussions

1.1 Results and Discussions

1.1.1 Standard curve of GRI in Phosphate buffer 7.2

For determination of drug entrapment efficiency and release of drug from nanosponge, a standard calibration curve was plotted using phosphate buffer solution at pH 7.2. The UV absorbance of Griseofulvin standard solutions in the range of 2-20 µg/ml of drug in buffer pH 7.2 showed linearity at λmax 295nm. The linear curve with regression coefficients should be near to 1 which was obtained from the calibration curve (Figure 29) and corresponding absorbance is shown in table 8. The line equation for phosphate buffer solution at pH 7.2 was found to be: Y = 0.0296X + 0.0801 (R^2=0.9932).

Table 8: Absorbance of various concentrations of GRI at λmax 295nm.

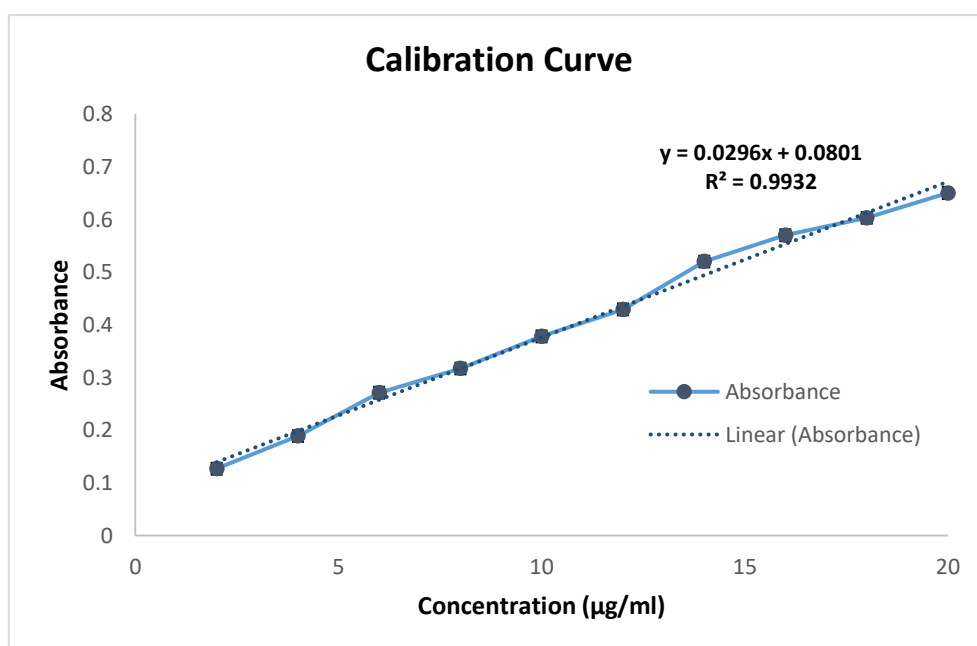| Concentration (µg/ml)	Absorbance
2	0.127
4	0.189
6	0.271
8	0.317
10	0.378
12	0.429
14	0.52
16	0.57
18	0.603
20	0.65

Figure 29: Standard calibration curve of GRI in phosphate buffer solution of pH 7.2

1.1.2 Melting point determination

According to IP melting point of a substance is defined as those points of temperature at which the substance begins to melt and is completely melted except as defined otherwise for certain substances. The melting point of pure griseofulvin was found to be 220-223°C. The reported melting point of griseofulvin is 224.5°C (n=3). Confirmation of melting point indicated the purity of sample [139].

1.1.3 Solubility study

Griseofulvin is very poorly soluble in water (0.2 g/L at 25 °C), sparingly soluble in ethanol and methanol, and soluble in acetone, chloroform, and dimethyl formamide, as per the given standard. An analysis of the drug's solubility in several solvents revealed that it was only minimally soluble in ethanol, chloroform, methanol, and acetic acid, but was easily soluble in N, N-dimethyl formamide (table 9) [139].

Table 9: Solubility of GRI in various solvents.

Sl.no.	Solvent	Observation
1.	N,N-dimethylformamide	Freely soluble
2.	Ethanol, Methanol, Chloroform, Acetone	Slightly soluble
3.	Water	Practically insoluble

1.1.4 Physical characterization

The sample of griseofulvin received was studied for its organoleptic characters such as colour, odour, and appearance as it is one of the first criteria for identification of compound and it shows properties which comply to standards as per IP. The details have been summarized in table 10. Prepared nanosponges were checked for uniformity, texture and appearance and found to be white, smooth and uniform in texture, and having a fluffy characteristic like cotton (figure 30).

Table 10: Physical properties of GRI

Sl no.	Property	Observation
1.	Visual appearance	Crystalline powder
2.	Color	Pale white
3.	Odour	Odorless
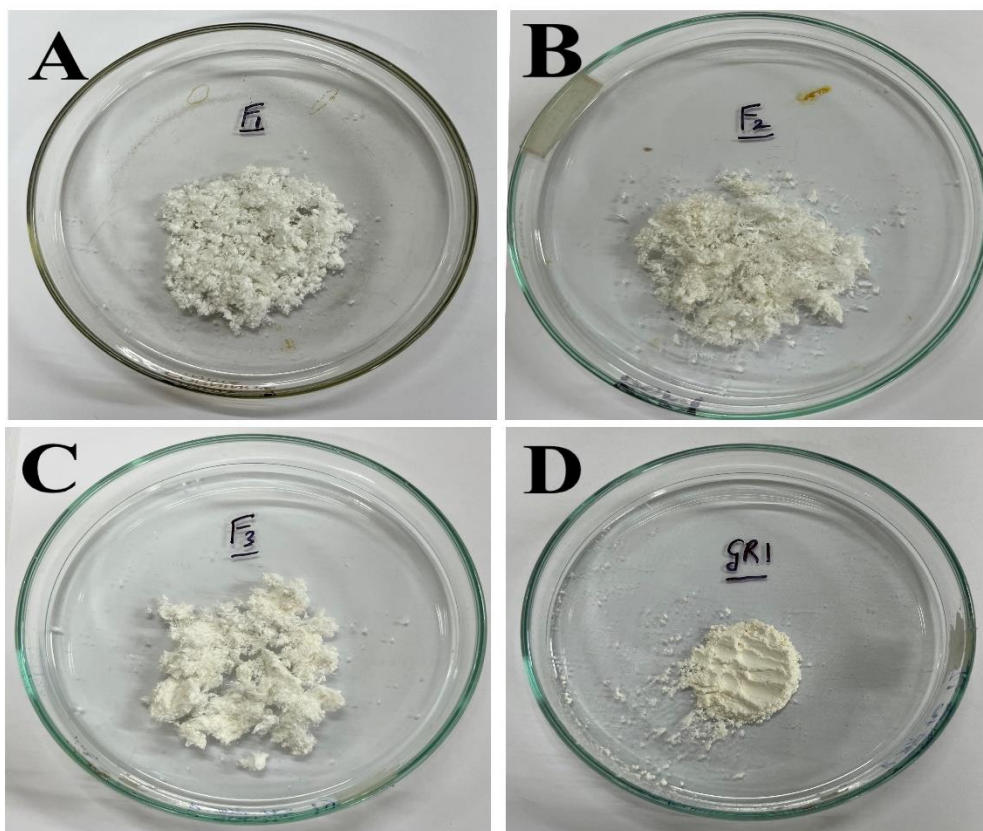
Figure 30: Nanosponges prepared by quasi emulsion solvent diffusion method. Where A: F1 formulation, B: F2 formulation, C: F3 formulation, D: griseofulvin.

1.1.5 Percentage yield and Entrapment efficiency

The interior structure of nanosponges is comprised of void spaces surrounded by a rigid scaffold network. As a result, across all three formulations, entrapment efficiency was found to be quite high, falling between 94.22% and 97.18%. Though passive loading of medication was followed, very small loss by leaching was detected due to stiffness of the polymer network resulting in high entrapment efficiency of the formulations.

By utilizing lyophilization in the last step of fabrication substantial amounts of nanosponges were produced. This resulted in higher practical yield and minimum product loss. Percentage yield was high and ranged between 86.54% and 91.33%. Table 11 summarizes the percentage yield and entrapment efficiency of the three formulations [140].

Table 11: Percentage yield and entrapment efficiency result of the formulations, (Formulation F4 is not mentioned as nanosponge formation did not occur.)

Formulation code	Percentage yield	Entrapment efficiency (%)
F1	91.33	97.18
F2	86.54	94.22
F3	88.25	94.42

1.1.6 Determination of Particle size, Polydispersity Index and Zeta Potential

Mean particle size, PDI and zeta potential values of prepared NS formulations are given in Table 12. The mean particle size was dependent on the quantity of polymers. Increasing the polymer fraction significantly increased the particle size. Particle size was also found to be dependent on crosslinker amount, and an increased concentration of crosslinker gave rise to a small particle size (F1) (figure 31). Polydispersity Index (PDI) is a measure of the range of size distribution. Values greater than 1 indicate that the distribution is poly-dispersed. F1 had the least observed PDI value 0.254. This shows that all the particles of these formulations are in monodispersed region i.e. are of similar size [140]. Electric charge on a nanoparticle surface is measured by zeta potential. Higher magnitudes of zeta potential indicate higher stability (more electrostatic repulsion between the particles), whereas a lower magnitude of zeta potential indicates a flocculated system whereby particles adhere together due to similar charges. Zeta potential values showed that the nanosponges had an agglomerating character due to minimal electrostatic repulsions [141].

Table 12: Mean Particle Size, PDI and Zeta potential values

Formulation	Particle size (nm)	Polydispersity Index	Zeta potential
F1	569.62	0.254	0.4
F2	814.26	0.451	-0.3
F3	864.33	0.405	0.2
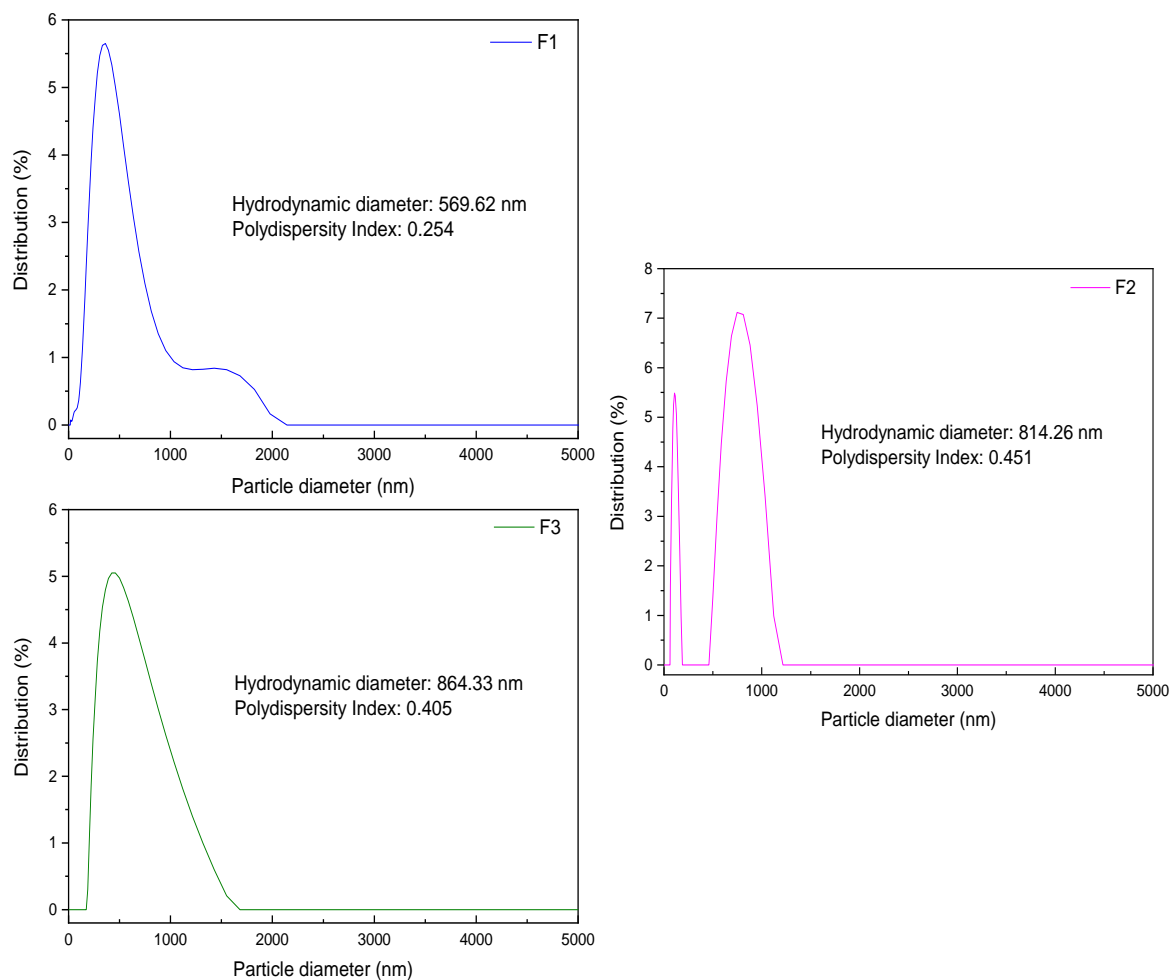
Figure 31: Particle size distribution of three nanosponge formulations: F1, F2 and F3.

1.1.7 Optical microscopy

Optical microscopy analysis was done at 100x magnification to observe the structures of drug loaded nanosponges but it was difficult to observe due to low magnification of trinocular microscope. The images exhibited a spongy and fluffy characteristic like cotton, but no definite shape of nanosponge could be determined (Figure 32). Further characterization through SEM was helpful.
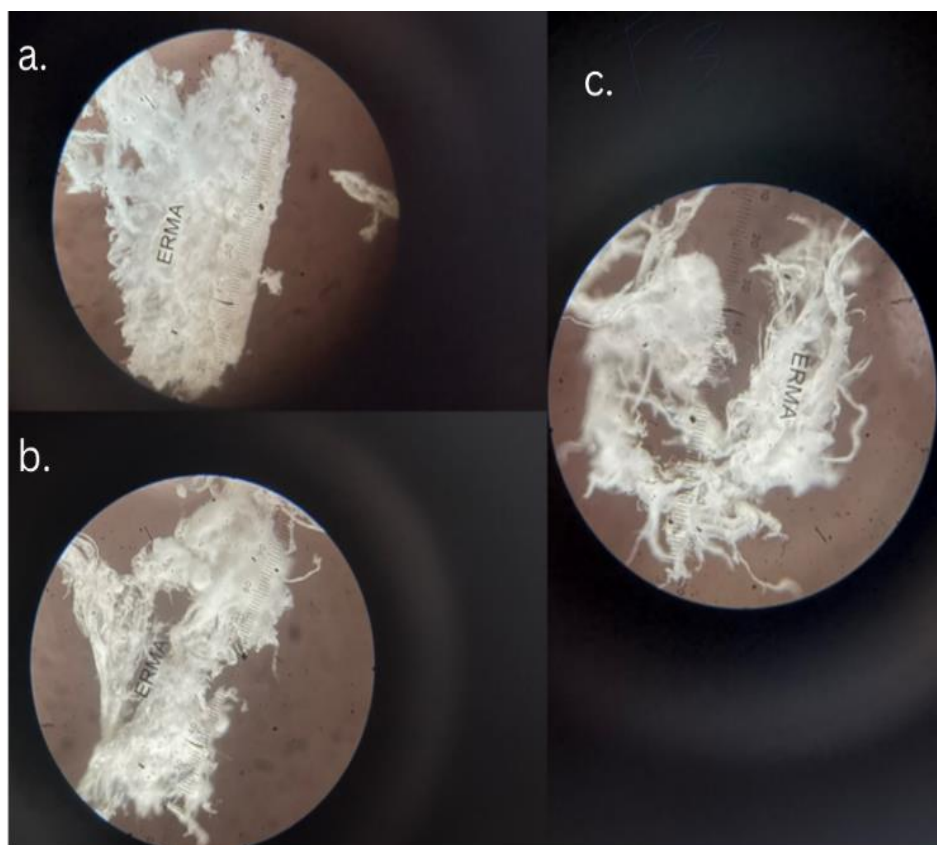
Figure 32: Images of Griseolfulvin nanosponge from trinocular microscope, where a: F1, b: F2, and c: F3.

1.1.8 FTIR (Fourier Transform Infrared Spectroscopy)

Figure 33 represents the FTIR spectrum of drug, blank nanosponge and drug-loaded nanosponges. Each graph was plotted as Wavenumber (cm^{-1}) vs. %Transmittance [142]. FTIR spectra of pure griseofulvin are reported at wave numbers 1708, 1660, 1619, 1587, 1505, 1470, 1428, 1363, 1277, 1248, 1187, 1153, 1064, 1062, 961, 889, 822, 801 and 682 cm^{-1}. Similar peaks were observed in FTIR spectra of drug sample at wave numbers 1704.63, 1656.23, 1613.72, 1584.85, 1503.95, 1464.8, 1428.1, 1359.95, 1271.28, 1240.38, 1192.8, 1154.8, 1071.78, 1053.34, 962.47, 886.45, 823.2, 800 and 678.35 cm^{-1}. In this FTIR spectra of drug, characteristic peak at wave number 678.35 cm^{-1} indicates presence of benzene derivative, 1359.95 cm^{-1} indicates O-H bend of aromatic ring, 1271.28 cm^{-1} indicates C-O stretch of alkyl aryl ether, sharp peak at 886.45 and 823.2 cm^{-1} indicates C-Cl stretch of chloro-benzene ring, peaks at 1704.63 and 1656.23 cm^{-1} indicates C=O stretch of lactum and three peaks at 1613.72, 1584.85 and 1503.95 cm^{-1} indicates C=C stretch of aromatic ring. Occurrence of only expected peaks for functional group at their respective wave number assured the purity of drug [140]. For formulations blank, F1, F2 & F3 peaks at 2928.74, 2974.63, 2974.67 and 2973.92 cm^{-1}

respectively indicate C-H stretching of ethylcellulose polymer. Strong and broad peaks at 1057.84, 1056.48, 1056.04 and 1057.91 cm^{-1} show C-O stretching of the polymer ethylcellulose used in formulations [143]. In FTIR spectra of the blank nanosponges, peak ranging from 1700 to 1750 cm^{-1} confirms the presence of the carbonate bond [144]. Strong band at 1728.95 cm^{-1} of the blank nanosponges indicates the C=O stretching and confirms nanosponges formation. Similar bands at 1728.87 cm^{-1} and 1730.4 cm^{-1} also indicate C=O stretching [66]. C-H bending vibrations are seen at 1445 and 1447.25 cm^{-1} [145]. In nanosponge formulations (F1-F3), there is broadening and disappearance of characteristic drug peaks, which shows that the drug has been successfully entrapped in the scaffold matrix. Due to drug entrapment, the characteristic peaks of the polymers have reduced in intensity.
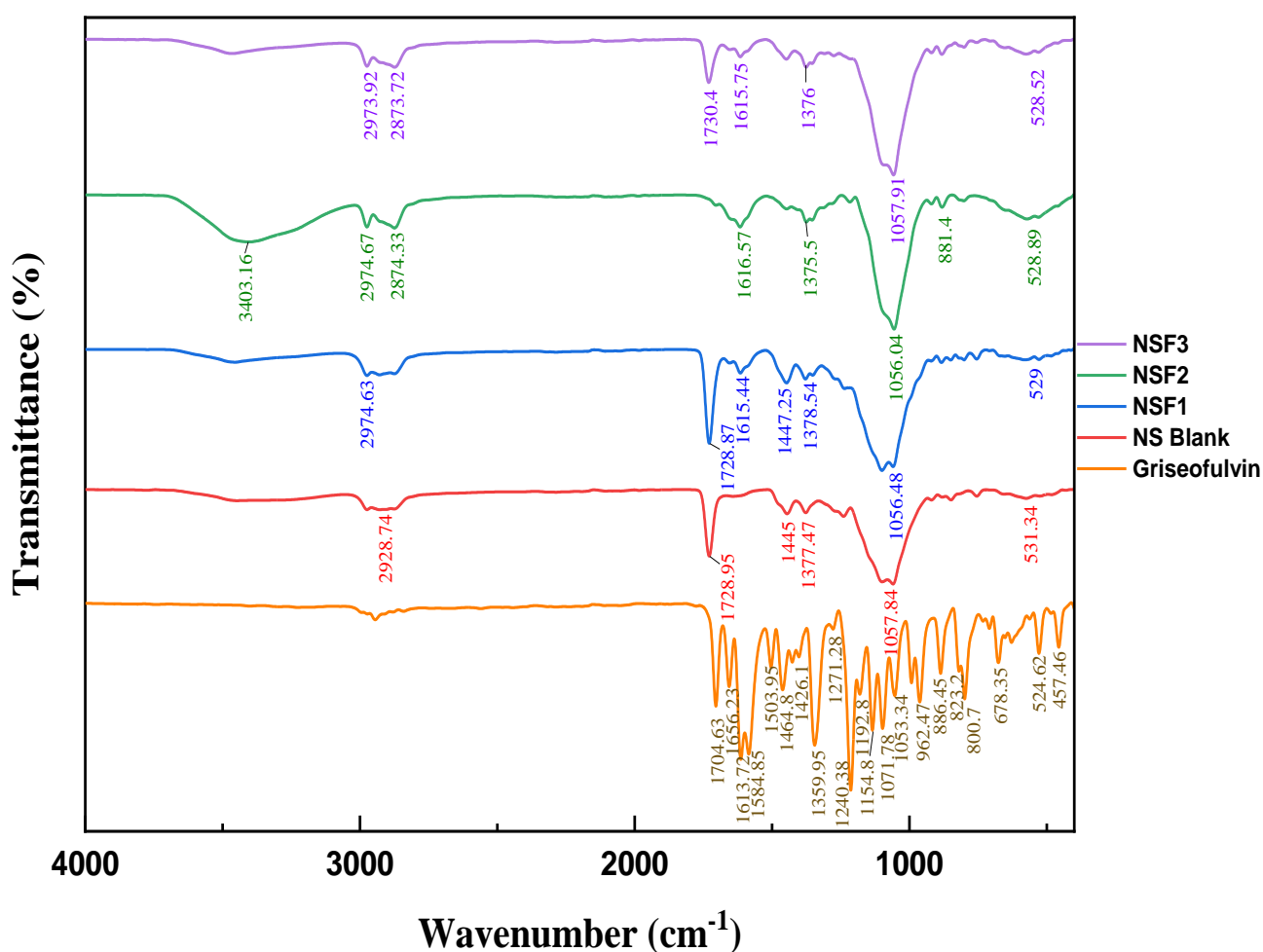

Figure 33: FTIR spectra of griseofulvin, blank nanosponge and drug loaded nanosponge (F1, F2 and F3).

1.1.9 PXRD (Powder X-ray Diffraction)

The evaluation of the diffraction peaks, width, shape, and position provided information about the sample's crystal defects, crystal size, crystalline phase, shape anisotropy, strain, and texture. For sample F1, F2 and F3, it was noted that a few characteristic peaks of griseofulvin had vanished, but the peaks that were visible were all of low intensity. This observation revealed that most of the drug was entrapped into nanosponges [146]. Griseofulvin shows sharp peaks at 10.985º, 13.467º, 14.847º, 16.766º, 19.52º, 20.53º, 21.901º, 22.80º, 24.13º, 26.92º, 28.73º etc. (2θ) amongst which 10.985º, 13.467º, 14.847º, 16.766º, 24.13º, 26.92ºand 28.73º were the most sharp and distinct peaks (figure 34) [139]. Blank nanosponges were distinctively different from drug loaded nanosponges as evident from the XRD spectra which show two broad peaks (Verifying amorphpus nature) [26]. The amorphous nature of nanosponges change when drug gets entrapped and the corresponding crystallinity increases from 17.69% to 53.56% for F1, 47.33% for F2 and 50.88% F3. All the distinct peaks observed in drug were reduced in intensity in F1, F2 and F3 nanosponges, due to successful drug encapsulation (Figure 35) [147].
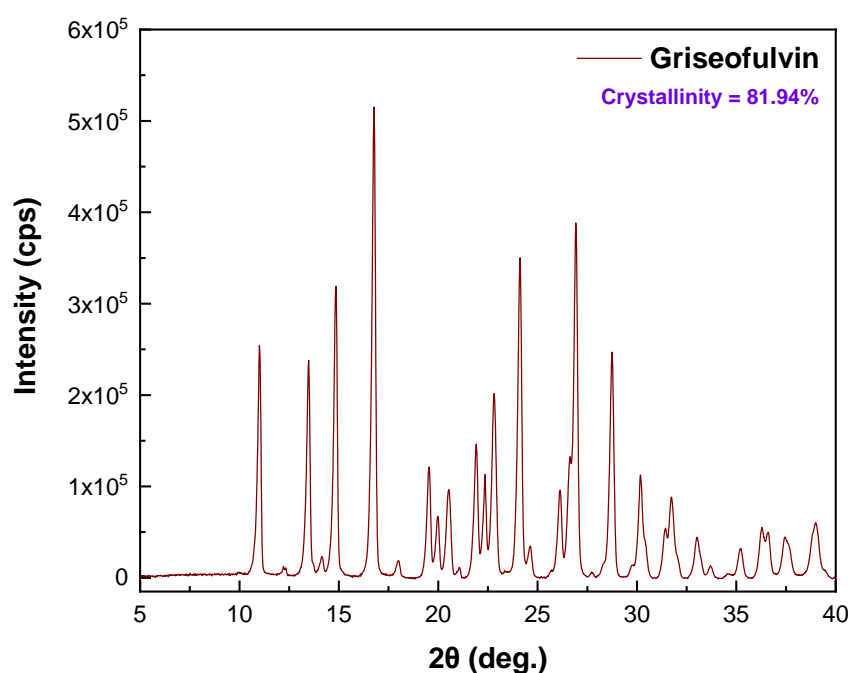
Figure 34: XRD spectra of GRI.
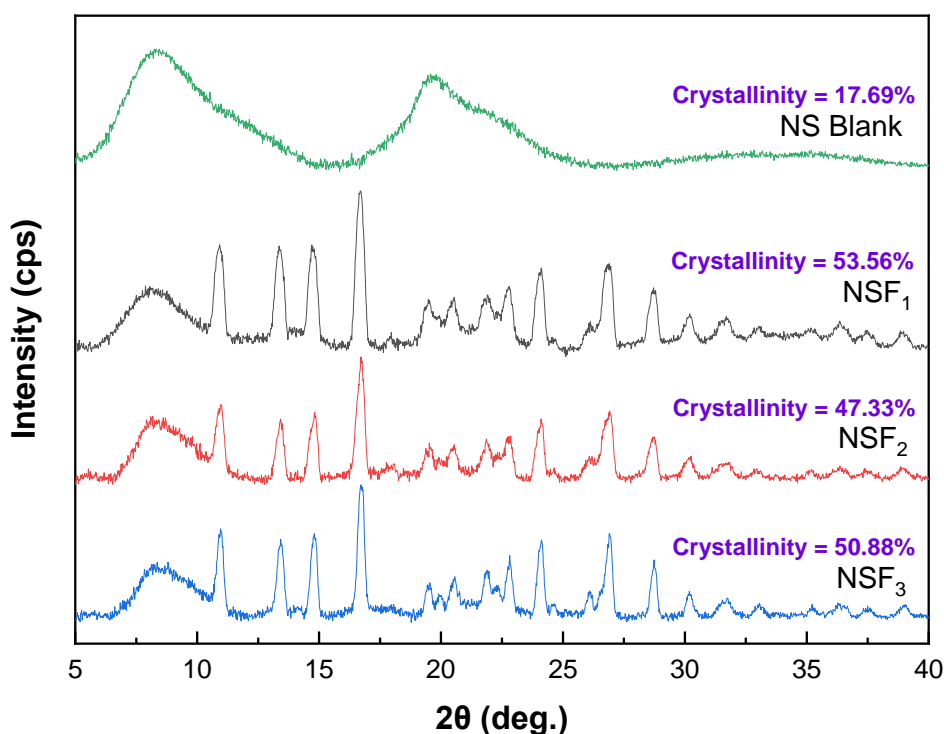
Figure 35: XRD spectra of blank nanosponge and formulations F1, F2 and F3.

1.1.10 DSC (Differential Scanning Calorimetry)

To determine if a complex forms between griseofulvin and nanosponges, DSC was used to study the components behaviour during heating. The complete disappearance of the melting peak of drug is commonly cited as proof that the active moiety has been successfully encapsulated in the nanosponge matrix. This could be because the crystalline part changed into an amorphous form when the inclusion mixture was made [148,149]. Griseofulvin shows a sharp endotherm at 223°C which represents its melting point. For the three formulations (F1, F2 and F3) a broad endothermic depression was observed starting at 227.27 °C (figure 36). This was possibly due to the melting of griseofulvin in drug loaded nanosponges [150]. The disappearance of the drug endotherm was checked in the formulations prepared by freeze-drying. This showed proof of physical interactions between the polymer, cross-linker and active moiety, resulting in loss of crystal structure of drug as well as inclusion complex formation [151]. The DSC findings validate the results from XRD spectra (figure 34,35) which also suggest a decrease in crystallinity of griseofulvin after fabrication of drug loaded nanosponges. Formulation F1

exhibited a glass transition region with its onset at 140.78°C. Absence of any characteristic peaks in the DSC thermograms indicate high nanosponge stability.
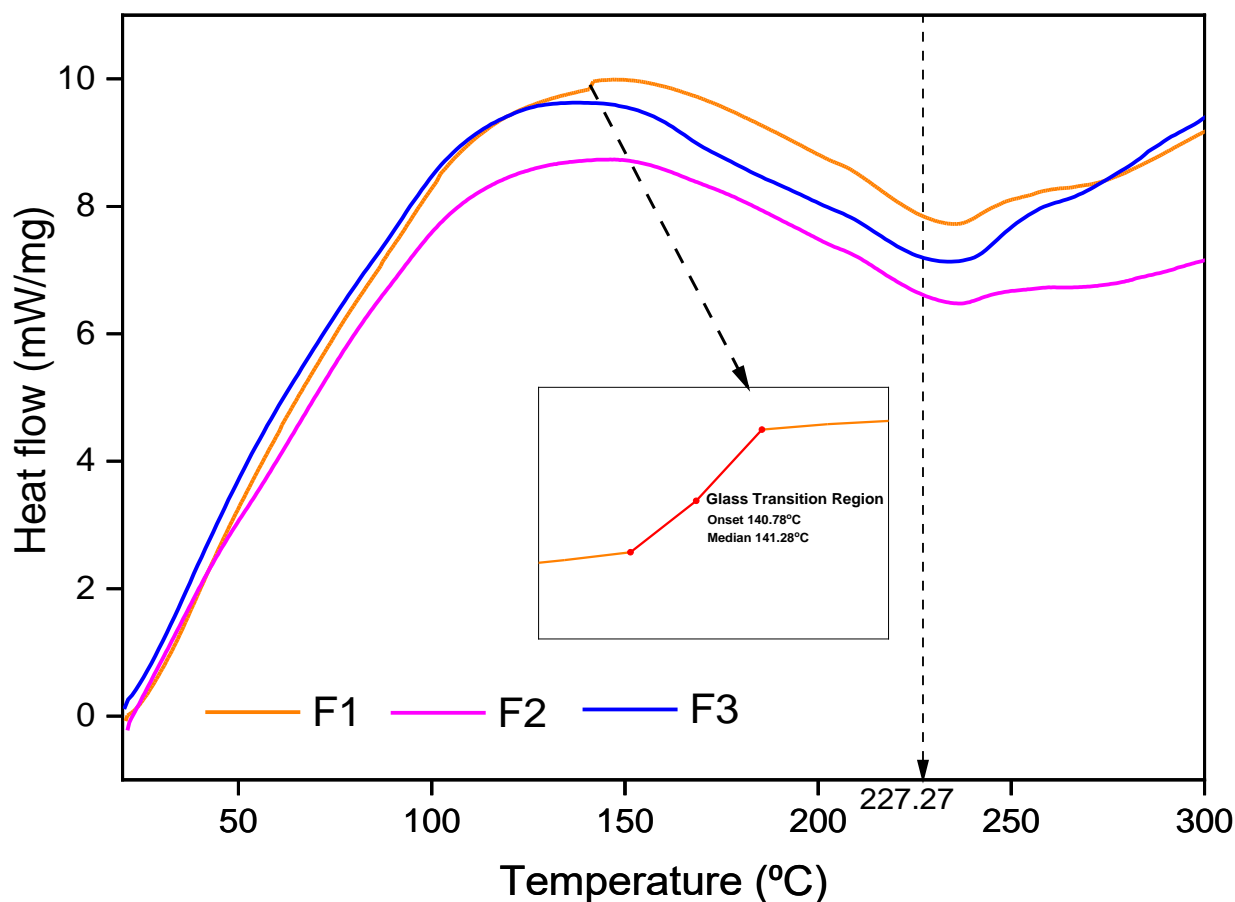
Figure 36: DSC thermogram of drug loaded nanosponges (F1, F2 and F3).

1.1.11 SEM (Scanning Electron Microscopy)

Particle morphologies are evaluated by SEM studies. SEM topography images of nanosponge before and after drug loading with 15000 X magnification are given in figure 37. The characteristic sponge-like morphology of nanosponges are observed in samples before drug loading (blank nanosponge) [152]. In a recent study, it is reported that characteristic sponge like morphology of nanosponges would not change after lyophilization process. The SEM image also concur with the study as lyophilization has been significantly employed during the preparation steps [153]. After drug loading, the smooth porous surface morphology of F1, F2 and F3 indicate drug entrapment into the porous matrix [26]. Polymer and crosslinker concentration also seemed to have an effect on the porous morphology of the nanosponges. As

evident from figure 36, F1 having an optimum concentration of etyhlcellulose and eudragit RS 100 (1:1), had porous diameter of different sizes ranging from 150-800nm. In F2, when 3:1 ratio of polymers were used a uniform porous diameter was observed throughout the sample in SEM. Noticeable changes were observed in F3 with rough and big porous diameters. This suggested that when ethylcellulose was used in highest concentration, it had a noticeable impact on the porosity [140].

It is evident that the prepared nanosponges have a spongy structure. The spongy structure was confirmed from optical microscopy images (Figure 31) as well as from SEM images [154]. The presence of fine orifices on the surface could be caused by diffusion of organic solvents (dichloromethane and ethanol) from the surface of formed nanoporous scaffold during preparation [155]. Also no residual or intact crystals of griseofulvin were observed on the nanosponge surfaces, indicating successful drug entrapment [125]. As explained by *Shende et al*, the extraporous nature of the nansoponge might be helpful for higher encapsulation of drug [15]. The morphological characterization by this microscopy showed that the nanosponges prepared by emulsion solvent diffusion technique, created scaffold of higher porosity. So it could be referred as polymer nature, polymer concentration and method of fabrication can influence surface morphology.

The inner structure of nanosponges consists of void spaces enclosed by a rigid scaffold network that may be constructed from both drug and polymer. Due to which the entrapment efficiency was found to be quite high in the range of 94.22% to 97.18% for all the formulations (F1, F2 and F3) [134]. Though passive loading of drug was followed, very minimal loss by leaching was observed due to rigidity of the polymer network. Therefore, it is evident that ethylcellulose and eudragit based nanosponges are potentially useful for encapsulation of relatively hydrophobic drug like griseofulvin.
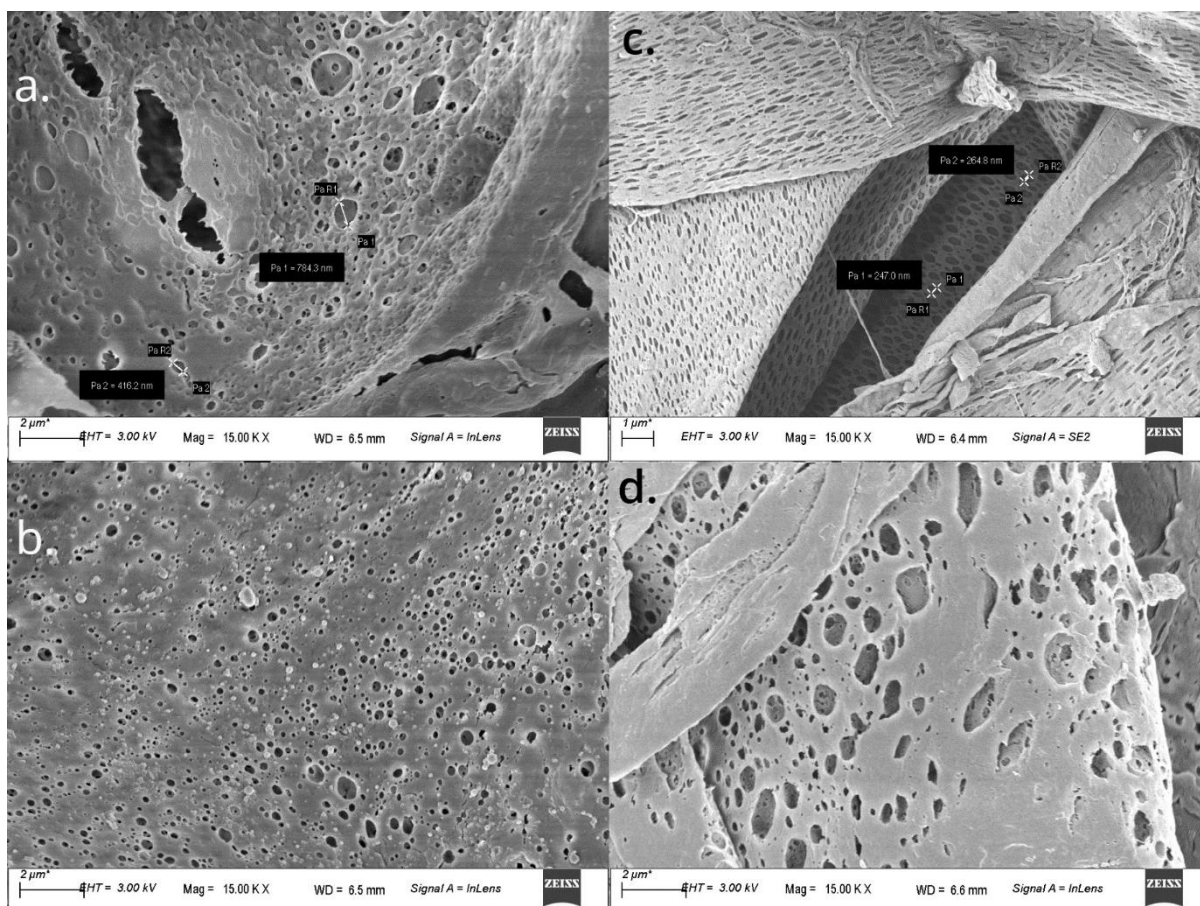
Figure 37: SEM images of all formulations, where a: blank nanosponges, b: F1, c: F2 and d: F3.

1.1.12 TEM (Transmission Electron Microscopy)

TEM analysis was studied to get more structural information of the nanosponges. The TEM images of sample F1 (figure 38) showed that the regular size and shape of the nanosponges were unaffected even after griseofulvin loading [125]. Drug entrapment could be attributed by the black particles encapsulated into the spherical agglomerates. Using Cliff-Lorimer equation (Eq. (1)), the relative concentrations of the elements were determined in the sample. 64.56% C, 36.25% O and 0.16% of Cl was obtained in the chemical composition analysis. Trace amounts of Cl in the sample indeed confirmed griseofulvin presence in the nanosponges.

$$\frac{C_a}{C_b} = K_{ab}\frac{I_A}{I_B} \qquad (1)$$

Cliff-Lorimer equation, where C_a and C_b are weight fraction of two elements, I_A and I_B are the peak intensities and K_{ab} is a constant depending on two elements and operating conditions.
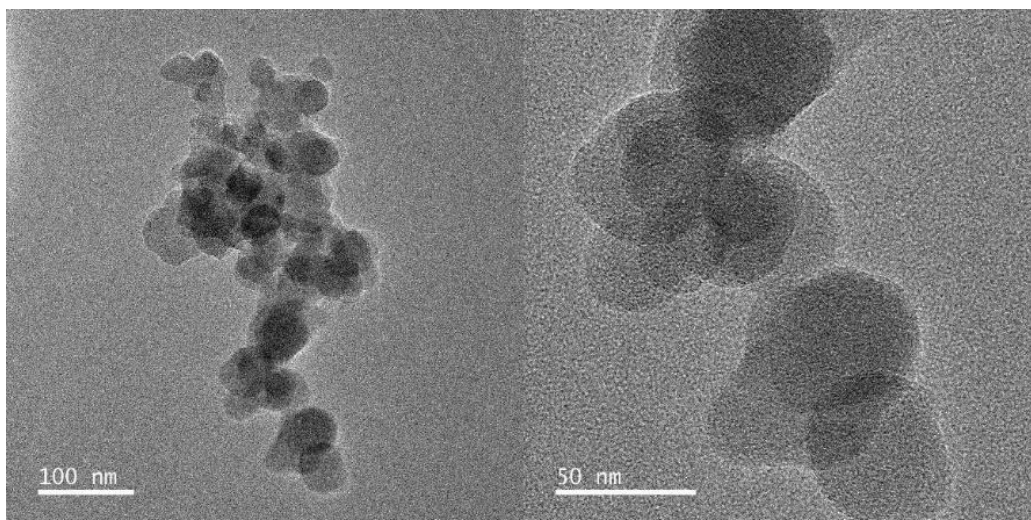
Figure 38: TEM images of F1 nanosponge, scale 100 and 50 nm.

1.1.13 *In-vitro* drug release study

We carried out *in vitro* release study on F1, F2 and F3 samples. F1 released 17.73% drug, F2 released 19% drug and F3 released 20.6% drug after 12 hrs. Further release study was carried out for 4 hrs and F1, F2 and F3 showed 22.86%, 23.54% and 25.16% drug release respectively. So, it is noticeable that the drug loaded nanosponges have more prolonged effect than drug alone (figure 39). Polymer composition of the nanosponge delivery system can have a direct influence on the release rate of entrapped drug [152]. It was also noted that increased cross-linking tends to slow down drug release, probably because increased crosslinking degree decreases the diffusion of the water within the drug delivery system, thus decreasing the drug release [156]. Similarly maximum release was observed in F3 (having no crosslinker) and minimum release was observed in F1 (with maximum amount of crosslinker present). The SEM micrographs also showed the samples having void spaces enclosed by a rigid scaffold network, this led to a very slow release of drug from the prepared nanosponges [157]. Individual dissolution calculations of all formulations have been summarized in table 13, 14 and 15.

Table 13: %CDR Calculation of F1 formulation (n=3)

Time	Absorbance	Concentration (µg)	Cumulative amount (In 100 ml)	Cumulative concentration (mg)	%CDR
1	0.104	0.807432432	80.74324324	0.080743243	0.807432432
2	0.17	3.037162162	303.7162162	0.303716216	3.037162162
3	0.218	4.658783784	465.8783784	0.465878378	4.658783784
4	0.258	6.010135135	601.0135135	0.601013514	6.010135135
5	0.312	7.834459459	783.4459459	0.783445946	7.834459459
6	0.342	8.847972973	884.7972973	0.884797297	8.847972973
7	0.399	10.77364865	1077.364865	1.077364865	10.77364865
8	0.424	11.61824324	1161.824324	1.161824324	11.61824324
9	0.455	12.66554054	1266.554054	1.266554054	12.66554054
10	0.485	13.67905405	1367.905405	1.367905405	13.67905405
11	0.561	16.24662162	1624.662162	1.624662162	16.24662162
12	0.605	17.73310811	1773.310811	1.773310811	17.73310811
13	0.646	19.11824324	1911.824324	1.911824324	19.11824324
14	0.682	20.33445946	2033.445946	2.033445946	20.33445946
15	0.737	22.19256757	2219.256757	2.219256757	22.19256757
16	0.757	22.86824324	2286.824324	2.286824324	22.86824324

Table 14: %CDR Calculation of F2 formulation (n=3)

Time	Absorbance	Concentration (µg)	Cumulative amount (In 100 ml)	Cumulative concentration (mg)	%CDR
1	0.168	2.969594595	296.9594595	0.296959459	2.969594595
2	0.224	4.861486486	486.1486486	0.486148649	4.861486486
3	0.26	6.077702703	607.7702703	0.60777027	6.077702703
4	0.287	6.989864865	698.9864865	0.698986486	6.989864865
5	0.333	8.543918919	854.3918919	0.854391892	8.543918919
6	0.364	9.591216216	959.1216216	0.959121622	9.591216216
7	0.431	11.85472973	1185.472973	1.185472973	11.85472973

8	0.466	13.03716216	1303.716216	1.303716216	13.03716216
9	0.51	14.52364865	1452.364865	1.452364865	14.52364865
10	0.575	16.71959459	1671.959459	1.671959459	16.71959459
11	0.596	17.42905405	1742.905405	1.742905405	17.42905405
12	0.645	19.08445946	1908.445946	1.908445946	19.08445946
13	0.676	20.13175676	2013.175676	2.013175676	20.13175676
14	0.731	21.98986486	2198.986486	2.198986486	21.98986486
15	0.757	22.86824324	2286.824324	2.286824324	22.86824324
16	0.777	23.54391892	2354.391892	2.354391892	23.54391892

Table 15: %CDR Calculation of F3 formulation (n=3)

| Time	Absorbance	Concentration (µg)	Cumulative amount (In 100 ml)	Cumulative concentration (mg)	%CDR
1	0.164	2.834459459	283.4459459	0.283445946	2.834459459
2	0.24	5.402027027	540.2027027	0.540202703	5.402027027
3	0.293	7.192567568	719.2567568	0.719256757	7.192567568
4	0.323	8.206081081	820.6081081	0.820608108	8.206081081
5	0.378	10.06418919	1006.418919	1.006418919	10.06418919
6	0.455	12.66554054	1266.554054	1.266554054	12.66554054
7	0.51	14.52364865	1452.364865	1.452364865	14.52364865
8	0.531	15.23310811	1523.310811	1.523310811	15.23310811
9	0.595	17.39527027	1739.527027	1.739527027	17.39527027
10	0.615	18.07094595	1807.094595	1.807094595	18.07094595
11	0.663	19.69256757	1969.256757	1.969256757	19.69256757
12	0.69	20.60472973	2060.472973	2.060472973	20.60472973
13	0.715	21.44932432	2144.932432	2.144932432	21.44932432
14	0.773	23.40878378	2340.878378	2.340878378	23.40878378
15	0.806	24.52364865	2452.364865	2.452364865	24.52364865
16	0.825	25.16554054	2516.554054	2.516554054	25.16554054
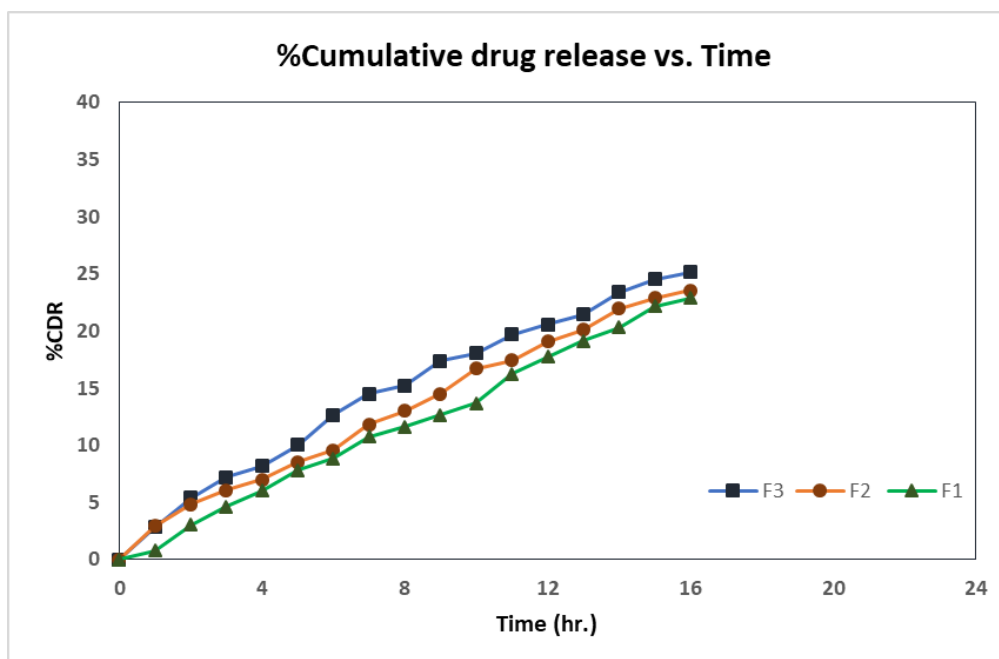
Figure 39: % Cumulative drug release vs. Time of F1, F2 and F3.

1.1.14 Release Kinetics

The release of a drug from the nanoparticle-based formulation depends on many factors including, pH, temperature, drug solubility, polymer amount, desorption of the surface-bound drug, drug diffusion through the nanoparticle matrix, nanoparticle matrix swelling and erosion, and the combination of erosion and diffusion. Nanosponge particle consists of a matrix system where the drug is physically and uniformly dispersed, the drug is released by erosion of the matrix. Rapid burst of drug release may happen owing to the weakly bound drug to the large surface area of the nanoparticle followed by a sustained release [158]. Korsmeyer-Peppas model describes drug release from a polymeric system considering non-Fickian mechanisms transport ($0.45<n< 0.89$) which occurs when the diffusion is entirely controlled by stress-induced relaxations of polymer chains. In the present work, the formulations F1, F2, and F3 show $R^2=0.9777$, $R^2=0.9893$, and $R^2=0.996$ respectively which indicate linearity; and the exponent (n) value of F2 and F3 is 0.7767 & 0.7863 respectively; indicating that these formulations show non-Fickian mechanism as per Korsemeyer-Peppas model. Whereas F1 differs from F2 and F3 as it shows the exponent value of 1.1038 which indicates that it follows super case II mechanism ($n>0.85$). Super Case-II release is the drug transport mechanism associated with stresses of polymer chains that swell in water or biological fluids followed by polymer disentanglement and erosion.

Putting release data of formulations (F1, F2 & F3) to Hixon- Crowell's model (Figure 42), the kinetic profiles show linearity as evident from R^2 values (Table 16). The Hixon–Crowell equation applies to pharmaceutical dosage forms such as tablets, considering that dissolution occurs in planes parallel to the tablet surface which causes the change in surface area and changes the diameter of the particles. In present formulations, diffusion occurs from each nanoparticle individually, and there is a change in surface area and the diameter of the nanoparticle as well as a change in volume due to surface swelling and erosion of biodegradable polymer. It may be the possible reason for its compliance with that of Hixon- Crowell's model. Higuchi model describes the release of drugs from an insoluble matrix as a square root of a time-dependent process based on the Fickian diffusion Equation. Drug release in these formulations does not show any initial lag period as happens in the case of the insoluble matrix (Figure 43). Formulation F3 shows linearity but F1 and F2 deviate from linearity, rather these profiles are biphasic in nature. Overall, this equation (Eq. (2)) serves to classify release profiles as either first-order or zero-order. When the exponent of release, n = 0.5, the system is classified as Fickian with diffusion driving first order release. If n greater than equal to 1, the model is non-Fickian and correlates with zero-order drug delivery, which is governed by forces like swelling and/or polymer chain relaxation. In the case of 0.5 < n < 1, drug release is determined by a combination of diffusion and swelling (mixed order). Hence it can be concluded that Formulation F1 is showing zero order release and F2 and F3 have a mixed order release [159,160].

$$\frac{M_i}{M_\infty} = Kt^n \qquad (1)$$

Korsmeyer-Peppas Mathematical Model. M_∞ represents the amount of drug at equilibrium, M_i represents the amount of drug released over time, K is the release velocity constant, and n is the exponent of release.

Based on the above explanation it is concluded that the mechanism of drug release well fits with that of the Korsmeyer-Peppas model (Figure 44).

Table 16: Summary of r^2 value of various models

Code	Zero order r^2	First order r^2	Higuchi r^2	Hixon-Crowell r^2	Korsmeyer-Peppas r^2	N
F1	0.9963	0.9959	0.9765	0.9963	0.9777	1.1038
F2	0.996	0.9965	0.9733	0.9963	0.9893	0.7767
F3	0.9864	0.9924	0.9921	0.9864	0.996	0.7836

Table 17: Calculation of zero-order kinetics

Time (hr)	Cumulative % drug release		
	F1	F2	F3
1	0.807432432	2.969594595	2.834459459
2	3.037162162	4.861486486	5.402027027
3	4.658783784	6.077702703	7.192567568
4	6.010135135	6.989864865	8.206081081
5	7.834459459	8.543918919	10.06418919
6	8.847972973	9.591216216	12.66554054
7	10.77364865	11.85472973	14.52364865
8	11.61824324	13.03716216	15.23310811
9	12.66554054	14.52364865	17.39527027
10	13.67905405	16.71959459	18.07094595
11	16.24662162	17.42905405	19.69256757
12	17.73310811	19.08445946	20.60472973
13	19.11824324	20.13175676	21.44932432
14	20.33445946	21.98986486	23.40878378
15	22.19256757	22.86824324	24.52364865
16	22.86824324	23.54391892	25.16554054
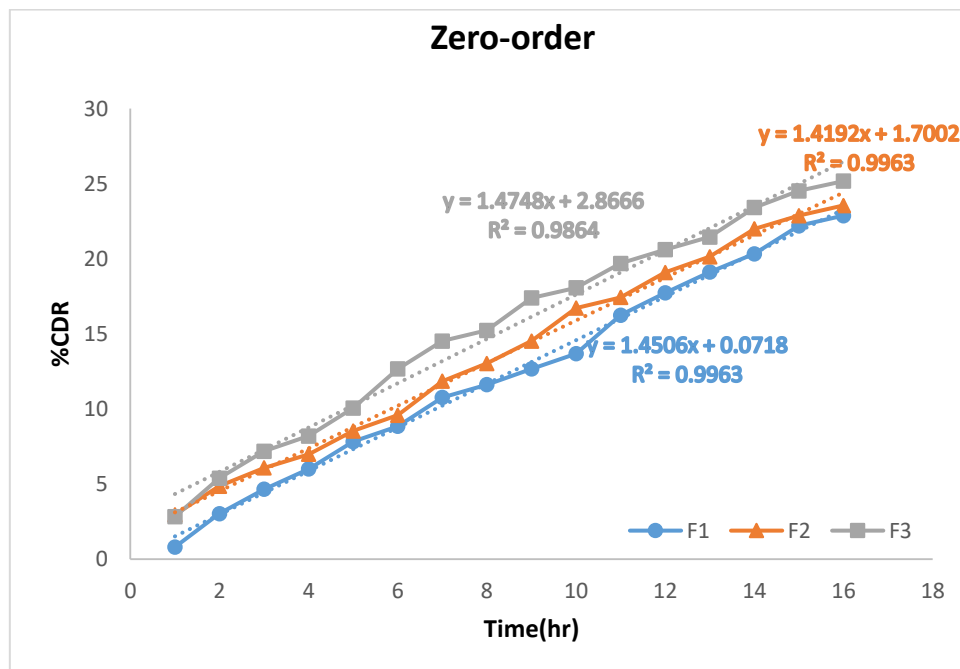
Figure 40: Zero-order release kinetics.

Table 18: Calculation of first-order kinetics

| Time (hr)	Log % Drug Release		
	F1	F2	F3
1	1.996479	1.986908	1.987512
2	1.986605	1.978356	1.975882
3	1.979281	1.972769	1.967583
4	1.973081	1.96853	1.962814
5	1.964569	1.961213	1.953933
6	1.959766	1.956211	1.941186
7	1.950493	1.945199	1.931846
8	1.946363	1.939334	1.928226
9	1.941186	1.931846	1.917005
10	1.936116	1.920543	1.913438
11	1.923002	1.916827	1.904756
12	1.915225	1.908032	1.899795
13	1.907851	1.902374	1.89515
14	1.901271	1.892151	1.884179
15	1.891021	1.887233	1.877811
16	1.887233	1.883412	1.874102
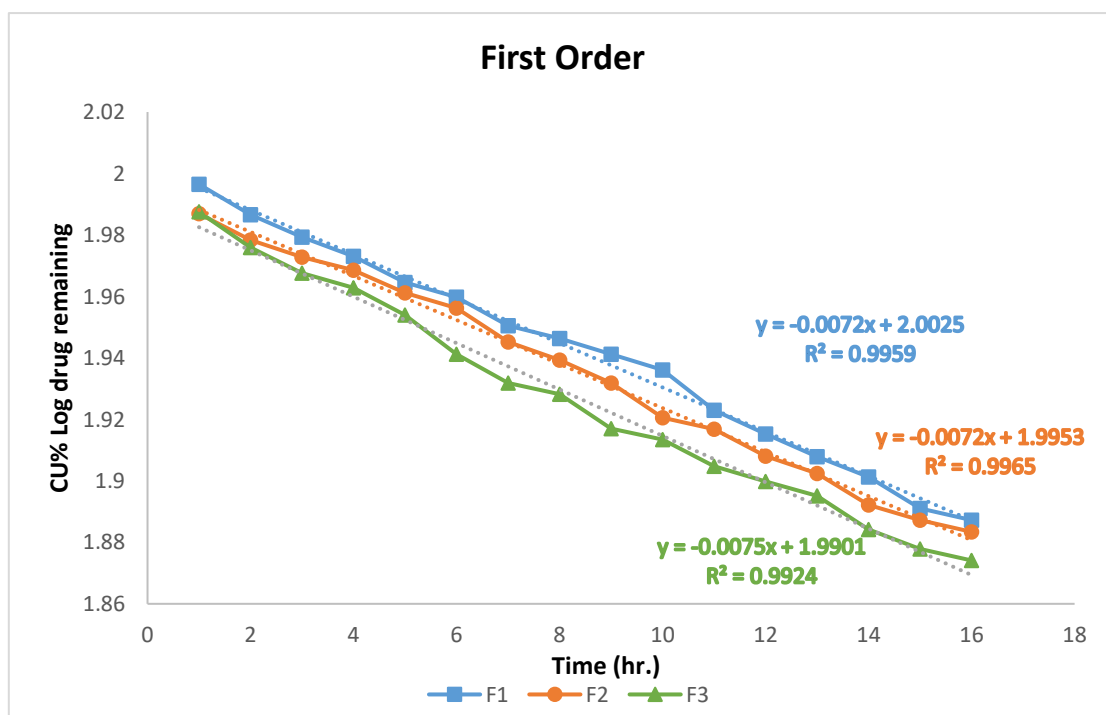
Figure 41: First-order release kinetics.

Table 19: Calculation of Hixon-Crowell model

Time	Cumulative % drug release			Cube root of % drug released		
	F1	F2	F3	F1	F2	F3
1	0.807432	2.969595	2.834459	33.06419	32.34347	32.38851
2	3.037162	4.861486	5.402027	32.32095	31.71284	31.53266
3	4.658784	6.077703	7.192568	31.78041	31.30743	30.93581
4	6.010135	6.989865	8.206081	31.32995	31.00338	30.59797
5	7.834459	8.543919	10.06419	30.72185	30.48536	29.9786
6	8.847973	9.591216	12.66554	30.38401	30.13626	29.11149
7	10.77365	11.85473	14.52365	29.74212	29.38176	28.49212
8	11.61824	13.03716	15.23311	29.46059	28.98761	28.25563
9	12.66554	14.52365	17.39527	29.11149	28.49212	27.53491
10	13.67905	16.71959	18.07095	28.77365	27.76014	27.30968
11	16.24662	17.42905	19.69257	27.91779	27.52365	26.76914
12	17.73311	19.08446	20.60473	27.4223	26.97185	26.46509
13	19.11824	20.13176	21.44932	26.96059	26.62275	26.18356
14	20.33446	21.98986	23.40878	26.55518	26.00338	25.53041
15	22.19257	22.86824	24.52365	25.93581	25.71059	25.15878
16	22.86824	23.54392	25.16554	25.71059	25.48536	24.94482

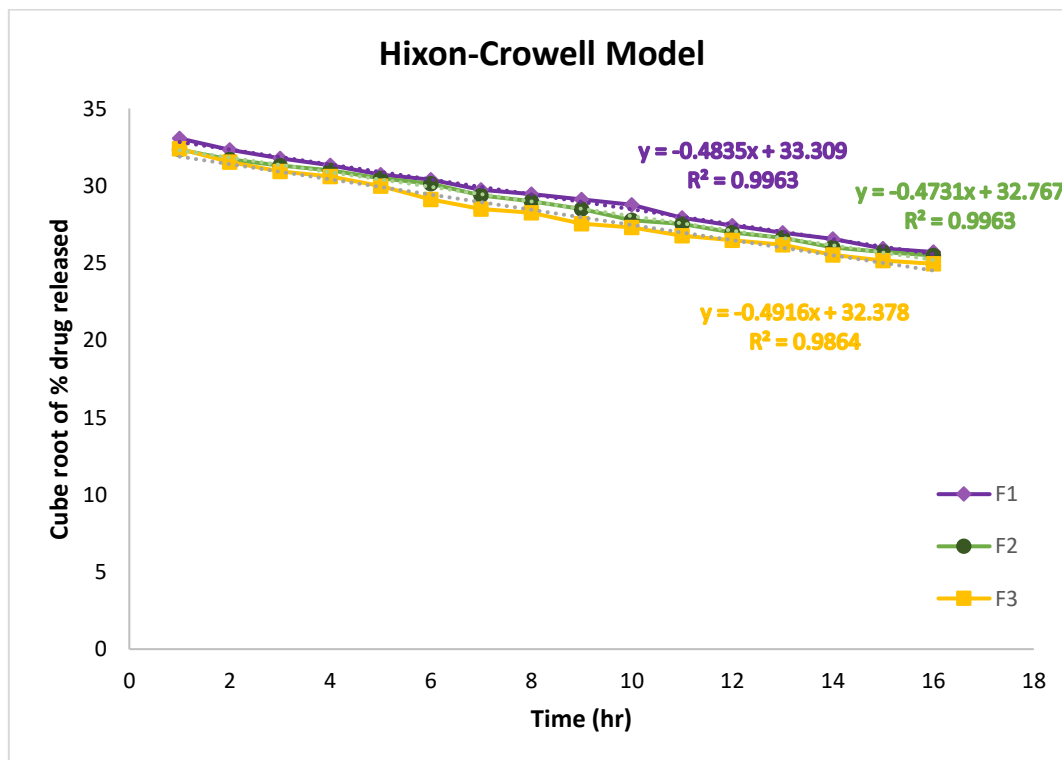**Figure 42:** Hixon-Crowell Kinetics.

Table 20: Calculation of Higuchi model

Time	Sq root of time	Cumulative % drug release		
		F1	F2	F3
1	1	0.807432	2.969595	2.834459
2	1.414213562	3.037162	4.861486	5.402027
3	1.732050808	4.658784	6.077703	7.192568
4	2	6.010135	6.989865	8.206081
5	2.236067977	7.834459	8.543919	10.06419
6	2.449489743	8.847973	9.591216	12.66554
7	2.645751311	10.77365	11.85473	14.52365
8	2.828427125	11.61824	13.03716	15.23311
9	3	12.66554	14.52365	17.39527
10	3.16227766	13.67905	16.71959	18.07095
11	3.31662479	16.24662	17.42905	19.69257
12	3.464101615	17.73311	19.08446	20.60473
13	3.605551275	19.11824	20.13176	21.44932
14	3.741657387	20.33446	21.98986	23.40878
15	3.872983346	22.19257	22.86824	24.52365
16	4	22.86824	23.54392	25.16554

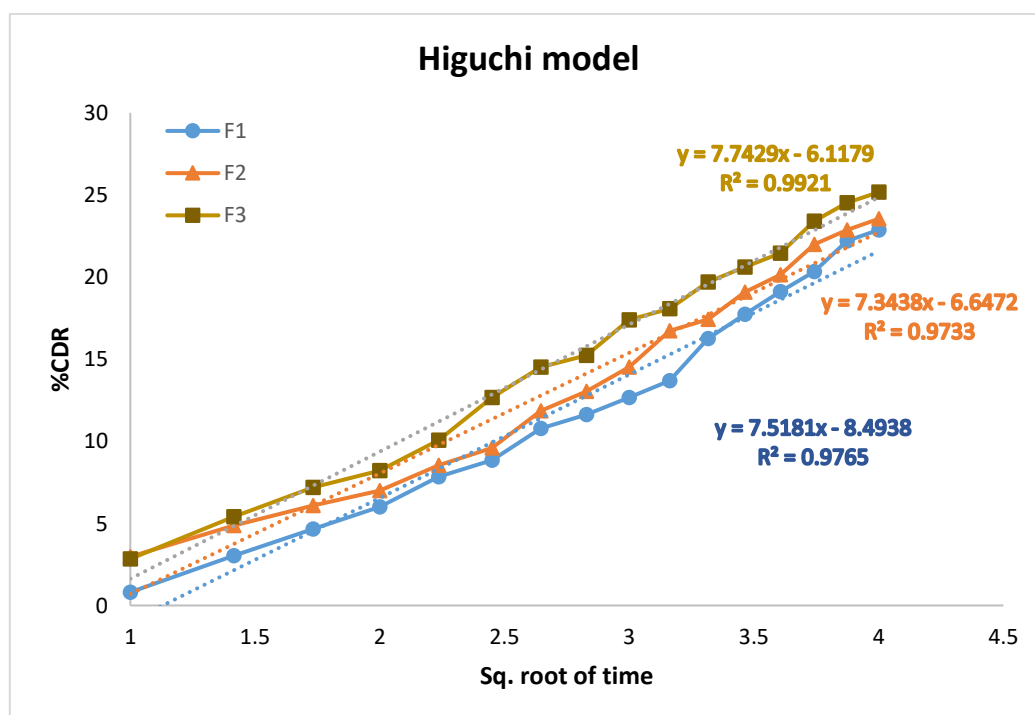**Figure 43:** Higuchi release kinetics.

Table 21: Calculation of Korsmeyar-Peppas model

| Log Time	Log Cumulative % Drug Release		
	F1	**F2**	**F3**
0	-0.09289	0.472697	0.45247
0.30103	0.482468	0.686769	0.732557
0.477121	0.668273	0.783739	0.856884
0.60206	0.778884	0.844469	0.914136
0.69897	0.894009	0.931657	1.002779
0.778151	0.946844	0.981874	1.102624
0.845098	1.032363	1.073892	1.162076
0.90309	1.06514	1.115183	1.182789
0.954243	1.102624	1.162076	1.240431
1	1.136056	1.223226	1.256981
1.041393	1.210763	1.241274	1.294302
1.079181	1.248785	1.28068	1.313967
1.113943	1.281448	1.303882	1.331414
1.146128	1.308233	1.342223	1.369379
1.176091	1.346208	1.359233	1.389585
1.20412	1.359233	1.371879	1.400806
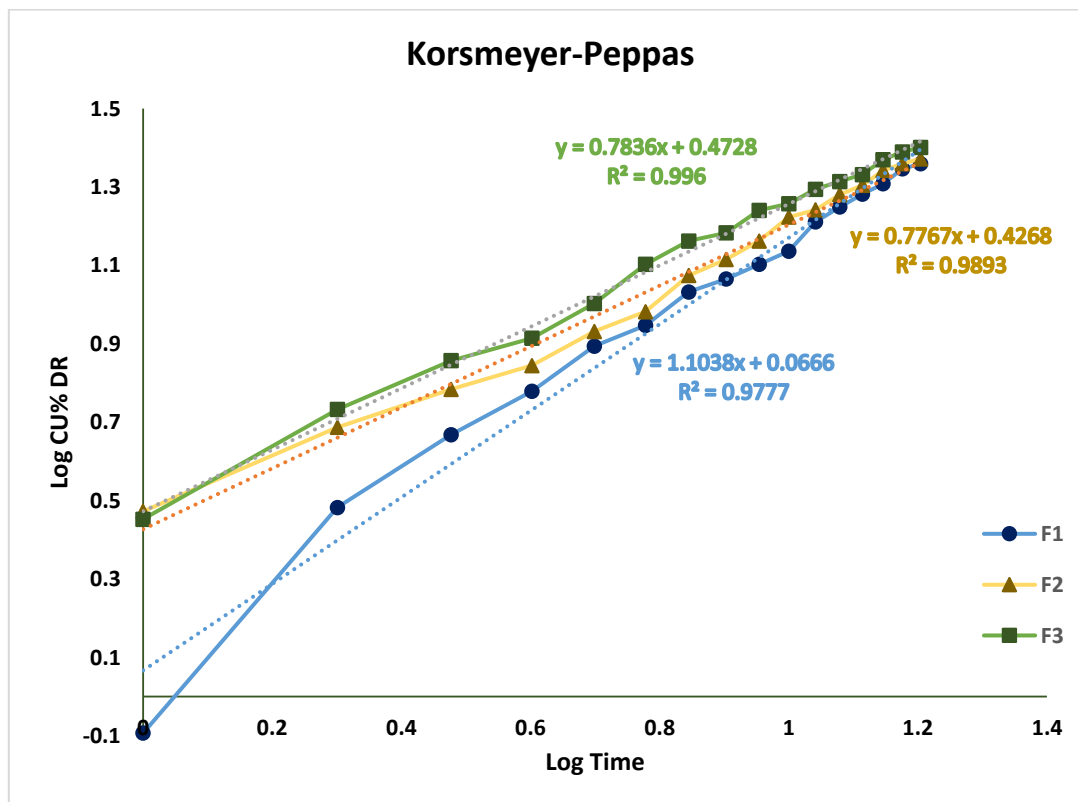
Figure 44: Korsmeyar-Peppas kinetics.
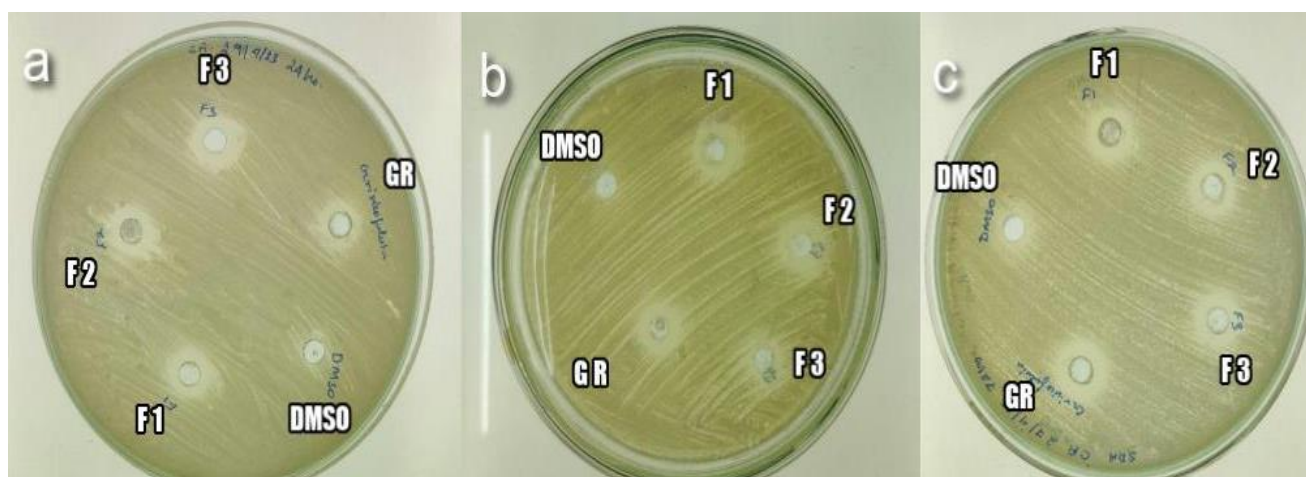
1.1.15 *In-vitro* antifungal assay

Figure 45: Antifungal activity assay, where a: after 24 hours, b: after 48 hours, c: after 72 hours.

In-vitro results of antifungal activity performed against the fungal strain *C. albicans* is represented in figure 45. All the formulations tested (F1, F2 & F3) were found to be active against *C. albicans*. Zone of inhibition (mm) exhibited by pure griseofulvin was 19 ± 0.1 after 24, 48 and 72 hrs. Formulation F1 showed zone of inhibition (mm) of 13 ± 0.2 after 24 hrs, 16 ± 0.1 after 48 hrs and 17 ± 0.1 after 72 hours. Almost similar observations were noted in F2 with zone of inhibition (mm) of 14 ± 0.2 after 24 hrs, 15 ± 0.3 after 48 hrs and 17 ± 0.1 after 72 hours. F3 exhibited a higher zone of inhibition (mm) of 15 ± 0.3 after 24 hrs, 17 ± 0.1 after 48 hrs and 19 ± 0.1 after 72 hrs in comparison to other formulations. An increase in zone diameter with a long time frame may be due to the release of more antifungal agent from the particulate formulation [161]. This observation is at par with the release studies performed earlier. F3 has showed a higher %CDR that any other formulations (figure 39).

According to classification of antimicrobial activity three levels are reported: strong activity (microorganism is very sensitive), moderate activity (microorganism is intermediate sensitive), and weak activity (microorganism is resistant). The zones of inhibition were interpreted using the Laboratory Manual of Standardized Methods for Antimicrobial Sensitivity Tests (Tendencia 2004; Table 22) [162].

Table 22: Zones of Inhibition Interpretative Standard for some important Test Microorganisms.

Test Organism	Interpretative Criteria		
	Sensitive	**Moderate**	**Resistant**
Candida albicans	≥ 18	14-17	≤ 13
Aspergillus niger	≥ 15	10-14	≤ 10
Escherichia coli	≥ 18	14-17	≤ 10
Aspergillus flavus	≥ 15	10-14	≤ 10
Bacillus subtilis	≥ 18	14-17	≤ 10
Staphylococcus aureus	20	-	19

As per the clause of antimicrobial activity, fabricated F3 formulation was considered to elucidate the highest antifungal activity and also exhibited a sustain release of griseofulvin throughout 72 hours. Larger the zone of inhibition, lower the minimum inhibitory concentration (MIC) and conversely the microorganisms are most susceptible to F3 [163]. Table 23 shows the mean zones of inhibition in different time intervals against *C. albicans* strain.

Table 23: Zone of inhibition diameter of pure drug and formulations F1, F2 and F3

Test Compounds	Zone diameters in mm at different time frames		
	24hrs	**48hrs**	**72hrs**
Griseofulvin	19	19	19
F1	13	16	17
F2	14	15	17
F3	15	17	19
DMSO	No zone of inhibition	No zone of inhibition	No zone of inhibition

Chapter 7
Summary and Conclusion

Summary and Conclusion

Nanosponges can carry both lipophilic and hydrophilic medicines, releasing them in a controlled and predictable fashion. Particle size and release rate can be adjusted by altering the polymer to cross-linker ratio. Controlled release and protection from physicochemical degradation of the active moieties are made possible by encapsulation of medicines into nanosponge. Nanosponges, because of their diminutive size and round shape, can be formulated into a variety of dosage forms, including parenteral, aerosol, topical, tablets, and capsules. These tiny mesh-like structures are five times more effective in delivering drugs for cancer than conventional ways, and they may transform the treatment of numerous diseases in future. By minimising the need for several dosing sessions and adverse effects, topical nanosponges may increase patient adherence and efficacy.

When used as part of a topical drug delivery system, nanosponges are able to keep medications in place on the skin for an extended period of time. Therefore, it draws the conclusion that nanosponges may have a significant function in the therapeutics of various diseases. Nanosponges, as nano-sized colloidal carriers, are small enough and porous enough to be quickly absorbed through the skin. They enhance the solubility of poorly soluble medicines and boost their bioavailability by binding them within the matrix. These nanospheres are made from a polymer and can encapsulate or suspend a wide range of compounds before being added to a finished gel, lotion, cream, ointment, liquid, or powder. Entrapping substances with this method reduce the potential for adverse reactions, boosts stability, adds sophistication, and expands the range of possible formulations. Incorporating nanosponges into topical drug delivery systems for retention of dose form on skin, as well as using oral drug delivery using bio-erodible polymers, particularly for colon specific delivery and controlled release drug delivery system, might improve patient compliance by offering site specific drug delivery system and prolonging dosing intervals.

Before preparation of the topical delivery system, pre-formulation studies are necessary for drug and polymers used in formulation. Characteristics were compared for physical mixture and formulation. For the drug candidate melting point was determined and its solubility was assessed. The λmax of GRI was determined and standard curve was plotted. Instrumental analysis (FTIR, PXRD and DSC) was performed for drug, blank nanosponge (having only polymers) and drug loaded nanosponges (drug + polymer) to check any interaction among ingredients. Particle size, PDI, Zeta Potential were also assessed for the nanosponges.

- From DSC study, it was concluded that crystalline drug may have converted to amorphous phase as it did not show any endothermic peak in the DSC thermogram like pure drug. The disappearance of the drug endotherm was checked in the formulations prepared by freeze-drying. This showed proof of physical interactions between the polymer, cross-linker and active moiety, resulting in loss of crystal structure of drug as well as inclusion complex formation.

- From FTIR spectra it was concluded that there was no chemical interference between drug and polymers. Some of the peaks of drug are not visible in the FTIR spectrum of Nanosponge formulation. It suggests that some functional groups of drugs form weak Vander Waals force with that of polymers. Due to drug entrapment, the characteristic peaks of the polymers also have reduced in intensity of drug loaded nanosponge when compared with blank nanosponge spectra.

- From PXRD data, it was well established that the drug lost its high crystallinity when being entrapped in the nanosponge matrix. Blank nanosponges were also distinctively different from drug loaded nanosponges as evident from the XRD spectra which showed two broad peaks.

- SEM and TEM studies gave a brief idea of the surface morphology of the nanosponges and small pores throughout the structure proved its high porosity.

- Particle size of the formulations ranged between 569.62nm to 864.33nm. PDI values indicated a monodispersed formulation and Zeta potential showed that the nanosponges agglomerated with each other due to similar charges.

- Antifungal sensitivity assay was successful and zone of inhibition was observed in all the formulations. Significant antifungal activity was observed against *C.albicans* just like pure drug alone, but the only difference was that the release of drug was slow and sustained from the nanosponges.

- Finally release kinetics and in-vitro release study showed that the drug loaded nanosponges follow Korsmeyer-Peppas model of release and the rate of release is slow and sustained with only 25% CDR (cumulative rate of drug release) in 16 hours, with no lag time. From the results it can be concluded that griseofulvin loaded nanosponges can be used as a means for antifungal drug delivery against various topical skin infections.

Chapter 8

References

List of References

1. S.P. Vyas, R.K. Khar. Targeted and Controlled Drug Delivery – Novel Carrier Systems: Molecular Basis of Targeted Drug Delivery. CBS Publishers and Distributors; New Delhi: 2012: 38-40.

2. Selvamuthukumar S., Anandam S., Kannan K., Manavalan R. Nanosponges: A Novel Class of Drug Delivery System – Review. Journal of Pharmacy & Pharmaceutical Sciences, 2012; 15(1): 103-11.

3. Patricia Vsan Arnum, Nanosponges – a controlled release nanoparticle system, shows promise in targeted drug delivery. 2016; 35(5): 56-60.

4. Preethi S., Ananya K.V, Patil A.B., Gowda D.V., Recent Review on Nanosponge. International Journal of Research in Pharmaceutical Sciences. 2020; 11(1): 1085-1096.

5. Benet Z.L., BCS and BDDCS. Bioavailability and Bioequivalence: Focus on physiological factors and variability. Department of Biopharmaceutical sciences, University of California, San Francisco, USA, 2007.

6. Ajay Vishwakarma et al: Nansoponges: A Benefication for Novel Drug Delivery. International Journal of Pharmaceutical Technology and Research. 2014; 6(1): 11-20.

7. Patricia Vsan Arnum, Nanosponges – a controlled release nanoparticle system, shows promise in targeted drug delivery. 2016; 35(5): 56-60.

8. Trotta F., Tumiatti V., Cavalli R., Rogero C., Mognetti B., Berta G. Cyclodextrin-based nanosponges as a vehicle for Antitumoral drugs. WO 2009/003656 AI; 2009.

9. Shivani S., Poladi K. Nanosponges – Novel emerging drug delivery system: a review, International Journal of Pharmaceutical Science and Research, 2015; 6(2): 529-540.

10. Hayiyana Z., Choonara Y.E., Makgotloe A., et al. Ester-Based Hydrophilic Cyclodextrin Nanosponges for Topical Ocular Drug Delivery. Curr Pharm Des. 2016; 22(46): 6988-6997. https://doi.org/10.2174/1381612822666161216113207

11. Ghurghure M.S., Ka K., Ys T., Ma P. Preparation and in-vitro evaluation of Itraconazole loaded nanosponges for topical drug delivery. Indo American Journal of Pharmaceutical Research. 2019; 9(04): 1999-2011

12. Salisbury D. Nanosponge drug delivery system more effective that direct injection. Nashville: Vanderbilt University; 2010, accessed on 06.01.23

13. Gholibegloo E., Mortezazadeh T., Salehian F., Forootanfar H., Firoozpour L., Folic acid decorated magnetic nanosponge: An efficient nanosystem for targeted curcumin delivery

and magnetic resonance imaging, Journal of Colloid and Interface Science, 2019; 556: 128-139

14. Jenning, V., Schäfer-Korting, M., Gohla, S. Vitamin A-loaded solid lipid nanoparticles for topical use: drug release properties. Journal of Controlled Release, 2000; 66(2-3): 115–126

15. Pawar S., Shende P., Diversity of β-cyclodextrin-based nanosponges for transformation of actives, International Journal of Pharmaceutics. 2019; 565: 333-350.

16. Shringirishi M., Prajapati K.S., Mahor A., Yadav P., Verma A., Nanosponges: a potential nanocarrier for novel drug delivery – a review. Asian Pacific Journal of Tropical Disease, 2014; 4(2): 519-526.

17. Rao M., Bhingole R.C. Nanosponge-based pediatric-controlled release dry suspension of Gabapentin for reconstitution. Drug Development and Industrial Pharmacy. 2015; 41(12): 1-8.

18. Taleb A.S., Moatasim Y., Gaballah M., Asfour H.M. Quercitrin loaded cyclodextrin based nanosponge as a promising approach for management of lung cancer and COVID-19, J Drug Deliv Sci Technolo, 2022; 77:103921-25.

19. Shankar S., Linda P., Loredana S., Francesco T., Pradeep V., Dino A., Michele T., Gianpaolo Z., Roberta C., Cyclodextrin-based nanosponges encapsulating camptothecin: Physicochemical characterization stability and cytotoxicity. Eur J Pharm Biopharm. 2013; 74(2):193-201.

20. Swaminathan S., Vavia P.R., Trotta F., Cavalli R. Nanosponges encapsulating dexamethasone for ocular delivery: formulation design, physicochemical characterization, safety and corneal permeability assessment. J Biomed Nanotechnol, 2013; 9(6): 998-1007.

21. Torne S.J., Ansari K.A., Vavia P.R., Trotta F., Cavalli R. Enhanced oral paclitaxel bioavailability after administration of paclitaxel-loaded nanosponges. Journal of Drug Delivery, 2010; 17(6): 419-25.

22. Ansari K.A., Torne S.J., Vavia P.R., Trotta F., Cavalli R. Paclitaxel loaded nanosponges: invitro characterization and cytotoxicity study on MCF-7 cell line culture. Curr Drug Deliv. 2011; 8(2): 194-202.

23. Rao M., Bajaj A., Khole I., et al. In-vitro and in-vivo evaluation of β-cyclodextrin-based nanosponges of Telmisartan. J Incl Phenom Macrocycl Chem, 2013; 77: 135-45.

24. Zainuddin R., Zaheer Z., Sangshetti J.N., Momin M. Enhancement of oral bioavailability of anti-HIV drug Rilpivirine HCl through nanosponge formulation. Drug Dev Ind Pharm, 2017; 43(12): 2076-84.

25. Omar, S.M., Ibrahim, F. and Ismail, A. Formulation and evaluation of cyclodextrin-based nanosponges of griseofulvin as pediatric oral liquid dosage form for enhancing bioavailability and masking bitter taste. Saudi Pharmaceutical Journal, 2020; 28(3):349-361.

26. Ansari K.A., Vavia P.R., Trotta F., Cavalli R. Cyclodextrin-based nanosponges for delivery of resveratrol: In vitro characterisation, stability, cytotoxicity and permeation study. AAPS PharmSciTech 2011; 12: 279-86.

27. Torne S., Darandale S., Vavia P., Trotta F., Cavalli R. Cyclodextrin-based nanosponges: effective nanocarrier for tamoxifen delivery. Pharm Dev Technol, 2013; 18(3): 619-625.

28. Cavalli R., Akhter A.K., Bisazza A., Giustetto P., Trotta F., Vavia P. Nanosponge formulations as oxygen delivery systems. International Journal of Pharmaceutics, 2010; 402(1-2): 254-257.

29. Momin M.M., Zaheer Z., Zainuddin R., et al. Extended delivery of Erlotinib glutathione nansoponge for targeting lung cancer. Artif Cells Nanomed Biotechnol, 2018; 46(5): 1064-75.

30. Lim K.M. Skin Epidermis and Barrier Function. Int J Mol Sci. 2021; 22(6): 3035. DOI: 10.3390/ijms22063035. PMID: 33809733; PMCID: PMC8002265.

31. Camilion J.V., Khanna S., Anasseri S., Laney C., Mayrovitz H.N. Physiological, Pathological, and Circadian Factors Impacting Skin Hydration. Cureus. 2022; 14(8):e27666. DOI: 10.7759/cureus.27666. PMID: 36072192; PMCID: PMC9440333.

32. José Pedro Lopes & Michail S.L. Pathogenesis and virulence of Candida albicans, Virulence, 2022; 13(1): 89-121, DOI: 10.1080/21505594.2021.2019950

33. Wakure B.S., Salunke A.M., Mane P.T., Nanosponges as novel carrier for topical delivery of Luliconazole – an antifungal drug, International Journal of Pharmaceutical Science and Research, 2021; 12(10): 5570-5583

34. Mahendra P. Morbidity and Mortality Due to Fungal Infections. J Appl Microbiol Biochem. 2017; 1(1):1-2.

35. Sawant B, Khan T. Recent advances in delivery of antifungal agents for therapeutic management of candidiasis. Biomed Pharmacother. 2017; 96:1478-90.

36. Sabra R, Branch R.A. Amphotericin B nephrotoxicity. Drug Saf. 1990; 5(2):94-108 https://doi.org/10.2165/00002018-199005020-00003.

37. Pfaller M.A., Diekema, D.J. Antifungal Drug Resistance: Clinical Impact and Opportunities for New Therapies. Clinical Microbiology Reviews. 2007; 20(3):531–567.

38. Smith H.C. Why Are Prescription Drugs More Expensive in the U.S. than in Other Countries? www.goodrx.com 19.10.22, accessed on 18.02.23.

39. Voltan AR, Quindos G, Alarcon KPM, Fusco-Almeida AM, Mendes-Giannini MJS, Chorilli M. Fungal Disease: Could Nanostructured Drug Delivery System be a Novel Paradigm for Therapy? Int J Nanomed. 2016; 11:3715-30.

40. Buchiraju R, Nama S, Sakala B, Chandu BR, Kommu A, Yedulapurapu N. Vesicular Drug Delivery System: An Overview. Res J Pharm, Biol Chem Sci. 2013; 4(3):463-73.

41. Madni A, Sarfraz M, Rehman M, Ahmad M, Akhtar N, Ahmad S, et al. Liposomal Drug Delivery: A Versatile Platform for Challenging Clinical Applications. J Pharm Pharm Sci. 2014; 17(3):401-26.

42. Stone N.R., Bicanic T, Salim R, Hope W. Liposomal Amphotericin B (AmBisome(®)): A Review of the Pharmacokinetics, Pharmacodynamics, Clinical Experience and Future Directions. Drugs. 2016; 76(4):485-500.

43. Muller R.H., Mader K, Gohla S. Solid Lipid Nanoparticles (SLN) for controlled drug delivery: A review of the state of the art. Eur J Pharm Biopharm. 2000; 50(1):161-77.

44. Omar S. M., Ibrahim F., Ismail A. Formulation and evaluation of cyclodextrin-based nanosponges of griseofulvin as pediatric oral liquid dosage form for enhancing bioavailability and masking bitter taste. Saudi Pharm J. 2020; 28:349–361. https://doi.org/10.1016/j.jsps.2020.01.016.

45. Conte C., Caldera F., Catanzano O., D'Angelo I., Ungaro F., Miro A., Pellosi D. S., Trotta F., Quaglia F. β-cyclodextrin nanosponges as multifunctional ingredient in water-containing semisolid formulations for skin delivery. J. Pharm. Sci. 2014; 103:3941–3949. https://doi.org/10.1002/jps.24203

46. Ahmed, M.M., Fatima, F., Anwer, M.K., Ibnouf, E.O., Kalam, M.A., Alshamsan, A., Aldawsari, M.F., Alalaiwe, A. and Ansari, M.J. Formulation and in vitro evaluation of topical nanosponge-based gel containing butenafine for the treatment of fungal skin infection. Saudi Pharmaceutical Journal, 2021; 29(5): 467-477.

47. Yang F., Yang J., Li, S. Nanosponges: A Novel Drug Delivery System. Journal of Pharmaceutical Sciences, 2009; 98(10): 3447-3453.

48. Rubio G.R., Oleveira de C.H., Rivera J., Contador T.N. The Fungal Cell Wall: Candida, Cryptococcus, and Aspergillus Species. Sec. Fungi and Their Interactions, 2020; 10: 1-13.

49. Yamamoto T., Kitamoto K., Fukuyama J., Yamada T. Caspofungin Disrupts the Cell Wall Architecture of Pathogenic Fungi and Increases Accessibility of the β(1-3)-Glucan Layer. Microbiology and Immunology, 2002; 46(2): 97-102.

50. van der Heiden H. J., Planta, R. J., de Koster C. G. Alpha-Agglutinin of Mating-Type Alpha Cells of Saccharomyces cerevisiae Interacts with the Carboxyl Terminus of Aga2p. Molecular and Cellular Biology, 1998; 18(9): 5159-5168.

51. Lathia K. R., Kulkarni A. P. Targeted Drug Delivery Strategies and Nanoparticles for Fungal Infections. The AAPS Journal, 2016; 18(2): 393-403.

52. Jain N.,Devi K.V., Dang R., Bhosale U. Microsponges: A novel drug delivery system. 2013; 15(81): 500-06.

53. Khopade A.J., Jain S., Jain N.K. The Microsponge. Eastern Pharmacist, 2012; 49-53.

54. Shrishail M Ghurghure et al. Nanosponges: A novel approach for targeted drug delivery system. International Journal of Chemistry Studies. 2018; 2(6): 15-23.

55. Divya P.S, Chacko A.J. Formulation and evaluation of trimethoprim loaded nanosponge ocular in- situ gel. International Journal of Pharmacy and Pharmaceutical Journals. 2018; 13(3):158-171.

56. Nagasamy Venkatesh et al. Nanosponges: a review. International Journal of Applied Pharmaceutics. 2018; 10(4), 1-5.

57. Amber V., Shailendra S., Swarnalatha S. Cyclodextrin based novel drug delivery systems. J pharmaceutics sci, 2012; 62: 23-42.

58. Rajeswari C., Alka A., Javed A., Khar R.K. Cyclodextrins in drug delivery: an updated review, AAPS PharmSciTech, 2013; 6(2): E329-357.

59. Farsana P., Sivakumar R., Haribabu Y. Hydrogel based Nanosponges drug delivery for topical applications – A updated review, 2021; 14(1): 527-530.

60. Iravani S, Varma RS. Nanosponges for Drug Delivery and Cancer Therapy: Recent Advances. Nanomaterials. 2022; 12(14):2440. https://doi.org/10.3390/nano12142440

61. Sherje A.P., Dravyakar B.R., Kadam D., Jadhav M. Cyclodextrin based nanosponges: a critical review. Carbohydrate Polymers, 2017; 173: 37-49

62. Li D., Ma M. Nanosponges for water purification. Clean products and processes. 2000; 2(2): 112-116.

63. Caldera F., Tannous M., Cavalli R. et al: Evolution of cyclodextrin nanosponges. International Journal of Pharmaceutics. 2017; 531(2): 470-79.

64. Trotta F., Cavalli R., Tumiatti W., Zerbinati O., Rogero C., Vallero R: Ultrasound – assisted synthesis of Cyclodextrin based nanosponges. 2013; EP 1 786 841 B1.

65. Hayiyana Z., Choonara Y.E., Makgotloe A., et al. Ester-Based Hydrophilic Cyclodextrin Nanosponges for Topical Ocular Drug Delivery. Curr Pharm Des. 2016; 22(46): 6988-6997. https://doi.org/10.2174/1381612822666161216113207

66. Darandale S.S., Vavia P.R. Cyclodextrin-based nanosponges of curcumin: formulation and physicochemical characterization. Journal of Inclusion Phenomena and Macrocyclic Chemistry. 2013; 75(3-4): 315-322.

67. Lembo D., Swaminathan S., Donalisio M., Civra A., Pastero L., et al. Encapsulation of acyclovir in new carboxylated cyclodextrin-based nanosponges improves the agent's antiviral efficacy. International Journal of Pharmaceutics, 2013; 443(1–2): 262–272.

68. Swaminathan S., Pastreo L., Serpe L., Trotta F., Vavia P., Aquilano D., Cavalli R. Cyclodextrin-based nanosponges encapsulating camptothecin: Physicochemical characterization, stability and cytotoxicity. European Journal of Pharmaceutics and Biopharmaceutics. 2010; 74(2): 193-201.

69. Lala R, Thorat A, Gargote C. Current trends in β-cyclodextrin based drug delivery systems. Int J Res Ayur Pharm, 2011; 2(5): 1520-1526.

70. Swaminathan S., Vavia P.R., Trotta F., Cavalli R. Nanosponges encapsulating dexamethasone for ocular delivery: formulation design, physicochemical characterization, safety and corneal permeability assessment. J Biomed Nanotechnol, 2013; 9(6): 998-1007.

71. Trotta F., Dianzani C., Caldera F., Mongnetti B., Cavalli R. The application of nanosponges to cancer drug delivery. Expert Opinion on Drug Delivery, 2014; 11(6): 931-941

72. Shankar S, Vavia PR, Francesco T, Satyen T. Formulation of Betacyclodextrin based nanosponges of Itraconazole. J Incl Phenom Macrocycl Chem, 2007; 57: 89–94

73. Shrestha S., Bhattacharya S. Versatile uses of Nanosponge in Pharmaceutical arena: A mini review. Recent patents on nanotechnology, 2020; 14: 1-8.

74. Cavalli R., Trotta F., Tumiatti W., Cyclodextrin-based nanopsonges for drug delivery. Journal of inclusion phenomena and macro chemistry. 2013; 56(1-2):209-213.

75. Nacht S., Krantz M., The Microsponge: A novel topical programmable delivery system. Chapter 15: In: Topical Drug Delivery Systems Edited by David W.O. and Anfon H.A., 2008; 42: 299-325.

76. Cavalli R., Trotta F., Tumiatti W. Cyclodextrin-based nanosponges for drug delivery. J. Incl. Phenom. Macrocycl. Chem, 2006; 56(1–2): 209–213.

77. Ahmed S., Sheraz A.M., Ahmed S., Anwar Z., Nanosponges: Characteristics, methods of preparation and applications, 2017.

78. Riyaz A.M., Shailesh T., et al. Nanosponges: the spanking accession in drug delivery- an updated comprehensive review. Pelagia Research Library. 2014; 5(6): 7-21.

79. Nag O.K., Delehanty J.B., Active Cellular and Subcellular Targeting of Nanoparticles for Drug Delivery. Pharmaceutics 2019; 11(10):543.

80. Subramanian S., Singireddy A., Krishnamoorthy K., Rajappan M. Nanosponges: A Novel Class of Drug Delivery System – Review. J Pharm PharmaceutSci, 2012; 15(1): 103-111.

81. Ramnik S., Nitin B., et al. Characterization of Cyclodextrin Inclusion Complexes – A review. J Pharm Sci Tech, 2010; 2(3): 171-183.

82. Wolfgang S. Sample preparation in Light scattering from and Nanoparticle Dispersions. Springer Berlin Heidelberg GmbH & Co. Int J Pharm, 2013; 344(1-2): 33-43.

83. Aithal K.S., Udupa N. et al. Physicochemical properties of drug cyclodextrin complexes. Indian Drugs, 2008; 32:293-305.

84. Duchene D. Vaution C., Glomot F. Cyclodextrin: their value in pharmaceutical technology. Drug Dev Ind Pharm, 2012; 12(11-13): 2193-2215.

85. Tayade P.T., Vavia P.P. Inclusion Complexes of Ketoprofen with β-cyclodextrins. Oral pharmacokinetics of Ketoprofen in human. Indian J Pharm Sci, 2012; 68(2): 164-170.

86. Renuka S., Kamla P. Polymeric Nanosponges as an alternative carrier for improved retention of econazole nitrate onto the skin through topical hydrogel formulation. Pharm Dev Technol. 2011; 16(4): 367-376.

87. Salunkhe A., Kadam S. et al. Nanosponges: a modern formulation approach in drug delivery system. World Journal of Pharmacy and Pharmaceutical Sciences. 2018; 7(2): 575-592.

88. Chen E., Benso B., Seleem D., et al. Fungal-host interaction: curcumin modulates proteolytic enzyme activity of Candida albicans and inflammatory host response in vitro. International Journal of Dentistry 2018; https://doi.org/10.1155/2018/2393146

89. Narayanan V.S., Muddaiah, S., et al. Variable antifungal activity of curcumin against planktonic and biofilm phase of different candida species. Indian J. Dent. Res, 2020; 31: 145–148.

90. Neelofar K., Shreaz S., Rimple B., Muralidhar S., Nikhat M., Khan L.A., Curcumin as a promising anticandidal of clinical interest. Can. J. Microbiol. 2011; 57(3): 204–210.

91. Moghadamtousi S.K., Kadir H.A., et al. Review on Antibacterial, Antiviral, and Antifungal Activity of Curcumin. BioMed Research International, 2014; 2014:186864. https://doi.org/10.1155/2014/186864

92. Song L., Zhang F., Yu J., Wei C., Han Q., Meng X., Antifungal effect and possible mechanism of curcumin mediated photodynamic technology against Penicillium expansum. Postharvest Biol. Technol, 2020; 167(2020): 111234-38.

93. Hu Y., Luo J., Kong W., Zhang J., Logrieco A.F., Wang X., Yang M. Uncovering the antifungal components from turmeric (Curcuma longa L.) essential oil as Aspergillus flavus fumigants by partial least squares. RSC Adv. 2015; 5(52): 41967–41976.

94. Gacem M.A., Gacem H., Telli A., Khelil A.O. Mycotoxins: decontamination and nanocontrol methods. In: Nanomycotoxicology. Elsevier, 2020; 189–196.

95. Kavitha K., Vijaya N., et al. Nanomaterials for antifungal applications. Nanotoxicity, 2020; 385–398.

96. Nerilo S.B., Romoli J.C.Z., Nakasugi L.P., et al. Antifungal activity and inhibition of aflatoxins production by Zingiber officinale Roscoe essential oil against Aspergillus flavus in stored maize grains. Ciencia Rural, 2020; 50(6):11-19.

97. Castellanos, L.M., Olivas, N.A., et al. In vitro and in vivo antifungal Activity of clove (Eugenia caryophyllata) and pepper (Piper nigrum L.) essential oils and functional extractsagainst Fusarium oxysporum and Aspergillus niger in tomato (Solanum lycopersicum L.). International Journal of Microbiology, 2020; 1-8. https://doi.org/10.1155/2020/1702037

98. Oliveira, R.C., Carvajal-Moreno M., et al. Essential oils trigger an antifungal and anti-aflatoxigenic effect on Aspergillus flavus via the induction of apoptosis-like cell death and gene regulation. Food Contr, 2020; 110:107038.

99. da Silva Bomfim N., Kohiyama C.Y., Nakasugi L.P., Nerilo S.B., et al. Antifungal and antiaflatoxigenic activity of rosemary essential oil (Rosmarinus officinalis L.) against Aspergillus flavus. Food Addit. Contam, 2020; 37(1): 153–161.

100. Zhu C., Lei M., Andargie M., Zeng J., Li J. Antifungal activity and mechanism of action of tannic acid against Penicillium digitatum. Physiol. Mol. Plant Pathol, 2019;107:46–50.

101. Choi H., Lee D.G. Lycopene induces apoptosis in Candida albicans through reactive oxygen species production and mitochondrial dysfunction. Biochimie, 2015; 115: 108–115.

102. Rai M., Ingle A.P., Pandit R., Paralikar P., Anasane N., Santos C.A.D. Curcumin and curcumin-loaded nanoparticles: antipathogenic and antiparasitic activities. Expert Rev. Anti Infect, 2020; 18(4):367–379.

103. Sadeghi-Ghadi, Z., Vaezi, A., et al. Potent in vitro activity of curcumin and quercetin co-encapsulated in nanovesicles without hyaluronan against Aspergillus and Candida isolates. J. Mycol. Med, 2020; 101014.

104. Gong L., Li T., Chen F., Duan X., Yuan Y., Zhang D., Jiang Y. An inclusion complex of eugenol into β-cyclodextrin: preparation, and physicochemical and antifungal characterization. Food Chem, 2016; 196: 324–330.

105. Chaudhari A.K., Singh V.K., et al. Improvement of in vitro and in situ antifungal, AFB1 inhibitory and antioxidant activity of Origanum majorana L. essential oil through nanoemulsion and recommending as novel food preservative. Food Chem. Toxicol, 2020; 111536-48.

106. Behbehani J.M., Irshad M., Shreaz S., Karched M., Synergistic effects of tea polyphenol epigallocatechin 3-O-gallate and azole drugs against oral Candida isolates. J. Mycolog. Med, 2019; 29(2): 158–167.

107. Wu L.P., Wang D., Li Z. Grand challenges in nanomedicine. Mater Sci Eng, C. 2020; 106:110302-08.

108. Bausell, R.Barker. The problem with science: the reproducibility crisis and what to do about it (New York, 2021; online edu, oxford academeic, 2021); https://doi.org/10.1093/oso/9780197536537.001.0001 accessed on 27.01.23.

109. Hofmann-Amtenbrink, M., Grainger, D.W. and Hofmann, H., 2015. Nanoparticles in medicine: current challenges facing inorganic nanoparticle toxicity assessments and standardizations. Nanomedicine: Nanotechnology, Biology and Medicine, 11(7):1689–1694.

110. Mathur M., Devi K.V. Potential of novel drug delivery systems in the management of topical candidiasis. Journal of drug targeting, 2017; 25(8): 685-703. https://doi.org/10.1080/1061186X.2017.1331352

111. Rajam P.R., Muthukumar R.K. An updated comprehensive review on Nanosponges – novel emerging drug delivery system. Research J. Pharm. And Tech, 2021; 14(8): 4476-4484.

112. Arika T., Yokoo M., Hase T., Maeda T., Amemiya K., Yamaguchi H. Effects of butenafine hydrochloride, a new benzylamine derivative, on experimental dermatophytosis in guinea pigs. Antimicrob. Agents Chemother. 1990; 34(11): 2250–2253.

113. Anwer M.K., Mohammad M., Ezzeldin E., Fatima F., Alalaiwe A., Iqbal M. Preparation of sustained release apremilast-loaded PLGAlga nanoparticles: In vitro characterization and in vivo pharmacokinetic study in rats. Int. J. Nanomed. 2019; 14: 1587–1595.

114. Rauber C.D.S., Guterres S.S. and Schapoval E.E. LC determination of citral in Cymbopogon citratus volatile oil. Journal of Pharmaceutical and Biomedical Analysis, 2005; 37(3): 597-601.

115. Aldawsari H.M., Badr-Eldin S.M., Labib G.S. and El-Kamel A.H. Design and formulation of a topical hydrogel integrating lemongrass-loaded nanosponges with an enhanced antifungal effect: in vitro/in vivo evaluation. International journal of nanomedicine, 2015; 10: 893-897.

116. Csermely P., Agoston V., & Pongor S. The efficiency of multitarget drugs: The network approach might help drug design. Trends in Pharmacological Sciences, 2005; 26(4): 178–182.

117. Abou T.S., Darwish A.B., Abood A. and Mohamed A.M. Investigation of a new horizon antifungal activity with enhancing the antimicrobial efficacy of ciprofloxacin and its binary mixture via their encapsulation in nanoassemblies: in vitro and in vivo evaluation. Drug Development Research, 2020; 81(3): 374-388.

118. Lembo D., Swaminathan S., Donalisio M., Civra A., Pastero L., et al. Encapsulation of acyclovir in new carboxylated cyclodextrin-based nanosponges improves the agent's antiviral efficacy. International Journal of Pharmaceutics, 2013; 443(1–2): 262–272.

119. Amer R.I., El-Osaily G.H., Gad, S.S. Design and optimization of topical terbinafine hydrochloride nanosponges: Application of full factorial design, in vitro and in vivo evaluation. Journal of Advanced Pharmaceutical Technology & Research, 2020; 11(1): 13-18.

120. Baline K., Hali F. Fonsecaea pedrosoi-induced chromoblastomycosis: About a case. Pan Afr Med J 2018; 30:187-191.

121. Chopra B.; Dhingra A.K.; Dhar K.L. Psoralea corylifolia, L. (Buguchi)—Folklore to modern evidence: Review. Fitoterapia 2013; 90: 44–56.

122. Kumar S., Trotta F., Rao R. Encapsulation of babchi oil in cyclodextrin-based nanosponges: Physicochemical characterization, photodegradation, and in vitro cytotoxicity studies. Pharmaceutics, 2018; 10(4): 169-178.

123. Anandam S.; Selvamuthukumar S. Fabrication of cyclodextrin nanosponges for quercetin delivery: Physicochemical characterization, photostability, and antioxidant effects. J. Mater. Sci. 2014; 49: 8140–8153.

124. Baloglu E., Karavana S.Y., Senyigit Z.A., Hilmioglu-Polat S., Metin D.Y., Zekioglu O., Guneri T. and Jones D.S. In-situ gel formulations of econazole nitrate: preparation and

in-vitro and in-vivo evaluation. Journal of Pharmacy and Pharmacology, 2011; 63(10): 1274-1282.

125. Osmani, R.A.M., Kulkarni, P.K., Shanmuganathan, S., Hani, U., Srivastava, A., Prerana, M., Shinde, C.G. and Bhosale, R.R. A 3^2 full factorial design for development and characterization of a nanosponge-based intravaginal in situ gelling system for vulvovaginal candidiasis. RSC advances, 2016; 6(23): 18737-18750.

126. Shende, Pravin K.,Trotta F., R. S. Gaud, Kiran D., Roberta C., and Miriam B., Influence of different techniques on formulation and comparative characterization of inclusion complexes of ASA with β-cyclodextrin and inclusion complexes of ASA with PMDA cross-linked β-cyclodextrin nanosponges. Journal of inclusion phenomena and macrocyclic chemistry, 2012; 74(1): 447-454.

127. H. Kansagra, S. Mallick, Microemulsion- based antifungal gel of luliconazole for dermatophyte infections: formulation, characterization and efficacy studies, J. Pharm. Investig. 2016; 46: 21-28.

128. Kapileshwari G.R., Barve A.R., Kumar L., Bhide P.J., Joshi M. and Shirodkar R.K. Novel drug delivery system of luliconazole-Formulation and characterisation. Journal of Drug Delivery Science and Technology, 2020; 55:101302-08.

129. K. Uchida, Y. Nishiyama, H. Yamaguchi, In vitro antifungal activity of luliconazole (NND-502), a novel imidazole antifungal agent, J. Infect. Chemother. 2004; 10: 216–219.

130. Patel A.R., Vavia P.R.: Effect of hydrophilic polymer on solubilization of fenofibrate by cyclodextrin complexation. Journal of inclusion phenomena and macrocyclic chemistry. 2006; 56: 247–251

131. Cilurzo F., Minghetti P., Sinico C. Newborn pig skin as model membrane in vitro drug permeation studies. AAPS PharmSciTech. 2007; 8(4):1–4.

132. Klarić Maja K., Mastelić J., Piecková E., Pepeljnak S. Antifungal activity of Thyme essential oil and thymol against moulds from Damp Dwellings. Letters in applied microbiology. 2007; 44:36-42.

133. Rezaei A., Khavari A., Sami M., Incorporation of thyme essential oil into the β-cyclodextrin nanosponges: Preparation, characterization and antibacterial activity, Journal of Molecular Structure, 2021; 1241:130610.

134. Sharma R. and Pathak K. Polymeric nanosponges as an alternative carrier for improved retention of econazole nitrate onto the skin through topical hydrogel formulation. Pharmaceutical development and technology, 2011; 16(4): 367-376.

135. Williams A.C., Barry B.W. Penetration enhancers. Adv Drug Del Rev 2004; 56: 603–618.

136. Arida A.I., Al-Tabakha M.M., Hamoury H.A.J. Improving the high variable bioavailability of griseofulvin by SEDDS. Chem. Pharm. Bull. 2007; 55(12):1713–1719.

137. Omar S.M., Ibrahim F. and Ismail A. Formulation and evaluation of cyclodextrin-based nanosponges of griseofulvin as pediatric oral liquid dosage form for enhancing bioavailability and masking bitter taste. Saudi Pharmaceutical Journal, 2020; 28(3):349-361.

138. Rao M.R., Chaudhari J., Trotta F., Caldera F. Investigation of cyclodextrinbased nanosponges for solubility and bioavailability enhancement of rilpivirine. AAPS PharmSciTech. 2018, 19(5):2358–2369.

139. Bhalekar R., Nagoba S., et al. Formulation and evaluation of nanosponges hydrogel for topical drug delivery containing griseofulvin. International Journal of Medicine and Pharmaceutical Sciences. 2020, 10(2): 57-70.

140. Shoaib Q., Abbas N., et al. Development and evaluation of scaffold-based nanosponge formulation for controlled drug delivery of naproxen and ibuprofen. Tropical Journal of Pharmaceutical Research, 2018; 17(8): 1465-1474.

141. Patel R.V., Agrawal K.Y. Nanosuspension: an approach to enhance solubility of drugs. Journal of advanced pharmaceutical technology & research, 2011; 2: 81-87.

142. Ahmed R.Z., Patil G., Zaheer Z. Nanosponges–a completely new nano-horizon: pharmaceutical applications and recent advances. Drug Dev. Ind. Pharm, 2013; 39(9): 1263–1272.

143. Patel D.M., Jani R., Patel Chhagan. Design and evaluation of colon targeted modified pulsincap delivery of 5-fluorouracil according to circadian rhythm. International journal of pharmaceutical investigation, 2011; 1: 172-81.

144. Anandam S., Selvamuthukumar S. Optimization of microwave assisted synthesis of cyclodextrin nanosponges using response surface methodology. J. Porous Mat, 2014; 21(6): 1015–1023.

145. Bragagni M., Maestrelli F., Mura P. Physical chemical characterization of binary systems of prilocaine hydrochloride with triacetyl-β-cyclodextrin. J. Incl. Phenom. Macrocycl Chem, 2010; 68(3–4): 437–445.

146. Bunaciu A.A., Udriştioiu E.G., Aboul-Enein H.Y. X-ray difraction: instrumentation and applications. Crit. Rev. Anal. Chem, 2015; 45(4): 289–299.

147. Sapino S., Carlotti M.E., Cavalli R., Ugazio E., Berlier G., Gastaldi L., Morel S. Photochemical and antioxidant properties of gamma-oryzanol in beta-cyclodextrin-based nanosponges. J. Incl. Phenom. Macrocycl. Chem, 2013; 75(1–2): 69–76.

148. Biliaderis C.G. Differential scanning calorimetry in food research-a review. Food Chem, 1983; 10(4), 239–265.

149. Cammenga H.K., Epple M. Basic principles of thermoanalytical techniques and their applications in preparative chemistry. Angew. Chem. Int. Ed. Engl, 1995; 34(11): 1171–1187.

150. El-Mallah Y., Yousef A., et al. Effect Of A Binary Blend Composed Of Poloxamer And PVP On Aqueous Solubility Of Griseofulvin. Int J Pharm Pharm Sci, 2014; 7(2): 121-125.

151. Li B., Wen M., Li W., He M., Xang X., Li S. Preparation and characterization of baicalin-poly-vinylpyrrolidone coprecipitate. Int J Pharm, 2011; 408:91-6.

152. Yaşayan G., Sert Ş.B., Tatar E., Küçükgüzel İ. Fabrication and characterisation studies of cyclodextrin-based nanosponges for sulfamethoxazole delivery. Journal of Inclusion Phenomena and Macrocyclic Chemistry, 2020; 97: 175-186.

153. Singh V., Xu J., Wu L., Liu B., Guo T., Guo Z., York P., Gref R., Zhang J.: Ordered and disordered cyclodextrin nanosponges with diverse physicochemical properties. RSC Adv, 2017; 7(38): 23759–23764 (2017). https://doi.org/10.1039/C7RA00584A

154. Sabzi E.N., Kiasat R.A. β-Cyclodextrin Based Nanosponge as a Biodegradable Porous Three Dimensional Nanocatalyst in the One-Pot Synthesis of N-Containing Organic Scaffolds. Catalysis Letters, 2018. https://doi.org/10.1007/s10562-018-2484-3

155. Al-Suwayeh S.A., Taha E.I., Al-Qahtani F.M., Ahmed M.O., Badran M.M. Evaluation of Skin Permeation and Analgesic Activity Effects of Carbopol Lornoxicam Topical Gels Containing Penetration Enhancer. Sci. World J, 2014; 1–9.

156. Wu Y., Joseph S., Aluru N.R.: Effect of cross-linking on the diffusion of water, ions, and small molecules in hydrogels. J. Phys. Chem, 2009; 113(11):3512.

157. Moglad H., Fatima F., Muqtader M., Devanathad V., Khalid A.M., F. Aldawsa, Development of Topical Antibacterial Gel Loaded with Cefadroxil Solid Lipid Nanoparticles: In vivo Wound Healing Activity and Epithelialization Study. Int. J. Pharmacol, 2020; 16: 298–309. https://doi.org/10.3923/ijp.2020.298.309

158. Laraceunte Mei-Li., Yu H.M., et al. Zero-order drug delivery: State of the art and future prospects. Journal of Controlled Release, 2020; 327: 834-856.

159. Mathematical models of drug release, Strategy to Modify Drug Release from Pharm. Syst. Elsevier, 2015; 63–86. https://doi.org/10.1016/b978-0-08-100092-2.00005-9

160.   Weidner J. Drug delivery. Drug Discov. Today. 2001; 6(4): 216-217 https://doi.org/10.1016/S1359-6446(02)02270-5.

161.   Sajorne R., Mabuhay-Omar J. Antimicrobial property of the epidermal mucus of Tilapia Oreochromis spp. 2020;

162.   Tendencia E.A., Disk diffusion method. In Laboratory manual of standardized methods for antimicrobial sensitivity tests for bacteria isolated from aquatic animals and environment. Southeast Asian Fisheries Development Centre-Aquaculture Department, Tigbauan, Iloilo, Philippines.2004, 13-29.

163.   Bauer A.W., Kirby W.M., Sherris J.C., Turck M. Antibiotic susceptibility testing by a standardized single disk method. American Journal of Clinical Pathology, 1996; 45(4): 493–496.

Chapter 9
Recent publications

Main Publications

1. **Prateep Sengupta**, Amrita Das, Debaldeb Datta, Jasmina Khanam, Kajal Ghosal, **Nanosponge: A New Platform for Antifungal Drug Delivery. Reactive and Functional Polymer (under review)**
2. Prateep Sengupta, Amrita Das, Jasmina Khanam, Pranab Kumar Mondal, Avirup Biswas, Jesil Mathew Arjan, Kajal Ghosal, **Griseofulvin loaded nanoporous scaffolds for topical antifungal drug delivery for extended duration. (patent under process)**

Related Publications

1. Amrita Das, Prateep Sengupta, Jasmina Khanam, Kajal Ghosal, **Magnetic Nanoparticles (MNP), A Novel Drug Delivery and Diagnostic Platform: A review on its Basic Concepts, Synthesis, Surface Coating and Applications. (under review)**